Chemical Aging and Influence of Manufacture on High Explosives

Le vieillissement chimique et l'influence de la fabrication sur les explosifs

A Thesis Submitted to the Division of Graduate Studies
of the Royal Military College of Canada
by

Tian Xiang Ma, CD, P.Eng

In Partial Fulfillment of the Requirement for the Degree of
Master of Applied Science in Chemistry and Chemical Engineering

September 2025

To

all ammunition and explosive practitioners in Canada,

your dedication continues to inspire.

Acknowledgement

The author wishes to take this opportunity to express his sincere gratitude and indebtedness to the staff and graduate students at Defence Research Development Canada (Valcartier), Munition Evaluation Testing Centre (Valcartier), Canadian Forces Ammunition Depot Dundurn, and Royal Military College of Canada (RMCC) for their invaluable support on this research.

Abstract

This study originated from a civil request from the Canadian National Railway (CNR) to the Department of National Defence (DND) for assistance to dispose of former US military munitions which were converted into civilian avalanche control use. They consisted of the 105 mm calibre recoilless munitions which were produced in 1954 and had been stored in ambient conditions. This study investigated the long-term ambient aging impacts and the influence from manufacturing on the 2,4,6-trinitrotoluene (TNT), Composition B (Comp B), and Composition A-3 (Comp A-3) using X-ray imaging, mechanical sensitivity tests, Electro-Static Discharge (ESD) sensitivity test, Scanning Electron Microscopy (SEM), and Thermal Gravimetry Analysis (TGA) - Differential Scanning Calorimetry (DSC) techniques. The TNT composition was further analysed by the Gas Chromatography – Mass Spectrometry (GC-MS).

The Comp A-3 composition consisted of Research Department Explosive (RDX) and inert wax mix. It had shown minimal measurable changes with respect to the mechanical, ESD and thermal sensitivity of the material. The X-ray and SEM images also revealed no discernable changes. This study concluded that there is no safety impact with respect to long-term ambient aging of the Comp A-3.

The TNT was found to have exhibited characteristics of thermally damaged materials on the surface level by SEM imaging. This resulted in the lowering of the friction resistance when compared to the known standards of the modern TNT. The cause of such reduction was attributed to the surface texture of the material which had an equivalent effect of increasing the surface area. The activation energy of the aged TNT was found to be 174 ± 31 kJ/mol with an R square value of 0.86 using the Kissinger method. However, this study noted that there

were non-linear properties in the Kissinger kinetic plot which resulted in the low R square value. The non-linear properties could be attributed by the multi-mechanism degradation behaviour of TNT. The TNT GC-MS analysis revealed only three impurities with low quantity when compared to a list of known impurities in the literature. However, difficulties were noted in the employment of the GC-MS techniques during the study. Thus, this study concludes that the aged TNT had retained its purity level with noted reduction in friction resistance due to thermal exposure.

The Comp B composition consisted of TNT and RDX. It was noted with similar defect as the aged TNT in its aging behaviour. There was a reduction in the friction resistance which was contributed by the aging of the TNT. The thermal sensitivity result revealed that the RDX was synthesized using the Bachmann process and was considered as the Type II RDX which contained a small quantity of His Majesty's Explosive (HMX). Based on the results from the Comp A-3, this study concludes that the aging of TNT had a predominant effect on the aging behaviour of the Comp B while the RDX had negligible effect.

In conclusion, the aging behaviours of the TNT, Comp B and Comp A-3 have been investigated using 71 years old samples which were stored in ambient conditions. The Comp A-3 was found to have no discernable changes with respect to aging while TNT was noted to have a reduction in friction resistances. The aging of Comp B was predominately affected by the aging of its TNT component while the RDX had negligible effects. No evidence was found to suggest the chemical stability of the explosives had been compromised. Thus, this study concluded that they can be safely stored and handled by the Canadian Armed Forces.

Résumé

Cette étude a été initiée par une demande civile de la Compagnie des chemins de fer nationaux du Canada (CNR) envers le département de la Défense nationale (DND). Cette demande civile a été fait pour obtenir de l'aide à éliminer les anciennes munitions militaires américaines, qui ont été converti pour un usage civil dans le contrôle des avalanches. Elles en consistaient des munitions sans recul de calibre 105 mm qui ont été produites en 1954 et ont été conservées dans des conditions ambiantes. Cette étude a examiné les impacts du vieillissement ambiant à long terme et l'influence de la fabrication sur le 2,4,6-trinitrotoluène (TNT), la Composition B (Comp B) et la Composition A-3 (Comp A-3) en utilisant des techniques d'imagerie par rayons X, des tests de sensibilité mécanique, un test de sensibilité aux décharges électrostatiques (ESD), une microscopie électronique à balayage (SEM) et une analyse thermogravimétrique (TGA) - calorimétrie différentielle (DSC). La composition de TNT a été analysée plus en détail par chromatographie en phase gazeuse – spectrométrie de masse (CG-SM).

La composition du Comp A-3 consistait d'un mélange d'explosif du département de recherche (RDX) et de cire inerte. Elle a illustré des changements mesurables minuscules, en ce qui concerne la mécanique, l'ESD et la sensibilité thermique du matériel. Les images aux rayons X et MEB n'ont également révélé aucun changement discernable. Cette étude a conclu qu'il n'y a aucun impact sur la sécurité en ce qui concerne le vieillissement à long terme à température ambiante du Comp A-3.

C'était constaté que le TNT présentait des caractéristiques de matériaux thermiquement endommagés au niveau de la surface lors de l'imagerie SEM. Cela a entraîné une diminution de

la résistance au frottement par rapport aux normes connues du TNT moderne. La cause de cette réduction a été attribuée à la texture de surface du matériel, qui avait un effet équivalent à l'augmentation de la surface. L'énergie d'activation du TNT vieillissant a été trouvée à 174 ± 31 kJ/mol avec une valeur R au carré de 0,86 en utilisant la méthode de Kissinger. Cependant, cette étude a noté qu'il existait des propriétés non linéaires dans le graphique cinétique de Kissinger, ce qui a entraîné la faible valeur R au carré. Les propriétés non linéaires pourraient être attribuées au comportement de dégradation à multi-mécanismes du TNT. L'analyse GC-MS du TNT a révélé seulement trois impuretés en faible quantité par rapport à une liste d'impuretés connues dans la littérature. Cependant, des difficultés ont été notées dans l'utilisation des techniques GC-MS pendant l'étude. Ainsi, cette étude conclut que le TNT vieilli avait conservé son niveau de pureté avec une réduction notée de la résistance au frottement en raison de l'exposition thermique.

La composition du Comp B se composait de TNT et de RDX. Nous avons noté des défauts similaires à ceux du TNT vieilli dans son comportement de vieillissement. Il y a eu une réduction de la résistance à la friction, qui a été attribuée au vieillissement du TNT. Le résultat de la sensibilité thermique a révélé que le RDX avait été synthétisé selon le procédé Bachmann et était considéré comme le RDX de type II, qui contenait une petite quantité d'explosif de Sa Majesté (HMX). Sur la base des résultats du Comp A-3, cette étude conclut que le vieillissement du TNT avait un effet prédominant sur le comportement de vieillissement du Comp B, tandis que le RDX avait un effet négligeable.

En sommaire, les comportements de vieillissement du TNT, du Comp B et du Comp A-3 ont été étudié en utilisant des échantillons âgés de 71 ans qui ont été conservé dans des

conditions ambiantes. Nous avons constaté que le Comp A-3 ne présentait aucun changement discernable en ce qui concerne le vieillissement, tandis que le TNT a montré une réduction de la résistance au frottement. Le vieillissement du Comp B était principalement affecté par le vieillissement de son composant TNT, tandis que le RDX avait des effets négligeables. Aucune preuve n'a été trouvée pour suggérer que la stabilité chimique des explosifs avait été compromise. Ainsi, cette étude a conclu qu'ils peuvent être conservés et manipulés en toute sécurité par les Forces armées canadiennes.

Statement of Work

In considering the behaviour of past munitions, it is often required for the candidate to have possessed an extensive range of skills and experience beyond that of many areas of graduate study. For example, a munition worker must have sufficient hands-on experience when using the pre-established standard operational procedures to handle ammunition and explosives, safety requires the presence and supervision of experienced and trained staff, and finally access to the licensed explosive ranges, facilities and equipment to conduct the study can become available at short notice. As a part time student, to undertake the full scope of the practical work would be unrealizable in a reasonable timeframe and may be practically impossible. Therefore, my role in the practical implementation of this project has been to provide supervision, coordination, and direction to all participants from various Department of National Defence (DND) organizations to perform the physical ammunition transportation, demilitarization, and conduct various tests.

Although impossible to complete all field and laboratory work, I have made it a priority to gain the necessary working knowledge and experience of the equipment and procedures used to enable the completion of this study. I have traveled to Defence Research Development Canada (DRDC) Valcartier and the Royal Military College of Canada (RMCC) to partake in the mechanical and electrostatic sensitivities testing, gas chromatography - mass spectrometry, scanning electron microscopy, and thermo-gravimetric analysis - differential scanning calorimetry. The work to analyse and interpret the test results have been solely my responsibility.

Table of Contents

List of Abbreviations

AAUNAC	Avalanche Artillery User of North America Committee
AOP	Allied Ordnance Publication
BC	British Colombia
BD	Base Detonating
BAM	Bundesanstalt fur Materialprufung
BAT	Battalion Antitank
CAF	Canadian Armed Forces
CFAD	Canadian Force Ammunition Depot
Comp B	Composition B
Comp A-3	Composition A-3
CNR	Canadian National Railway
CJOC	Canadian Joint Operational Command
DAOD	Defence Administrative Order and Directives
DNB	Dinitrobenzene
DND	Department of National Defence
DNT	Dinitrotoluene
DPA	Diphenylamine
DRDC	Defence Research and Development Canada
DSC	Differential Scanning Calorimetry
DTA	Differential Thermal Analysis

EC	Ethyl Centralite
EPA	Environmental Protection Agency
EOD	Explosive Ordnance Disposal
ESD	Electro-Static Discharge
GC	Gas Chromatography
HE	High Explosive
HEP-T	High Explosive Plastic – Tracer
Hexamine	Hexamethylenetetramine
HPLC	High Performance / Pressure Liquid Chromatography
HMX	His Majesty's / High Melting-point Explosive
LCEP	Life Cycle Environmental Profile
MADx	Munition Accident Database
MS	Mass Spectrometer
MoTI	Ministry of Transportation and Infrastructure
METC	Munition Evaluation and Testing Centre
MNT	Mononitrotoluene
MSIAC	Munition Safety Information Analysis Center
NATO	North Atlantic Treaty Organization
NB	Nitrobenzene
NC	Nitrocellulose
NG	Nitroglycerine
NQ	Nitroguanidine

PBX	Polymer/Plastic Bonded Explosive
PBXN	Polymer/Plastic Bonded Explosive Navy
PD	Point Detonating
PETN	Pentaerythritol Tetranitrate
RDX	Research Department Explosive (cyclotrimethylene trinitramine)
RMCC	Royal Military College of Canada
SEM	Scanning Electron Microscopy
SPCC	Single Pour Controlled Cooling
STANAG	Standardized Agreement
TGA	Thermal Gravimetric Analysis
TNT	2,4,6-trinitrotoluene
UN	United Nations
WCOT	Wall Coated Open Tubular
WWI	World War I
WWII	World War II

List of Figures

List of Tables

Chapter 1 Introduction

1.1 Hypothesis

Early production of chemical explosives can be traced back to ancient China and dated to the 10th century A.D. It consisted of the mixing of charcoal, sulfur and nitrate salts to form what is now known as gunpowder. (Kelly, 2004) In the context of energetic materials, these readily available materials were considered inert when separated. However, when mixed, they had the potential to react and produce work from their gaseous products upon initiation. Moisture is known to render the gunpowder inert and is detrimental to the performance of the material. As a result, the lifespan of gunpowder greatly depends on exposure to moisture, and its service life can vary depending on the exposure. The shift to organic based energetic material in the 19th century provided significant improvement in the material performance. However, the inherent degradation of the energetic material continues to remain as a challenge in its lifecycle management. Furthermore, exposure to hot climatic conditions will enhance degradation and expedite the de-stabilization of these energetic materials, potentially with catastrophic consequences.

The present work focuses on the aging effects of explosives. Particularly, the chemical composition of energetic materials contained within 105 mm calibre recoilless munitions aged under ambient environmental conditions. Under normal circumstances, these ammunitions would have been consumed or otherwise demilitarized. They contain a number of related materials which presents a unique opportunity for analytical studies.

The hypothesis of this work supposes that these materials will display chemical aging based on their composition. Their relative decay will be related to the known properties of the material, and their behaviours determined by artificial aging. In particular, there will be minimal TNT, Comp B, and Comp A-3 degradation. The sensitivities of these materials will remain at similar level to the modern explosives.

This work has the opportunity to shed light on the production of the subject materials which predate modern-day chemical analysis. These munitions represent an early production of the 105 mm calibre recoilless ammunition during the Korean War era from the US. It supposes that the quality of production would be at similar level when compared to the modern artillery shells despite of wartime production. It is proposed that the TNT impurities will be of similar proportion to the current manufacturing quality. The RDX contained within the Comp B and Comp A-3 would be synthesized using the Bachmann method, such that they would contain a noticeable percentage of HMX impurities.

1.2 Introduction to Energetic Material

Under the influence of Taoism, the invention of energetic material was linked to the search for immortality by the alchemists for profit. The earliest energetic material used dated back to around the 10th century A.D. It was known as the *huo yao* or, “fire drug”, and was used as a pyrotechnic element during holiday celebrations. (Kelly, 2004) By the end of the 13th century, the potential of these materials had been recognized and fully adopted to use as an aid to breach the walls of castles and cities during conflict. (Ahkavan, 2011)

Today, the term energetic material describes a man-made chemical composition that is capable of producing a detonation or deflagration or pyrotechnic effects. (Ahkavan, 2011) Based on their applications and chemical properties, there are various subcategories and methods to differentiate energetic materials. Within the context of this research, energetic materials are divided into three classes based on their corresponding responses upon initiation in an unconfined state. Energetic materials that can produce a deflagration are referred to as propellants. Deflagration is a surface combustion effect in which the rate of reaction depends on the burning surface area. It is commonly referred to as rapid burning. Explosives are energetic materials that can produce a physical shockwave travelling through the material at supersonic speed. This is known as a detonation. Lastly, pyrotechnics are materials that can produce pyrotechnical effects such as smoke, flare, and fireworks. However, they represent a distinctive and diversified class of materials and present a different scope to the current analysis. This paper will be focusing on explosives and using propellants as a comparison within energetic materials.

In the context of military application, propellants and explosives are often found in artillery ammunition components for different purposes. A generic artillery ammunition contains the fuze, projectile, and cartridge case shown in Figure 1. Propellants are commonly found in cartridge cases or in bags. They are used to accelerate and thus to impart the muzzle velocity for projectiles in a gun system. There are two types of cartridge ammunition: fixed cartridge and semi-fixed cartridge. Figure 1 illustrates an example of a fixed cartridge ammunition which the cartridge is crimped to the projectile. Semi-fixed cartridge ammunition refers to the separation of projectile and propellant cartridge case. The bagged propellants are

commonly used in large calibre artilleries such as the Modular Artillery Charge (MAC) system used in the 155 mm howitzer gun system. It allows the operator to adjust the propellant amount depending on the range required. Alternatively, propellants can also be used to actuate a device through the generation of gases such as pilot ejection seats and airbags in a car system. (Akhavan, 2011)

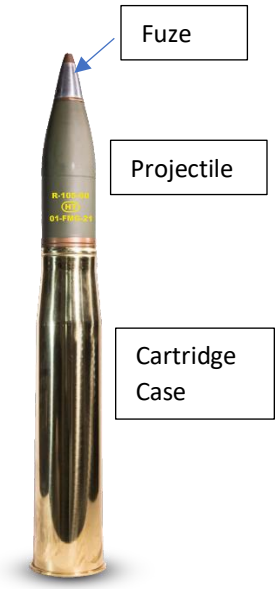

Figure 1. Generic Artillery Ammunition (MSM Group, 2025)

Explosives are usually used in the main charge of the projectile and in the fuze components of an artillery ammunition. Common forms of explosives are 2,4,6-trinitrotoluene (TNT) and cyclotrimethylenetrinitramine which is also known as the Research Department Explosive (RDX). They are mostly found in the projectile and used for destruction purposes. However, explosives used in the fuze component are designed to initiate the main charge in the projectile. They do not deliver the same scale of destruction power and contain smaller

quantities than the explosives used in the projectile. Examples of explosives found in the fuze components are tetryl and lead azide. Explosives contained in the fuze element are generally referred to as primary explosives, and explosives contained in the projectile are referred to as secondary explosives. The difference between primary and secondary explosives is their relative sensitivities to external stimuli. Primary explosives are chemical compositions with relatively higher sensitivity to external stimuli and can be easily initiated when compared to secondary explosives. When the fuze element and the projectile are assembled, they formed a coupling relationship known as the "explosive train", shown in Figure 2. This is used to maximize the safety of the ammunition until the point of use. (Payne, 2010)

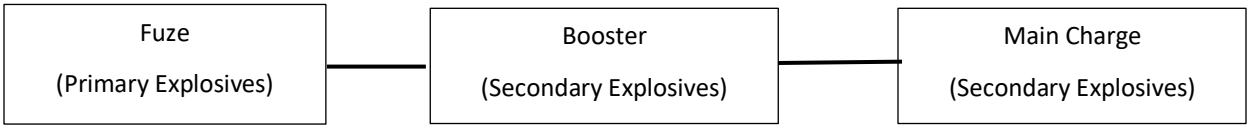

Figure 2. Illustration of Explosive Train

The decomposition process for both explosives and propellant going from reactant to product is known as oxidation-reduction reactions. Oxidation reaction describes the loss of electrons, and reduction reaction describes the gain of electrons. (Tro, 2008) During the reactions, the transfer of electrons between molecules or atoms is accompanied by the release of internal chemical energy. However, for organic molecules it is often beneficial to consider the same fundamental process in terms of the chemical cleavage of relatively weak bonds and the overall formation of stronger bonds, with a consequent release in energy. Notably, a majority of the energetic materials are made up of carbon, hydrogen, nitrogen and oxygen atoms. Consequently, the corresponding products of a complete combustion reaction for an

energetic material would consist of carbon monoxide (CO), carbon dioxide (CO_2), water (H_2O), and nitrogen (N_2). (Cooper, 1996)

Given the decomposition of energetic materials does not spontaneously occur, activation energy is needed to overcome the energy barrier in order for the decomposition reaction to occur. This can be achieved by an external stimulus, but on the molecular level, materials have the potential to disperse an applied stimulus in the form of kinetic energy via molecular motions. (Todd, 2020) If the stimulus is sufficient to exceed the capacity of kinetic molecular motion to absorb the energy, the covalent bonding between the molecules starts to cleave. (Todd, 2020) This is further driven by the desire of each molecule to minimize the free energy of the system. (Spice, 1964) The energy released from the cleavage further contributes to raising the temperature in the material. (Cooper and Kurowski, 1996) Thus, a chain reaction is formed to accelerate the decomposition of other adjacent molecules. The transition from deflagration to detonation occurs when the rate of the decomposition increases to almost an instantaneous one, due to the confinement of pressure. Reaction then accelerates beyond the sound velocity of the material (Ahkavan, 2011), hence forming a detonation shock wave.

In essence, both propellants and explosives are used in different artillery ammunition components. The difference between propellant and explosives is their responses upon initiation. Propellants deflagrate at a slower rate than explosive detonation. Depending on the relative sensitivity, explosives are further divided into primary and secondary explosives. The division is for the purpose of safe management during their lifecycle. In a chemical context, the initiation of propellant and explosives can occur by a stimulus that exceeds the material's rate to absorb. This paper focuses on the long-term effects on munitions stored at ambient

conditions during which the degradation is only likely to transition to initiation at the end state of decomposition.

1.3 History of Recoilless Rifle Ammunition and Civilian Avalanche Control in North America

Since the invention of the gun system, the work on minimizing the recoil of the gun system has been a central focus to improve the efficiency of the firing rate of the weapon. Recoil is the resulting force from firing a projectile in the gun system. Such force is equal in magnitude, but opposite in direction when compared to the force imparted on the projectile. The recoil force would drive the gun system rearwards and, it would therefore require re-calibration prior to the next engagement. The concept of the recoilless gun system utilizing Newton's third law was first realized by combining two guns firing back-to-back with different payloads in 1914. (Olcer and Levin, 1976) Throughout both world wars, various recoilless weapon designs had emerged. At the end of World War II (WWII), the US had developed a man-portable and shoulder-fired 57 mm calibre recoilless gun system. It was deployed in European and Pacific theatres and known as the M18. Driven by their success in action, a subsequent model was developed using a larger calibre in the 75 mm class known as the M20 and deployed in action. However, the development of the 105 mm calibre recoilless rifle and their munitions came to a halt as the US was de-mobilizing resources in the post WWII era in 1947. (Olcer and Levin, 1976)

In response to the Korean war, the 105 mm calibre recoilless rifle program was reactivated. An early prototype of a 105 mm calibre recoilless rifle was developed and designated as the M27 recoilless rifle system, shown in Figure 3. The M27 was deployed overseas and saw action in Korea. The mobility of the weapon system coupled with its

capability of direct heavy artillery support had demonstrated a tactical advantage on the frontline. This drove the formation of the 105 mm Battalion Antitank (BAT) within the infantry formation level and led to extensive use of the M27. Driven by new operational requirements to defeat armour target at a further distance, a new recoilless rifle was developed based on the existing M27 gun design. This new recoilless rifle was later designated as the M40. Subsequent ammunition used for the M40 was designated as 106 mm calibre to avoid confusion even though the actual gun bore diameter was 105 mm. As a result of the M40 recoilless rifle development and the new 106 mm calibre designation, the remaining 105R mm calibre ammunition and the M27 recoilless rifle were listed as military surplus for sale and retired from active service in the early 1950s. (Olcer and Levin, 1976; Abromeit, 2004)

The current study subjects are munitions designated for use with the M27 recoilless weapon. In a conventional lifecycle of an ammunition, they are usually exhausted in operation or demilitarized at a designated facility. It is uncommon for military surplus or retired ammunition to be recycled into civilian applications such as avalanche control.

Figure 3. M27 105 mm Recoilless Rifle Replica (Armourguy, 2018)

Prior to the use of military artillery on avalanche control in North America, ski resorts and state departments in the US often used civilian avalanche blasters who usually carried the explosives and hand-threw them from ridges, trams, or helicopters to trigger an avalanche. However, this practice exposed avalanche blasters to adverse conditions and resulted in multiple deadly accidents, partly due to the un-reliable commercial safety fuzes used. (Perla, 1976)

The use of military artillery in avalanche control had been implemented in Europe prior to WWII and was introduced by Monty Atwater to the US. Monty was a former WWII gunner and saw the application of military artillery in avalanche control during his military service in Europe. He became a snow ranger in the US Forest Service upon his retirement from active service. In 1949, he led a successful test firing conducted by the US National Guard using a 75 mm French howitzer in Utah. The success drove the US Forest Service to allow US National Guard troops to fire military weapons into the National Forests for avalanche control purpose. However, such a solution was deemed unworkable since the troops were not stationed nearby and travel would be interrupted due to avalanche hazards. Monty took the matter into his own hands and fired the weapon himself, despite rules that only the military was allowed to use the artillery to conduct avalanche control operations at that time. His success motivated the US Forest Service and US Army to amend the policy to allow civilian snow rangers to fire the military artillery and eliminated the need to deploy the National Guards. Monty's success was widely recognized at that time and prompted various trials to use military artillery in avalanche control in other ski resorts and departments. Subsequent test firings concluded that the recoilless rifle systems were the most optimal for civilian avalanche control. The light-weight

design and ease of transportation of the recoilless weapon system coupled with the low cost of military surplus sales, it quickly became the backbone of avalanche control and was used across various other state highway departments and the US Forest Service. (Abromeit, 2004)

The British Colombia (BC) Ministry of Transportation and Infrastructure (MoTI) is believed to have trialed and adopted the use of 105 mm calibre recoilless ammunition to conduct avalanche control. The BC MoTI joined the Avalanche Artillery Users of North America Committee (AAUNAC) in the late 1980s to procure the 105 mm calibre recoilless ammunition, receive update on ammunition surveillance, and standardize training for civilians using military weapons. (Abromeit, 2004)

The subject munitions in this paper consisted of two natures. They are High Explosive (HE) nature containing TNT and Comp B, and High Explosive Plastic – Tracer (HEP-T) nature containing Comp A-3. These early versions of the 105 mm calibre recoilless rifle and munitions have never been in Canadian Armed Forces (CAF) service. They were procured via the AAUNAC from the US as military surplus by the BC MoTI for the Coquihalla Highway avalanche control program in the 1990s. (Abromeit, 2004; Evens, 2024) These munitions were manufactured in the early 1950s and believed to be the last of the 105 mm calibre recoilless ammunition manufactured with the "105R" designation. Based on known records, they have not been deployed overseas. These munitions had been stored in Kamloops, BC since the late 1980s. (CJOC, 2019) They were later declared as surplus by BC MoTI and transferred to the Canadian National Railway (CNR) for avalanche control purpose in the early 1990s. CNR received approximately 1000 rounds of the ammunition consisting of two natures (HE and HEP-T) and relocated them to Terrace, BC. The ammunition was used by the Northwest Avalanche Solution

Ltd. for avalanche control in the Prince Rupert to Terrace railway corridor in BC under the direction of CNR. CNR joined the AAUNAC to ensure training and the use of standard operating procedures for civilian workers operating the 105 mm calibre recoilless weapon system in the 1990s. Unlike the US, there was no policy to regulate civilian use of military artillery in Canada other than the relevant labour safety standard which stated, “must be used in the manner recommended by the manufacturer”. (Evens, 2024)

This practice continued until 2015 when the CNR was notified by the US army that the surveillance of the ammunition had ended due to exhaustion of the US inventory. Therefore, CNR could no longer comply with the BC Occupational Health and Safety Regulation due to lack of confirmation on the ammunition serviceability. Subsequently, CNR ceased the 105 mm calibre recoilless rifle avalanche program and ended its AAUNAC participation in 2015. (Evens, 2024; CJOC, 2019)

In the summer of 2019, CNR reached out to the Department of National Defence (DND) regarding the disposal of military munitions retired from the avalanche control program. DND disposed of the propellant due to safety concerns and re-converted the projectiles into target munitions for Explosive Ordnance Disposal (EOD) training. A small quantity of the projectiles was sent to Defense Research and Development Canada (DRDC) for study and examination.

1.4 Introduction to Ammunition Aging

Aging is a natural phenomenon and a complex issue. It refers to the deterioration of the ammunition and its components when exposed to the expected operational and storage environments continuously or intermittently. There are a wide range of materials used in an

ammunition item other than explosives such as metals, plastics and rubbers to ensure their serviceability in these environments. While aging impacts the ammunition overall, the degree of these impacts varies between the materials.

There are three established degradation mechanisms with respect to the aging deteriorations of ammunition. They are known as Chemical, Mechanical and Thermomechanical. (NATO AOP 46, 2022) The chemical aging mechanism is also referred to as thermal aging because it describes the chemical change of the material as a result of exposure to different temperatures. Some energetic materials will inherently degrade at ambient temperature such as nitrocellulose (NC) and nitroglycerine (NG) to form undesired nitrate esters. The mechanical aging mechanism describes the repeated exposure of material to an applied force. One of the most common in-service considerations of new ammunition is the exposure to vibration from various transportation methods. When subjected to a vibration force over a period of time, cracks or voids could be developed within the material and they would negatively impact the expected performance of the material. Lastly, thermomechanical aging refers to the effects on the material when subjected to a combination of both thermal and mechanical aging mechanisms at the same time. This aging mechanism is commonly found in energetic materials used in air-launched munitions when subjected to rapid pressure and temperature changes. Aging limits the service life of such munitions, as defined by their flight hours.

The current study subjects are 105 mm recoilless munitions with a fixed cartridge and two different natures, M323 High Explosives (HE) and M326 High Explosives Plastic – Tracer (HEP-T). These munitions were designed to be used on the land environment and at a short

range to engage in anti-armour combat. Based on the available records (US Technical Manuals, 1977), they contain the following energetic materials listed in Table 1.

Table 1. Current Study Energetic Materials (US Technical Manuals, 1977)

Ammunition Components	M323 HE Nature	M326 HEP-T Nature
Projectile	TNT, Comp B	Comp A-3
Fuze	Tetryl, Lead Charge	Tetryl, Lead Charge
Propellant	M10	M10
Tracer	Not Applicable	Unknown

The study focus of the present work is on the chemical aging effects in the ammunition. Based on historical records and visual inspection, these munitions have been in storage for over 70 years, and they showed minimal signs of environmental deterioration. Thus, the mechanical and thermomechanical aging effects are believed to have minimal impacts on the munitions.

1.4.1 Chemical Aging of Propellant

There are three principal types of gun propellants based on their chemical composition. They are known as single-based, double-based and triple-based propellants. Single-based propellant contains nitrocellulose (NC) as the major component. Double-based propellant contains NC and is mixed with nitroglycerine (NG). Lastly, triple-based propellant contains a mixture of NC, NG and nitroguanidine (NQ). (Akhavan, 2011) Within these three types of propellants, NC is a common ingredient and has been studied thoroughly for its degradation due to aging and exposure to heat.

NC is produced via the use of nitric acid and sulphuric acid to substitute the targeted hydrogen atom in the cellulose material with the NO_2 group. This process is known as nitration. (Akhavan, 2011) While the details of this process will be discussed at a later section, the resulting product, NC, from the nitration process can decompose at ambient temperature which impacts the long-term stability of the material. This slow decomposition of NC is referred to as de-nitration which refers specifically to the process by which the NO_2 group breaks away from the oxygen atom within the cellulose structure (represented as R), shown in Equation 1.

Equation 1. De-nitration in NC (Lussier and Gagnon, 1996)

As with almost all chemical reactions, de-nitration requires an input of energy, known as the activation energy of the reaction. Different reactions have different activation energies. Through empirical studies of propellants stored at 25°C for 10 years, the decomposition mechanism has been identified as the de-nitration for storage of NC with exposures under 60°C. The value of 80 kJ/mol has been accepted as the activation energy. (NATO STANAG 4582, 2007) This low level of activation energy was believed to be attributed to the low binding energy in the O-N bond. When comparing this to a typical C-H bond, the binding energy of the O-N bond in Equation 1 is less than half of the C-H binding energy. As a result of the low activation energy, NC is sensitive to thermal exposures and de-nitration can occur at ambient temperature in storage. (Lussier and Gagnon, 1996)

The de-nitration of NC is a homolytic bond breaking reaction, in which both the products carry an unpaired electron in their outer valence shells. This is illustrated by the dots in Equation 1. The reaction further creates two highly reactive radical molecules, the decomposed nitric ester (RO) and the nitrogen dioxide (NO_2). Given their unpaired valence electrons, they will bond to the nearby organic molecules to gain stability, generating another radical in what is know as a propagation step. Subsequent reactions with oxygen and water at ambient conditions will create products that further catalyze the generation of more NO_2 , such as nitric acid. When the radical molecules bond to oxygen or water molecules forming other nitrogen species, they will release additional heat as a by-product from the exothermic reaction. This additional heat would back feed into the de-nitration reaction due to its thermal sensitivity and create more radicals. This is a self-sustained and auto-catalyzed reaction. It could lead to excessive heat buildup in a localized region overtime inside the NC and significantly increases in the decomposition rate. The ultimate consequence of de-nitration is self-ignition. (Druet and Asselin, 1988)

Stabilizers are added during the manufacturing process of propellants to ensure a stable service life of the NC. The purpose of the stabilizers is to remove the nitrogen dioxide radicals by bonding with them. This eliminates the subsequent propagation reactions of NO_2 radicals which limits the formation of other nitric derivatives. Stabilizers can only stop the auto-catalyzing nature of de-nitration when they bond to the nitrogen dioxide radicals and prevent further exothermic reactions. (Lussier and Gagnon, 1996) However, the inherent de-nitration of NC persists, and stabilizers can only prolong the service life of NC while an adequate quantity lasts. Based on commonly used stabilizers, diphenylamine (DPA) and ethyl centralite (EC), the

current Canadian approach assumes a constant activation energy and constant rate of reaction for temperatures below 60°C which corresponds to the CFAD magazine storage condition. Thus, the lifetime of NC can be estimated using the Arrhenius equation, shown in Equation 2. (STANAG 4582, 2007; AOP48, 2008; Miles, 1972) The Arrhenius equation can be used to estimate the kinetic rate of the reaction (K) from an identified reaction mechanism which represented by the activation energy (E_a) and the reaction temperature (T). While the Arrhenius constant (A) is determined empirically, the gas constant (R) is known.

$$K = Ae^{\frac{-E_a}{RT}}$$

Equation 2. Arrhenius Equation

The lifetime in storage could be predicted using the mathematical model on the rate of reaction and activation energy. However, the actual decomposition of NC with exposure to operational environment and temperature fluctuation has not been taken into consideration. Therefore, the stability of NC could be misrepresented by accepting the constant rate of reaction assumption. The Canadian climate zone fits into the NATO A3 intermediate category which can see temperature ranges between 28°C to 39°C during the summer in ambient conditions. (AECTP 230, 2009) However, overseas deployment could expose propellants to temperatures as high, or beyond, 71°C inside shipping containers and in hot climate conditions (Netherland Public Prosecution Office, 2020). Previously deployed and returned munitions from Afghanistan were noted with an abbreviation “TFA” which stands for Task Force Afghanistan in their lot numbers. The purpose of such abbreviation is to highlight the ammunition operational exposures, and to signal the priority to consume in the inventory management. Higher

temperature will increase the reaction rate which will increase the consumption of stabilizers. To prevent the catastrophic consequence of self-ignition due to depletion of stabilizers in propellants, a munition health surveillance program has been developed to monitor periodically the level of remaining stabilizers in the propellant. Based on the percentage of the remaining stabilizers, the propellant is assigned to a service life and subjected to another re-assessment at the end of the assigned life. (Lussier and Gagnon, 1996)

The current study subjects contain the M10 propellant based on known records (US TMs, 1977). M10 propellant is a single base propellant, and it consists of 98 % NC, 1 % DPA, and 1 % potassium sulfate (Kirchner et al, 1993). According to the Munition Accident Database (MADx), two magazine fires in the US were reported in 1998 and 2007. They were attributed to M10 propellant in storage with unknown age and history. (MSIAC MADx, 1998; MSIAC MADx, 2007) The M10 propellant contained in the current subject munitions was more than 70 years old, and the munition surveillance program ceased in 2015. While the percentage of remaining stabilizers in the propellant was not tested, it was assessed as a high risk to continue to store the munitions in their original fix-cartridge configuration due to the age of the propellant and lack of stabilizer confirmation. Therefore, the propellants were separated from the projectiles for immediate disposal and have been excluded from this study.

1.4.2 Chemical Aging of Energetic Materials

The current research subject munitions contain TNT, Comp B, and Comp A-3 in the projectiles and lead charge and tetryl in the fuze section. While the exact chemical compound of the lead charge is unknown, it is presumed to be a mixture of lead azide and lead styphnate. Lead styphnate was used as the primary ignition composition due to the high volumes of high

temperature gas it produces, and lead azide was widely used in detonators because of its readiness to undergo deflagration to detonation transition and its high capacity to initiate secondary explosives. (Akhavan, 2011) TNT and tetryl are pure explosive compounds while Comp B and Comp A-3 refer to formulations of explosives. According to the current standard, Comp A-3 consists of 90.8% RDX and 9.2% polyethylene; and Comp B consists of 59.5% RDX, 39.5% TNT and 1% wax. (NATO AOP 26, 2011) Due to the complicated design of the fuzes and the sensitivity of primary explosives contained within, it was assessed as a high risk to dismantle the fuze. Therefore, the lead charge and tetryl have been excluded in this study. Thus, this study will be focusing on the TNT, Comp B and Comp A-3.

As seen in the previous section, temperature plays a significant role in terms of the decomposition rate of reaction. Even at room temperature, de-nitration would still occur in NC. In comparison to the propellant, the explosives contained in the subject munitions are commonly known to be more stable with respect to thermal exposure in ambient conditions. This common understanding of explosive stability could be attributed to explosives having a higher activation energy than NC. Notably, the activation energy for NC stored at ambient condition is approximately 80 kJ/mol (STANAG 4582, 2007; AOP48, 2008) while the activation energy for a primary explosive such as lead azide is 160 kJ/mol. (Akhavan, 2011) The activation energies for the remaining explosives are listed in Table 2. To predict the decomposition of the explosives, a common approach is to use an accelerated aging method to simulate the storage conditions under ambient conditions by using an elevated temperature for a shorter and specific period of time. This method uses the Arrhenius equation of temperature dependency and assumes the material decomposition reaction does not change with respect to

temperature, in which the activation energy will remain constant. (Gorzynski and Maycock, 1974) However, the inaccuracy of this method lies in the activation energy values listed in Table 2, and the assumption that the decomposition mechanism remains unchanged with respect to different temperatures. The values in Table 2 are the known activation energies for the rapid initiation of explosives, and they do not necessarily represent the activation energies of the long-term decay mechanisms in ambient conditions.

Table 2. Activation Energies of the Explosives and NC

Ammunition Component	Energetic Materials	Activation Energy (kJ/mol)
Cartridge Case	NC (under 60°C)	80
Fuze	Lead Azide	160
	Lead Styphnate	184
	Tetryl	217
Projectile	TNT	222
	RDX	199

(Akahavan, 2011; NATO STANAG 4582, 2007; Maksacheff and Whelan, 1986)

Previous explanations by Lussier and Gagnon on NC de-nitration were attributed to the low binding energy between the O and N atoms at ambient conditions, resulting in low activation energy. (Lussier and Gagnon, 1996; Bohn, 2017) This binding energy refers to the energy required in order to break the bond. However, it only forms part of the activation energy. As discussed by Bohn, beside the known thermal cleavage of de-nitration, there are two other decomposition mechanisms at low ambient temperatures for NC. They are de-nitration by hydrolysis and the cellulose chain breakage by hydrolysis. These three distinctive

mechanisms have different activation energies respectively. However, the overall effect of actual NC decomposition is a combination of these mechanisms; the activation energy of 146 kJ/mol is obtained for temperatures between 60°C and 90°C, and the activation energy 86 kJ/mol is obtained for temperatures below 60°C. (Bohn, 2017) The value of 80 kJ/mol is selected based on a conservative approach and published in NATO standards. (STANAG 4582, 2007)

When compared to explosive decomposition mechanisms, the decomposition rate would be relatively small. This is based on studies using live samples from various conflicts which have reported minimal changes and no impact to the safety of the material. (Geneva International Centre for Humanitarian Demining, 2019; Simoens and Lefebvre, 2024). However, as long as the temperature is above absolute zero, the decomposition reaction would continue to occur to some extent. (Cooper, 1996) The current study has the potential to investigate the impact of individual decomposition mechanisms at low temperature with respect to TNT and RDX which are the energetic materials contained in Comp B and Comp A-3.

1.4.3 Chemical Aging of TNT at Ambient Condition

The current understanding of TNT stability is derived from its parent structure. When compared to NC which has a polymer chain structure, TNT has a ring structure from toluene which contains a benzene ring and is known for its stability, as illustrated in Figure 4 below.

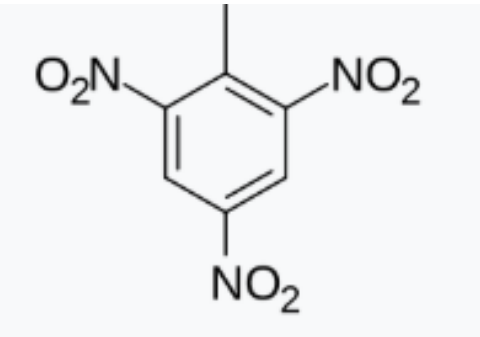

Figure 4. TNT structure (Wikipedia Image, 2025)

The stability of benzene is due to the resonance effect. As pointed out by Spice, the resonance effect is referring to the two equally possible and equivalent structures of molecule bonding. The actual structure is a hybrid version of the variants. (Spice, 1964) In addition, the six-electron ring provides an additional 'aromatic' stabilization based on the distribution of bonding and antibonding orbitals.

However, unlike NC in which the de-nitration inherently occurs, this process has a negligible effect on the TNT service life. Instead, the 'decay' in TNT is attributed to by-products formed during the manufacturing process. TNT is produced from toluene through nitration using nitric acid and sulphuric acid. During the process, TNT isomers and other undesired products such as dinitrotoluene (DNT) are removed using purification. Nonetheless, small amounts of them can remain as impurities and impact the melting point of TNT as a finished product. Pure TNT has a melting point around 80.7°C. (Akhavan, 2011) However, depending on the quantity of impurities that remains, the melting point could be suppressed (Wilson, 1985), and the melting of TNT could occur during the service life of the material. Repeated melting and cooling can produce localized low-melting regions in which impurities are concentrated in a similar process to that used constructively in zone refining. (Zhang et al, 2018) In the current

study application, the impurities decrease the melting point of TNT which cause the TNT to melt in localized areas. The liquified TNT allows the impurities to migrate and concentrate during thermal cycling and re-crystallization. As a result, the melting point would be further supressed due to increasing concentrations of impurities at the localized region. This is known as TNT exudation, and it was a common phenomenon that had been reported in munitions manufactured in the early 1920s when the production quality of TNT was low. (Voigt, 1983) TNT exudation in ammunition, except where the design allows, is considered as unsafe and non-suitable for service. (MSIAC, 2020) In the current study, TNT exudation is not expected due to mild climatic storage conditions experienced by the munitions. The mild climatic exposure can be suggested by the fact that the M10 propellants which they contain have not self-ignited despite their age.

Studies using various methods and different aged samples have attempted to determine the mechanism of TNT decomposition in ambient conditions, and their related serviceability with respect to aging. However, they have not reached a consistent conclusion. Using a computational model, the thermal decomposition of TNT is postulated by Cohen et al. at room temperature (25°C). This mechanism is known as the C-H alpha Attack, illustrated in Figure 5.

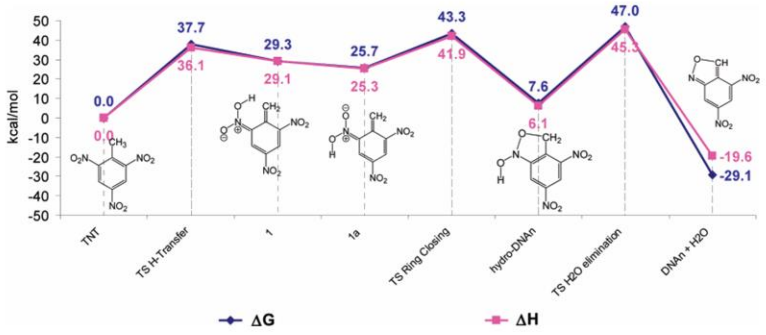

Figure 5. Proposed TNT Decomposition at Room Temperature (Cohen et al, 2007)

Cohen et al.'s approach is based on a purely unimolecular degradation mechanism, and it does not consider the impurities involved within TNT and the intermolecular relationships such as hydrogen bonding and crystal structure. The proposed activation energies for the molecular transformation are strictly related to the bond dissociation energy. The hypothesized C-H alpha attack mechanism has not been observed in various simulated and actual aging studies.

Using unknown age and service history of decanted TNT from old munitions, another study conducted by Ahmad et al. reported a lower activation energy of 203.4 kJ/mol when compared to a serviceable TNT at 217.78 kJ/mol. Their study implied aging had increased the sensitivity of TNT to friction and shock based solely on the difference of activation energies and without conducting sensitivity testing. The change in activation energy with respect to aging was believed to be an ingress of moisture, impurities creating voids, etc. (Ahmad et al, 2016) However, the reported change in activation energy is within 10% margin of the literature value of 222 kJ/mol in Table 2. In addition, the reference serviceable TNT was reported to have a lower melting point than the aged sample which indicates that the quality of TNT might be different. A similar study using different qualities of TNT conducted by Pouretedal et al. concluded that the activation energies can be different according to the purity of TNT. Notably, their study predicted a lifespan of approximately 477 days in an aluminium container for a military graded TNT based on 100 % mass loss at 25°C. (Pouretedal et al, 2017) However, their study was based on the kinetic parameters obtained through a simulated aging at an elevated temperature above the meting point of TNT which does not necessarily represent the long-term decay mechanism of TNT at ambient conditions. Their study result also contradicts other life study results which are based on actual remnants of war.

A different approach using the gas evolution in an accelerated aging study found that the storage life of TNT to be around 37 years at 55 °C based on the maximum acceptable volume of gas evolved at 2 mL from a 5 g sample. However, the study also pointed out that different acceptable criterions could result in different life limitation assessment. The aged TNT was noted to decompose at lower temperatures which indicated a change in stability, but the reaction mechanism and gas composition had not been determined. (Narang et al, 1993)

Using WWI samples collected from the Belgian EOD team, Simoens and Lefebvre concluded that there was no significant increase in sensitivity with aging and no significant difference in energetic content compared to the unaged materials. (Simoens and Lefebvre, 2024) Their result is mirrored by a US army study, in which they investigated the possibility to reuse previous TNT booster charges in the new 155 mm calibre projectile productions. Driven by a reduction of cost initiative on the reuse of energetic material in 1991, TNT samples from 1969 and 1944 era munitions were compared with recent manufactured samples in 1991 with respect to their performance and sensitivity. The study found minimal changes of the aged TNT with respect to aging and subsequently recommended the re-use of those old TNT boosters in new ammunition production. (Hopewell and Betts, 2000)

In summary, the parent structure of TNT brings inherent stability as an energetic material which establishes the general understanding on the longevity of the material. However, impurities from the manufacturing process pose a risk to lower the melting point of TNT and reduce its serviceability in hot climate zones. The aging of TNT has been studied using various methods and approaches. However, no consistent conclusion has been made regarding the serviceability of the material in relation to aging.

1.4.4. Chemical Aging of RDX at Ambient Condition

Similar to the common understanding on TNT stability, RDX is another well-known explosive that is stable in ambient conditions. While RDX lacks the benzene structure in TNT, as shown in Figure 6, it shares a similar six-member ring as TNT. Unlike TNT which has a melting point at 80 °C, RDX has a melting point at approximately 203 °C. (Miles, 1972) Thus, during the normal logistic and operational life cycle, melting is not expected.

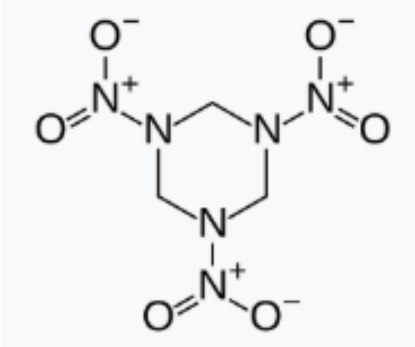

Figure 6. RDX Structure (Wikipedia Image, 2025)

There are two observed polymorphs of RDX under ambient conditions. They are known as alpha and beta RDXs. The polymorphism of RDX is referring to the six-member ring structure in which there can be an existence of multiple different molecular structures of the same molecule known as conformations under various conditions. The alpha-RDX is referring to the chair conformational structure with two nitro-groups in the axial positions. While the beta-RDX is also in the chair conformational structure and all nitro-groups in the axial positions. Both the alpha-RDX and beta-RDX are stable at ambient conditions. (Brady et al, 2017) However, the beta-RDXs would convert to the alpha form in the presence of excessive alpha-RDX. (Miles, 1972) In addition, the activation energy for the interconversion between the beta-RDX and

alpha-RDX are less than 5 kCal/mol (21 kJ/mol) while the activation energy of RDX is in the order of 50 kCal/mol (209 kJ/mol). (Brady et al, 2017; Miles, 1972) Thus, only the alpha-RDX is considered in this study.

Experimental work by Miles characterized the three phases of RDX decomposition based on the heating rate data obtained at discrete temperature ranges during a Differential Thermal Analysis (DTA). The three phases of RDX decomposition are known as induction, acceleration and decay. The induction period described the input of energy to reach the melting point of RDX. Miles demonstrated that when maintained at a constant temperature of 192 °C which is below the melting point of RDX, and in excess of 6.5 hours, it has no measurable chemical rate changes. The induction period followed by the acceleration period, in which the heating rate rapidly increased in the liquified stage of RDX to reach the self-ignition point. The decay period is the deceleration of the heating rate on the DTA. In addition, the activation energy was found to be constant over these three phases of RDX decomposition at approximately 50 kCal/mol which is 209 kJ/mol. (Miles, 1972)

While the work of Miles focused on the decomposition of RDX above the melting point, the postulated three phases of decomposition based on the kinetic rate obtained experimentally mirrored the work done by Batten and Murdie. But Miles's conclusion on the induction period of RDX having no measurable chemical changes contradicted the work from Batten and Murdie. Batten and Murdie demonstrated that RDX would decompose below its melting point. The decomposition was believed to be dependent on the geometry and the weight of the sample due to sublimation and interaction with gaseous decomposition products. However, the actual mechanism was not determined. Three distinctive activation energies were

found to correlate with Miles's postulated three phases of decomposition for RDX. The activation energies for induction, acceleration and decay decomposition phases are 49 kCal/mol (205 kJ/mol), 43 kCal/mol (180 kJ/mol), and 62 kCal/mol (259 kJ/mol) respectively in the temperature range from 170 - 198 °C. (Batten and Murdie, 1969) Another long-term aging study conducted on the explosives under the influence of deep space exposures revealed that RDX had a 1 % weight loss in 10 years due to sublimation. This study is based on accelerated aging which represents 10 years of storage at 66 °C and at near vacuum pressure (10^{-6} Torr). (Gorzynski and Maycock, 1974). The purpose of this study was to determine the suitability of the material to be used on a spacecraft. RDX was ruled out due to the mass change overtime. However, this study does not consider the serviceability of RDX in ambient conditions.

Additionally, the activation energy for RDX sublimation was found to be 114 kJ/mol by Gershanik et al. at 60 °C. It further estimated the lifetime of RDX as a 20-micron diameter particle at room temperature to be four months based on experimental molecular diffusion rate and vapour pressure. (Gershanik et al, 2010) However, Gershanik et al. work was primarily focusing on the security related applications in which explosive residuals can be detected from people and their belongings if they have been involved in preparation or transport of explosives. Their lifetime prediction does not have the same applicability as material aging study in ambient conditions.

To summarize, the longevity of RDX in storage is attributed to its high activation energy for decomposition. Unlike the low melting point of TNT, RDX has a high melting point which is approaching its ignition temperature and is considered unsafe to melt. (Akhavan, 2011) RDX has two polymorphs under ambient conditions. However, while both polymorphs are

thermodynamically stable, alpha-RDX is the dominant form and hence it will be the sole focus in this study. Studies demonstrated that, RDX can decompose below its melting point. While the actual mechanism remains unclear, experimental data suggested three phases of decomposition with distinctive activation energy differences. However, these decompositions occur at an elevated temperature which is above the ambient conditions. (Batten and Murdie, 1969) Other studies have attempted to study the aging effect of the RDX for a different application, and their studies have inconsistent results.

1.5 Manufacturing of Propellant and Explosives

The synthesis of energetic materials often uses a chemical process known as nitration. Nitration introduces one or multiple nitrogen dioxide groups (NO_2) into an organic molecule (Akhavan, 2011). This nitration process is applicable to both propellant and explosives. There are three commonly used types of nitration. Namely, they are C-, N-, and O-nitration. They are defined by the atom to which the nitrogen dioxide groups are attached. Nitrocellulose (NC) is synthesized using O-nitration because the nitrogen dioxide group is attached to the oxygen atom (Akhavan, 2011). The current research subject munitions containing TNT which is synthesized using C-nitration and RDX which is synthesized using N-nitration.

While the chemical synthesis process is known as nitration, the actual chemical mechanism of nitration involves the use of sulfuric acid (H_2SO_4) to generate the nitrating agent and electrophilic substitution to replace the hydrogen atom with the nitrogen dioxide group in the molecule. The organic molecule is first mixed in solution with nitric acid (HNO_3) and sulfuric acid. In theory, the use of sulphuric acid could be bypassed since the nitric acid provides the nitronium ion (NO_2^+) as the nitrating agent for the nitration reaction. The organic molecule

could be nitrated by the sole use of nitric acid. Nitric acid in high concentration will undergo self-dissociation according to Equation 3, and it will generate the nitronium ion (NO_2^+) by itself. However, the yield of the nitronium ion is extremely small. Once the nitronium ion is expended by nitration, a water molecule is generated as a by-product. (Gillespie et al, 1948)

$$3HNO_3 \rightleftharpoons NO_2^+ + NO_3^- + HNO_3,H_2O$$

Equation 3. Self Dissociation of Nitric Acid (Gillespie et al, 1948)

The addition of water molecules by the above reaction will lower the concentration of the nitric acid, and further, the nitronium ion generation in Equation 2 will be prevented by the water molecule acting as a base. Instead, a different chemical equilibrium will subsequently be established, as shown in Equation 4. Nitric acid will donate a proton to the water molecule. (Gillespie et al, 1948)

$$HNO_3 + H_2O = NO_3^- + H_3O^+$$

Equation 4. Nitric Acid and Water Equilibrium

In practice, the mechanism of continuous generation of the nitronium ion requires the presence of the sulfuric acid. The purpose of the sulphuric acid is the protonation of the nitric acid to generate the nitronium ion. (Kogelbaur et al, 2000; Westheimer and Kharasch, 1946) Sulphuric acid is a stronger acid than the nitric acid. As such the nitric acid will act as a base to give up the hydroxide ion (OH^-) and producing a nitronium ion (NO_2^+) while the sulphuric acid will produce the proton (H^+). (Tro, 2008) Once the nitronium ion is expended by nitration, the hydroxide ion will accept the proton from the sulphuric acid, as shown in Equation 5. However,

the strong acidity nature of the sulphuric acid will remain, and it will couple with the high concentration to donate an additional proton to the hydroxide ion forming a H_3O^+on the right-hand side of Equation 5. (Gillespie et al, 1948) Additionally, others have also reported that using other strong acids such as boron trifluoride (BF_3) and hydrogen fluoride (HF) have a similar effect as sulphuric acid on nitration. (Gillespie et al, 1948) Freizel pointed out that the formation of nitronium ions from mixtures of nitric acid and sulfuric acid is based on the excessive molar ratio of sulfuric acid as shown in Equation 5.

$$HNO_3 + 2H_2SO_4 = NO_2^+ + H_3O^+ + 2HSO_4^-$$

Equation 5. Formation of Nitronium Ion (Gillespie et al, 1948)

Other researchers have shown that, based on the variations of organic materials and reaction temperatures, the required concentration ratio between nitric acid and sulfuric acid varies differently from Equation 5. This variation of ratios also has an impact on the product yield in addition to the reaction temperature and the speed of stirring (Kroger and Fels, 2000; Rahaman et al, 2009)

Another chemical aspect of the nitration process is the substitution of the nitronium ion and the elimination of the proton from the organic molecule. There are two types of chemical substitution. They are known as electrophilic and nucleophilic substitutions. Both substitutions have similar mechanism that involve transfer of electrons and forming bonds, however they differ based on the ability to accept or donate electrons in the attacking group. Nitration is an electrophilic substitution due to the ability of the nitrating agent (NO_2^+) to accept an additional electron, while the molecule has one less valence electron. On the molecular level, the

nitronium ion (NO_2^+) from the nitric acid acts as the nitrating agent to bond to the organic molecule at the C, N, or O atom by forming an intermediate molecule. (Olah, 1970) Subsequently, the organic molecule eliminates a proton (H^+) and thus it completes the substitution reaction.

In short, nitration is the main process to synthesize propellants and explosives from organic molecules. Nitration involves the use of nitric acid and other strong acids such as sulphuric acid. The purpose of that strong acid is the protonation to the nitric acid which would act as a base medium to generate the nitronium ion. Nitronium ion is used as the nitrating agent in nitration. The synthesis is an electrophilic substitution of the nitronium ion to the organic molecule.

1.5.1 Manufacturing of TNT

TNT was first prepared by Wilbrand in 1863. The military application of TNT started prior to WWI as a replacement to picric acid and had become a standard explosive to all armies during WWI. (Akhavan) TNT was synthesized from toluene using C-nitration. Modern production of TNT using nitration is broken down into various steps in which toluene is first nitrated to mononitrotoluene (MNT) and nitrated again to obtain TNT. (Gawrysiak and Jarosz, 2021) However, the aromatic nature of toluene raised challenges regarding positional selectivity of the nitronium ion during the initial nitration. The ortho, para and meta nitration positions on the toluene molecule would later impact the quality of the finished product by forming asymmetrical TNT isomers, as shown in Figure 7. (Kroger and Fels, 2000)

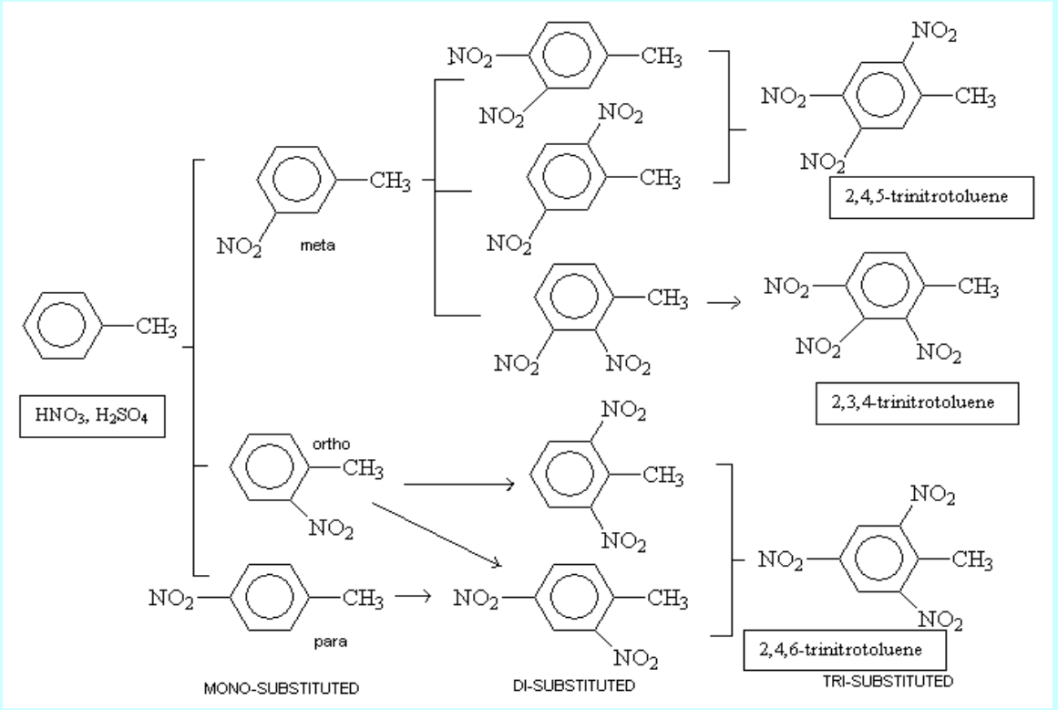

Figure 7. Nitration from Toluene (University of Bristol, 2025)

In addition to the asymmetric TNT isomers shown in Figure 7., Muraour and Munroe pointed out that other impurities could be formed as a result of the nitration process. (Muraour and Munroe, 1924) However, the primary concern of TNT impurities is the suppression of melting point which then causes exudation. Using commercial graded TNT and doping with 2,3,4-TNT and 2,4-DNT, Wilson noted that in localized small areas, where the impurities are dominant, the melting point could be as low as 37 °C. (Wilson, 1985) The subsequent re-crystallization of the exudated TNT during thermal cycling has an irreversible effect which the crystalline structure would grow omni-directionally. The re-crystallized TNT exudate also has a weak and brittle nature which has been further implicated in premature in-bore detonations in artillery accidents. (Wilson, 1981) Gawrysiak and Jarosz pointed out that the finished TNT could contain as much as 4 - 4.5 % of asymmetrical TNT isomers and other associated impurities while the

available qualitative criteria to assess is based solely on the melting point of the finished product. (Gawrysiak and Jarosz, 2021)

As a result, the manufacturing of TNT focuses mainly on the elimination of TNT isomers and their impurities. Early methods for the purification of TNT have been captured by Muraour and Munroe and are known as the “sellite” process. The sellite process uses a sodium sulfite salt (Na_2SO_3) and hydrochloric acid (HCl) solution to target the asymmetrical TNT isomers by replacing the nitro group (NO_2) in the ortho position to another nitro group with a hydrogen sulfite (HSO_3) group, as shown in Figure 8. (Muraour and Munroe, 1924) The mechanism is known as a nucleophilic substitution in which the attacking hydrogen sulfite group is a nucleophile molecule and the corresponding nitro group is released. The subsequent sulphonated product is soluble in water and can be washed out by water. (Hariri et al, 2019) This dissolved impurity mixture is known as the red water due to the colour of the solution. However, the sellite process was banned in the early 1980s due to the environmental toxicity of the red water. Subsequent purification methods using ammonium sulfate and other compounds have been studied by other researchers. (Mundy and Spencer, 1981) The current study subject TNT is manufactured in the 1950s and is believed to have been purified using the sellite process.

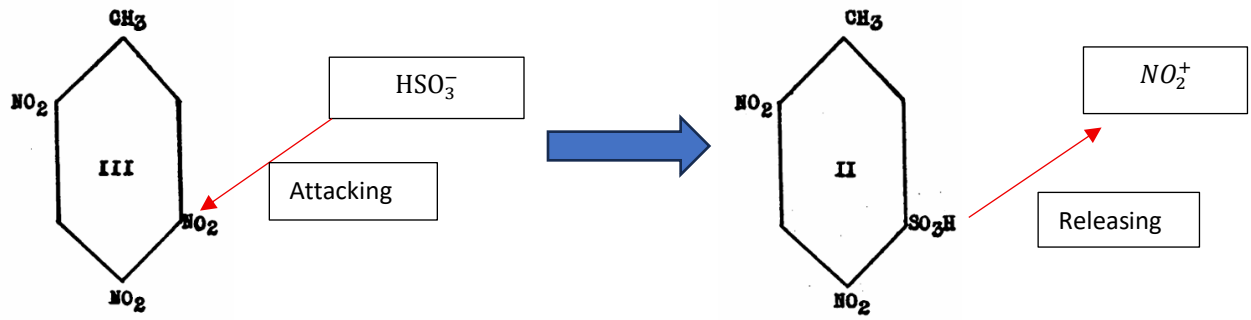

Figure 8. Sellite Purification Process (Muraour and Munroe, 1924)

1.5.2 Manufacturing of RDX

This chemical composition was known by various aliases in different countries since its development was held in secret during WWII. These circumstances also resulted in multiple synthetic approaches. It was referred to as the Cyclonite in the US, Hexogen in Germany, and T4 in Italy. (Agrawak, 2010) Today, it is more commonly known as the Research Department Explosive (RDX), named after the Research Department of the Royal Arsenal in Woolwich, UK. The discovery of RDX was linked to medicinal use by Henning in 1899. (Ahkavan, 2011) However, due to the inefficient yield and the cost to mass produce, the explosive potential of RDX was not realized until WWII. There are three known approaches to synthesize RDX. They are known as the Direct Process, McGill Process, and the Bachmann Process.

Under the Direct Process approach, hexamethylenetetramine (hexamine) was directly nitrated in the presence of high concentration nitric acid at a high molar ratio of nitric acid to hexamine to form RDX. The mechanism of nitration was first proposed by the British Research Department and was assumed to be a complete and symmetrical disassembly of the hexamine and re-assembly of the subsequent product to form RDX, as shown in Figure 9. The proposed mechanism was regarded as a fact without conclusive evidence at that time. It was based on an impurity compound, known as cyclonite oxide, found after evaporation in the post nitration phase. The reaction intermediate from the symmetrical disassembly of hexamine was never isolated. (Vroom, 1945)

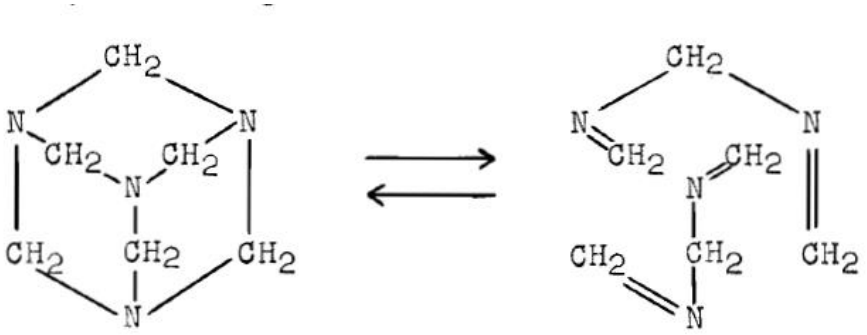

Figure 9. Disassembly of Hexamine (Vroom, 1945)

In 1941, Linstead hypothesized that the six-member ring structure of RDX was inherited from a cascade of continuous N – N nitration from hexamine by nitric acid, as shown in Figure 10. Linstead's ring hypothesis was circulated in secrecy during wartime and was reviewed in Vroom's kinetic study on the mechanism of direct nitration of hexamine post war. An intermediate compound, known as PCX, was isolated and identified from Linstead's proposed mechanism by Vroom in 1947. (Vroom, 1945) This has been the accepted mechanism for the Direct Process to manufacture RDX.

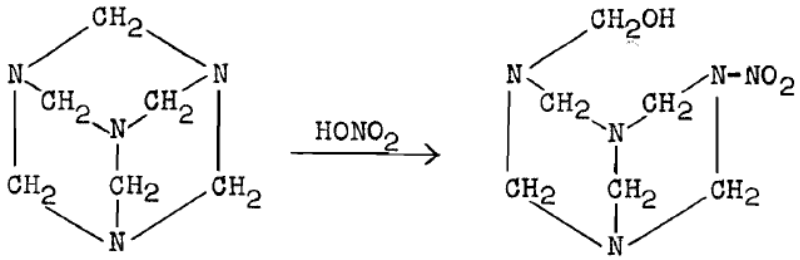

Figure 10. Linstead's Ring Hypothesis (Vroom, 1945)

Other attempts were also made to synthesize RDX and improve the product yield. Driven by the lack of hexamine, McGill University had developed another method to condense

formaldehyde and ammonium nitrate to form RDX solid without the use of Hexamine. (Edward, 1942) This was later known as the McGill process. In 1949, a new method was proposed by Bachmann and Sheehan, to synthesize RDX using hexamine, formaldehyde and ammonium nitrate. Their method achieved the highest product yield and has been widely regarded as the modern day RDX synthesis process. (Bachmann and Sheehan, 1949) This process is also referred to as the combined process since it combined both the direct process and McGill process. The current subject munition is presumed to have been synthesized using the Bachmann method.

1.5.3 Formulation of Composite Explosives

During the lifecycle of an ammunition, it is subjected to various conditions that could impact the stability and serviceability of the explosive, such as thermal cycling and logistical vibrations. Additionally, the inherent nature of the energetic materials would complicate the material's stability and serviceability in storage, transportation, and military applications. The result of these combined factors had driven the development of composite explosive using organic polymers or other binding materials to improve the mechanical properties and to reduce the sensitivity. (Szala, 2021) In the current study subject, RDX as a chemical has a crystal solid form in ambient conditions, (Bachmann and Sheehan, 1949) and it is very sensitive to initiation by impact and friction. (Akhavan, 2011) In practice, RDX crystals are coated with wax to reduce its sensitivity to initiation, and the process is known as desensitization. (Akhavan, 2011; Szala, 2021) The purpose of desensitization is to use wax to absorb and dissipate the heat generated when the crystals rub against each other and to absorb the heat by the endothermic melting of the wax prior to initiation. (Szala, 2021) The coating process is achieved by adding molten wax to a mixture of water and RDX crystals during rapid stirring at above the melting point of the

wax. After a period of stirring, the crystals would be coated with the wax to form small grains. Once stirring is stopped, they will settle rapidly to the bottom of the container. (Eyster and Weltman, 1945) Upon drying, the coated RDX could be pressed into shells.

Manufacturers tend to protect the key information on the components of the explosive by withholding the full physio-chemical specifications of explosives. This is due to the strategic nature of the information on explosives used, such as the wax used in desensitization process. Nonetheless, the availability of the raw material within the geographical location of the country often gives indication to the components used within explosive manufacturing of that particular country. For example, palm wax is used in equatorial countries due to the abundance of palm trees in those regions. (Szala, 2021)

Composition B (Comp B) is a type of composite explosives that contains 59.5 % RDX, 39.5 % TNT and 1 % wax by weight according to the current standard. (NATO AOP 26, 2011) Historically, the ratio of Comp B varies between RDX, TNT and the desensitized wax; and it was known as the cyclotol during WWII. (Akhavan, 2011; Szala, 2021) The development of Comp B is believed to be driven by the castability of TNT which has a relatively low melting point at approximately 80 °C and the relatively high explosive output of the RDX. During WWII, RDX was not used as a main filling in the UK, but instead it was added to molten TNT to increase the explosive power by casting into shells and bombs for military applications. (Akhavan, 2011) However, it has been pointed out that the settling of RDX crystals in the molten TNT is unavoidable during the casting process which results in regions with different RDX:TNT ratio during solidification. Such differences in homogeneity of the composition may be deemed unacceptable in certain applications. (James, 1965)

Composition A-3 (Comp A-3) is another type of composite explosive developed by the US, and it consisted of 90.8 % RDX and 9.2 % polyethylene wax according to the standard (NATO AOP 26, 2011). The development of Comp A-3 originated from the need to find a substitute to replace the beeswax used by the British in their RDX and beeswax mixed semi-plastic explosives at the end of WWII. (Eyster and Weltman, 1945) While effective, the beeswax is a natural product that suffers from low melting point at approximately 68 - 70 °C. (Szala, 2021) The effect of the low melting point would cause the sensitivity of the explosive to increase since the effective coating will be reduced once the wax melts. Previous investigation on suitable wax replacement realized that the physical properties of petroleum waxes could be a good desensitizer for RDX (Eyster and Weltman, 1945), and polyethylene was chosen according to later studies.

In conclusion, the formulation of composite explosives is driven by the desire to reduce explosive sensitivity to initiation and to achieve higher energetic outputs. The current study subject munitions were manufactured in the US in the early 1950s, and they contain RDX and desensitized wax. Based on available standards, the desensitized wax used during manufacturing is believed to be polyethylene wax and sourced locally within the US.

Chapter 2 Methods

2.1 Demilitarization

The subject munitions were transported by CNR from Terrace, BC to the Canadian Force Ammunition Depot (CFAD) Dundurn. The demilitarization of the munitions was completed by the staffs at the CFAD Dundurn. Upon arrival, the munitions were immediately segregated and quarantined due to the uncertainty of the propellant stabilizer level. The cartridge case was removed via a cartridge case separator to extract the projectile, shown in Figure 11. The cartridge case separator uses hydraulic power to unseat the projectile from the cartridge crimping and thereby separating the cartridge and the projectile. (Cline, 2024)

Figure 11. Cartridge Separator (Cline, 2024)

The propellant was poured from the perforated cartridge case into a grounded anti-static discharge bag for temporary collection and storage. The collected propellant was later disposed via electrical initiation and open burning on a designated burn tray table. The primer remained in the empty cartridges. They were manually functioned via a percussion strike in a specially designed apparatus shown in Figure 12. Upon completion, the primer and flash tube

were hydraulically extruded from the cartridge case for separate disposal shown in Figure 13. (Cline, 2024)

Figure 12. Percussion Firing Stand (Cline, 2024)

The fuzed projectiles were repackaged into a 105 mm projectile standard package and re-purposed for the EOD training target ammunition for the CAF. A small number of the projectiles was sent to the Munition Evaluation and Testing Center (METC) Valcartier which subsequently performed the de-fuzing operation on the projectile.

Figure 13. Primer Puncher (Cline, 2024)

2.2 X-Ray Photography

The X-Ray imaging was completed by the staffs at the METC Valcartier. Prior to the de-fuzing operation, five rounds of each nature were X-rayed using a Linatron M3A linear accelerator at a 3 MeV energy level. The HE nature projectiles were divided into 3 sections, bottom, top and middle to accommodate the view of the X-ray photos. The HEP-T projectiles were divided into 2 sections. The projectiles were each photographed at 0°, 45°, 90° and 135°. A total of 12 X-ray photos for each project were obtained for HE nature, and 8 X-ray photos for each projectile for the HEP-T nature.

2.3 Material Extraction

The de-fuzing operation was conducted by the staffs at the METC Valcartier and on the explosive range. The setup consisted of an explosive safety barrier, a work bench, leaver arm, extension metal piping, and a solid metal weight shown in Figure 14. The projectile was secured on the work bench. The leaver arm was attached to the fuze through an adapter for the Point Detonating (PD) fuze, and a different adapter was used for the Base Detonating (BD) fuze. The extension arm was installed with the weight to maximize leverage and produce torque. A temporary ladder was set up to hold the weight via an electro-magnet. The initiation was done through releasing the electro-magnet to let the weight drop. Therefore, the gravitation force on the weight generated the torque to turn the fuze on the projectile. A stopper using lumber was placed at parallel level to the projectile to prevent over torquing from the leaver arm. (Brassard, 2024)

Figure 14. De-Fuzing of Projectile (Brassard, 2024)

The de-fuzed projectiles were photographed and sent to DRDC Valcartier for material extraction. The Comp B was extracted via heating the de-fuzed projectile to melt the explosives. A second sample of the Comp B and the Comp A-3 were extracted remotely using machining techniques to grind the energetic material inside the shell. The TNT samples were scraped from the booster after opening the packaging.

2.4 Analytical Testing

The extraction of the explosive samples was completed by the staffs at the DRDC Valcartier. Additionally, recently manufactured explosive samples from DRDC Valcartier were provided to assist in the investigation of the impact from the long-term ambient aging process. However, the focus of this paper will be on the explosive fillings from the 105 mm recoilless munitions. The detailed manufacturing information of each explosive sample is listed in Table 3. The DRDC samples were extracted from various munitions and stored in conductive plastic containers. Those containers are subsequently put inside ammunition metal cans which have been stored at ambient conditions. While the history of the previous environmental exposure

remained uncertain, they are presumed to have remained in ambient conditions since their manufacture date.

Table 3. Recently Manufactured Explosive Data

Explosive	Manufacture Date	Production Lot Number
Comp A-3	01-01-1997	RD-Grenade-01
TNT	26-10-2005	SNP 144/2004
Comp B	2005	DDP05L008-012

2.4.1 Mechanical Sensitivity Testing

The mechanical testing was completed by the staffs at the DRDC Valcartier. The friction sensitivity test was done in accordance with the UN Test 3, type b (i) using the Bundesanstalt fur Materialprufung (BAM) Friction Apparatus manufactured by Julius-Peters KG, Berlin, Germany. The apparatus had an extended loading arm with six different pre-determined positions to attach a weight. The friction force was estimated from a look-up table based on the position of the weight attachment on the loading arm and the weight itself. A volume of 40 mm^3 sample in powder form was measured by a cylindrical instrument and placed on top of a porcelain plate. The plate was then secured on the friction apparatus with the loading arm and the peg clamped onto the sample. The porcelain plate would move horizontally while the peg remained stationary, thus creating friction against the test sample. The sample response was based on the operator observation and is divided into no reaction, decomposition, ignition, crackling and explosion. The test result was assessed based on the highest increment at which no response was observed from six consecutive trials.

The impact sensitivity test was performed in accordance with the UN Test 3, type a (ii) using the BAM Fallhammer Apparatus manufactured by Julius-Peters KG, Berlin, Germany. The apparatus was capable of using a drop weight of 1, 5 or 10 kg. In addition, the drop height could be adjusted to 10, 20, 30, 40 and 50 cm. The combination of the drop weight and height represented the impact energy used during testing. A sample volume of 40 mm^3 was measured using a cylindrical instrument. The sample was placed between two vertical metal cylinders with a gap of 2 mm and was held in position by a rubber "O" ring. The weight held at specific height was then released remotely and collapses the gap between the two metal cylinders. The sample response was based on operator observation and was divided into no reaction, decomposition, and explosion. The test result was assessed based on the lowest impact energy at which at least one observed response occurred in six consecutive trials.

2.4.2 Electrostatic Discharge (ESD) Sensitivity Test

The ESD sensitivity test was completed by the staffs at the DRDC Valcartier. The ESD sensitivity was carried out with an ESD simulator manufactured by Franklin Applied Physics under ambient condition. The ESD simulator was designed to simulate the static electric energy output of the human body by varying the capacitance and resistance of the circuitry. The current test setup used a 5 kΩ resistor and a 2000 pF capacitor at 25 kV which represented an energy level of 0.625 J. The sample was placed in the Spaenaur nylon washer in an open sample cell configuration, and the sample had a volume of approximately 32 mm^3 based on the washer dimensions. The washer was glued to a metal plate which was placed in the holding fixture and the discharge needle was adjusted to its lowest position. The gap between the needle and

sample was approximately 0.5 mm. The reaction responses were divided into no reaction, ignition and detonation and were based on 10 consecutive trials.

2.4.3 Thermal Sensitivity Test

The thermal sensitivity test was completed by the staff at the RMCC. The thermal sensitivity test consists of Thermogravimetric Analysis (TGA) and Differential Scanning Calorimetry (DSC). This is achieved with the use of the Netzsch STA Jupiter F3 instrument with a silicon carbide (SiC) furnace and a type S sample carrier. The crucible was made of aluminium oxide and had a pierced lid. The crucible had a volume of approximately 85 µL and had a pierced lid. The choice of the lit was due to the potential volatility of the material while venting the excessive pressure during gas evolution from the explosive.

The TGA/DSC was completed in an argon atmosphere which was different from the commonly used nitrogen atmosphere. The intend of the inert protective gas atmosphere was to protect the machinery during the phase transition of the sample as the heat raises while the carrier gas is used to remove potential volatile products from the system.

A background run was completed using the empty sample crucible against the reference empty crucible. A sample of approximately 1 mg was weighed prior to placing in the crucible. The protective gas flow rate was set at 20 mL/min, and the carrier gas flow rate was set at 50 mL/min. All samples were flushed out by the carrier gas upon completion of the TGA/DSC run and prior to the next run.

2.4.4 Scanning Electron Microscopy (SEM)

The SEM was completed by the graduate students at the RMCC. The SEM was done by using a Quanta FEG 450 manufactured by the company FEI. A small quantity of the sample was placed on a 12mm diameter black carbon conductive sticker manufactured by Agar Scientific. The sticker was supported by an aluminium specimen mount with 0.5" slotted head and 0.125" pin which was manufactured by Ted Pella Inc.

Prior to placing the sample inside the SEM, the system was vented with nitrogen gas to operate the door mechanism and prevent the ingress of other undesired particles. The aluminium specimen was screwed down onto the mound in the SEM machine. A photo was taken prior to inserting the specimen into the SEM. This photo was later used to maneuver the electron gun to examine the particles on the specimen. After the insertion of samples and door closure, the specimen height was adjusted to achieve a working distance of 10 mm from the electron gun to the sample particles, and the system vacuum was set to "High". The spot size was set to 6. The SEM images were taken using various power levels and different dwell times under the secondary electron mode.

2.4.5 Gas Chromatography – Mass Spectrometry (GC-MS)

The GC-MS was completed by the staffs at the RMCC. The GC-MS was done by using the Thermo-Scientific ISQ 7000 Single Quadruple GC-MS system with the Al 1310 auto-sampler. The Restek Rtx-TNT column with 6 m x 0.53 mm x 1.5 µm was installed inside the system as the main column after an inert guard column. The purpose of the inert guard column is to ease the pressure gradient between the GC and the MS environment. The system was pre-calibrated

using existing standards at 1 ppm by single ion monitoring to confirm retention times, and the calibration standard analytes were prepared by serial dilution with acetonitrile to a concentration of 1, 10 and 100 ppb. The carrier gas used was helium and it was set at a standard constant rate of 1 mL/min. The injection chamber was heated to 240 °C. An inert liner was used to mix the carrier gas and the vaporized sample prior to injection into the column. The split injection method was used to bleed off some of the sample to waste at the split point before the column. The bleed off ratio was set at 10:1. This was done to improve the result resolution. An inert narrow column (0.1 mm) was used before the main column in the GC. The purpose of the inert column was to ease the pressure gradient between the vacuum environment of MS and the positive flow rate environment in the GC.

The main GC column diameter was 0.53 mm Wall Coated Open Tubular (WCOT) and an adapter was used to reduce the diameter to 0.25 mm to fit into the MS inlet. The carrier gas and the sample were both injected into the MS. However, the carrier gas would not impact the result since the ionization voltage was set to 70 eV. Various mass to charge ratios were used to introduce selectivity in order to obtain the desired results. The selected molecular ions were fed into the dynode electron multiplier to convert into electrical signal and display the results.

Chapter 3 Results

There are seven samples in total; two samples contain TNT, three samples contain Comp B and two other samples contain Comp A-3. These samples are distinguished by the following nomenclature method. The samples which are extracted from the 105 mm calibre recoilless munitions will be referred to as the "aged" samples. The samples which are provided by DRDC Valcartier will be referred to as the "recent" samples. The aged TNT sample is extracted from the booster and the aged Comp B is extracted from the main charge of the HE nature ammunition. Of note, two different methods of extraction were used to extract the Comp B and resulted in two different samples. They are noted as "aged (melt)" and "aged (machine)" for differentiation purpose. The aged Comp A-3 sample is extracted from the main charge of the HEP-T nature ammunition.

The detailed results are captured in the appendices for all the samples. Results that contain no measurable or insignificant changes will not be discussed in this paper and can be found in the appendices. However, this paper will focus on results that contain meaningful differentiation when compared to the literature data. Additional illustrations and examples will be employed to present the interpretation of the results in this chapter as well.

3.1 X-Ray Photography

The use of X-ray photography as a method of quality control is a common practice in the current munition manufacturing industry. The requirement for explosive charges is that they should form a continuous filling without cracks, fissures or failures to case or container bond. In general, the X-ray images of all samples conform to this requirement, as shown in Appendix A.

However, an abnormality was noticed in which various small black shadows occurred near the top region of all five HE nature projectiles which indicates lower density spots inside the round, as shown in Figure 15. and Figure 16. below. These projectiles contain the TNT booster and Comp B as the main filling. Two of these projectiles were later chosen to be de-fuzed and the explosive fillings were extracted for further analytical testing. Such data cannot be informative alone and cannot be examined in the extracted material since the extraction process would have destroyed such structures.

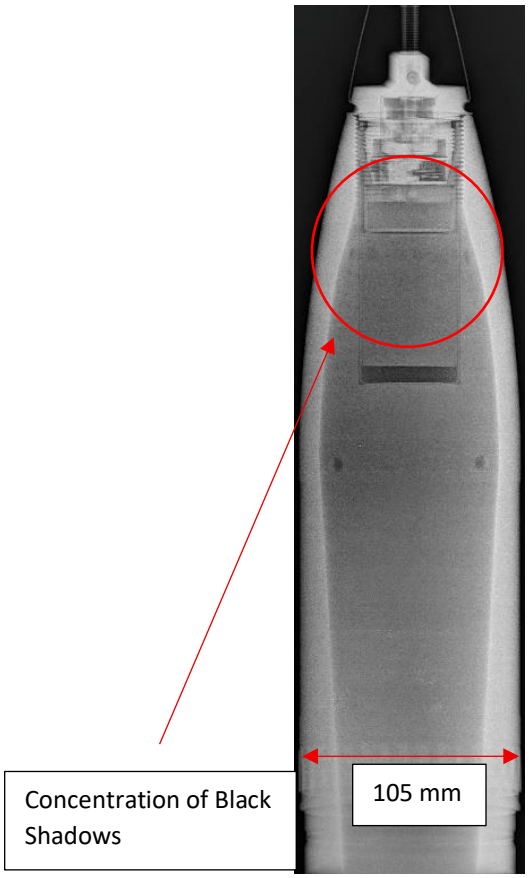

Figure 15. HE Nature Projectile Middle View at 45°

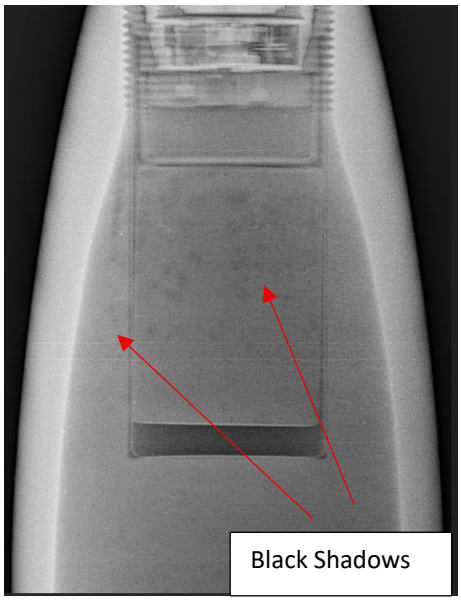

Figure 16. Close-Up on HE Projectile Booster Region

These HE nature projectiles contained Comp B as the main filling and the TNT booster. The image obviously represents a 2-dimensional image of a 3-dimensional structure. The outline of the booster is clearly visible and the existence of the black shadows outside the booster boundary suggests that they are related to the Comp B material rather than the TNT inside the booster. These black shadows appear to concentrate towards the nose section. The X-rayed photographs at 0°, 45°, 90° and 135°, as shown in Figure 17, show that the shadows did not gravitate toward a particular angle or orientation, since their appearances are in similar pattern and concentration regardless of those angles.

During the CNR storage site visit in 2019, it was revealed that all munitions were stored in their original packaging in a horizontal direction, shown in Figure 18. Based on the available records, the munitions had been stored in the current position for more than 30 years. Therefore, it is believed that the cavitations have no mobility and are unaffected by gravity.

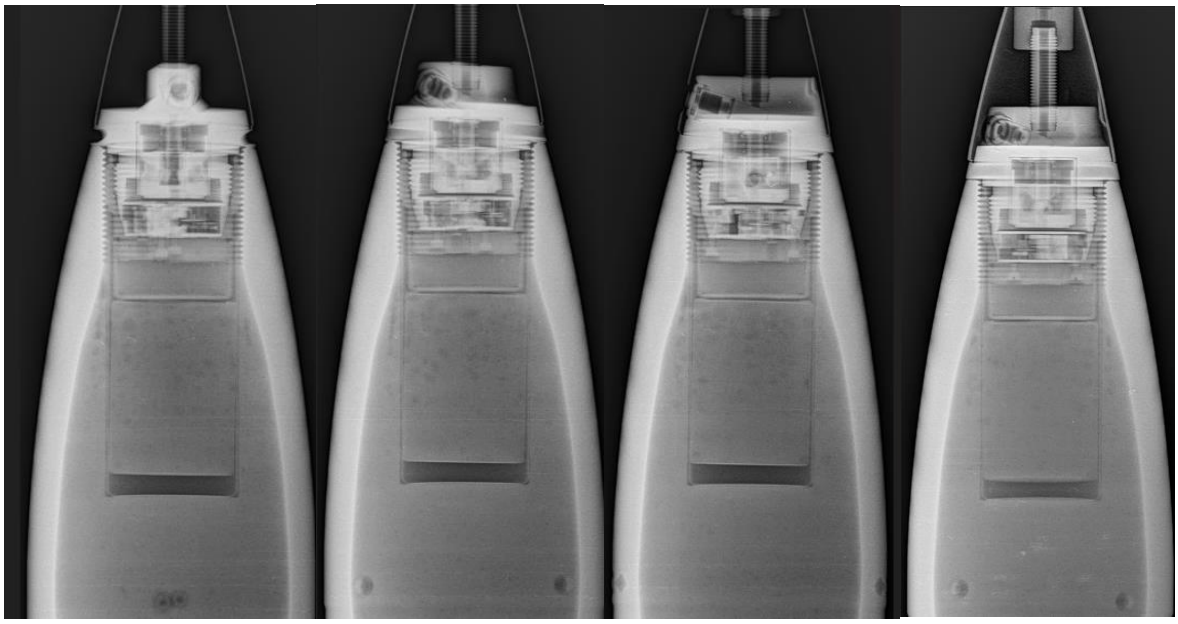

Figure 17. X Ray Photographs at 0°, 45°, 90° and 135°

Figure 18. CNR Storage Site Inspection in 2019 (CJOC)

Thus, they did not occur as a result of long-term aging but rather during the manufacturing process. It can be suggested that they represent a poor quality of production. This will be discussed in Chapter 4.

3.2 Sensitivity Testing (ESD and Mechanical)

In general, the purpose of the sensitivity tests is to assist in determining the appropriate UN classification of the energetic materials when stored and transported as dangerous goods. The sensitivity of the explosive can be divided into three subcategories: electro-static sensitivity, thermal sensitivity, and mechanical sensitivity. This section will focus on the results obtained using the electro-static discharge test, as shown in Appendix B, the BAM impact and friction tests, as shown in Appendix C and D. The thermal sensitivity results will be presented in the following section.

The summarized results from the ESD and mechanical tests are presented in Table 4. The results from individual sensitivity tests and their corresponding responses are presented in the appendices. The overall sensitivity results are at similar levels when the aged and the recent samples are compared to the literature data. Despite the numerical differences in the friction and impact results between the recent and the aged samples, majority of their results were within one test increment difference. Therefore, this study believes that they do not bear significant differentiation in terms of long-term aging impacts. However, the anomalies being the friction sensitivity of the aged and recent TNT samples which have significant numerical differences when compared to the literature data, as well as the aged Comp B friction results. These will be discussed further in Chapter 4.

In addition, the impact result for the recent TNT sample is also considered as an anomaly. The aged TNT sample demonstrated impact resistance beyond 80 J while the recent TNT sample was only at 7.5 J. The aged TNT sample impact result is consistent with the known values of beyond 80 J and TNT is known to have high resistance against mechanical stimuli such

as impact and friction. (UN, 2023; Dylong et al, 2022) An investigation to the cause of the recent TNT displaying low impact resistance is outside the scope of this study. Therefore, this study will be focusing on the aged TNT sample results.

Table 4. Summary of Sensitivity Results

Sample	ESD Result (J) Reaction Type	BAM Impact (J) Reaction Type	BAM Friction (N) Reaction Type
Aged TNT	> 0.625 No Reaction	> 80 No Reaction	160 Decomposition
Recent TNT	>0.625 No Reaction	7.5 Decomposition	120 Ignition
Aged Comp A-3	>0.625 No Reaction	20 Decomposition	160 Decomposition
Recent Comp A-3	>0.625 No Reaction	15 Decomposition	240 Ignition
Aged Comp B (Machined)	>0.625 No Reaction	15 Decomposition	96 Ignition
Aged Comp B (Melted)	>0.625 No Reaction	20 Explosion	120 Decomposition
Recent Comp B	>0.625 No Reaction	15 Explosion	160 Ignition

The ESD test is also known as the spark test. It is specifically designed to examine the response of the explosive when an electro-discharge event occurs through a bare human hand. (Kennedy, 2010) This paper uses Fisher's model and has adopted 25 kV at an appropriate capacitance as a reasonable equivalent to the electro-static voltages acquired by personnel under various environmental circumstances. (Fisher, 1989) All samples reported no reaction

when subjected to the ESD test at 25 kV, for which the corresponding energy level is 0.625 J. While there are other tests at higher energy levels to simulate other possible contact scenarios, such as helicopter electrostatic discharge for naval vertical replenishment at sea. Those tests are only conducted with an all-up-round configuration, rather than the bare explosive material. The ESD test results suggested that there is no measurable change with respect to the long-term aging on all samples. In particular, the bare human hand contact with the current explosive samples is safe.

3.3 Thermal Sensitivity

The combined TGA/DSC results can provide the thermal behaviour of the explosive when subjected to a constant heating rate in an inert gas (Ar) environment. This is also known as the thermal sensitivity of the explosive. The melting and reaction, onset and peak temperatures, heat released or absorbed, and mass loss profiles of the explosive can be extracted from the TGA/DSC results. While the thermograms for all the samples are presented in the Appendix F, the features of a thermogram and the method used to interpret will be illustrated using the recent Comp A-3 thermogram as an example which is shown below in Figure 19.

In Figure 19, the DSC portion is plotted in blue while the TGA portion is plotted in green. While both TGA and DSC data are presented as a function of temperature on the x-axis, the TGA data is represented on the y-axis as a percentage of the input sample mass loss and the DSC data is represented on the y-axis as a change in the energy. Notably, a positive change on the DSC data represents an endothermic reaction while the negative change represents an exothermic reaction. As illustrated in Figure 19, an endothermic spike is observed starting at

186.7 °C with a peak temperature at 199.5 °C. This corresponds to the melting of the sample during which energy is absorbed. However, an exothermic reaction starts upon the melting and has a peak temperature at 241.5 °C. This corresponds to the decomposition reaction of the sample and releases heat energy. The area under the DSC curve represents the total heat released or absorbed during the reaction.

The TGA data provides the mass loss profile of the sample which can be used to approximate the activation energy of the reaction using the Kissinger method. The Kissinger method assumes a first order reaction kinetic model and was a simplified from the generic kinetic rate equation, shown in Equation 6. The kinetic rate equation consisted of two parts and was represented by two different functions. The $f(\alpha)$ was a function which represented the order of the reaction while $K(T)$ was the Arrhenius equation. The Kissinger equation, shown in Equation 7, was derived by taking the first differential from the Equation 6 with respect to time. The Kissinger method further assumes that the temperature which the maximum rate of mass loss is tied to a specific heating rate. (Singh et al, 2019, Blaine and Kissinger, 2012)

$$\left(\frac{d\alpha}{dt}\right) = f(\alpha)K(T)$$

Equation 6. Generic Kinetic Rate Equation

$$\ln\left(\frac{\phi}{{T_{max}}^2}\right) = \ln\left(\frac{AR}{E_a}\right) - \frac{E_a}{RT_{max}}$$

Equation 7. Kissinger Kinetic Equation (Singh et al, 2019)

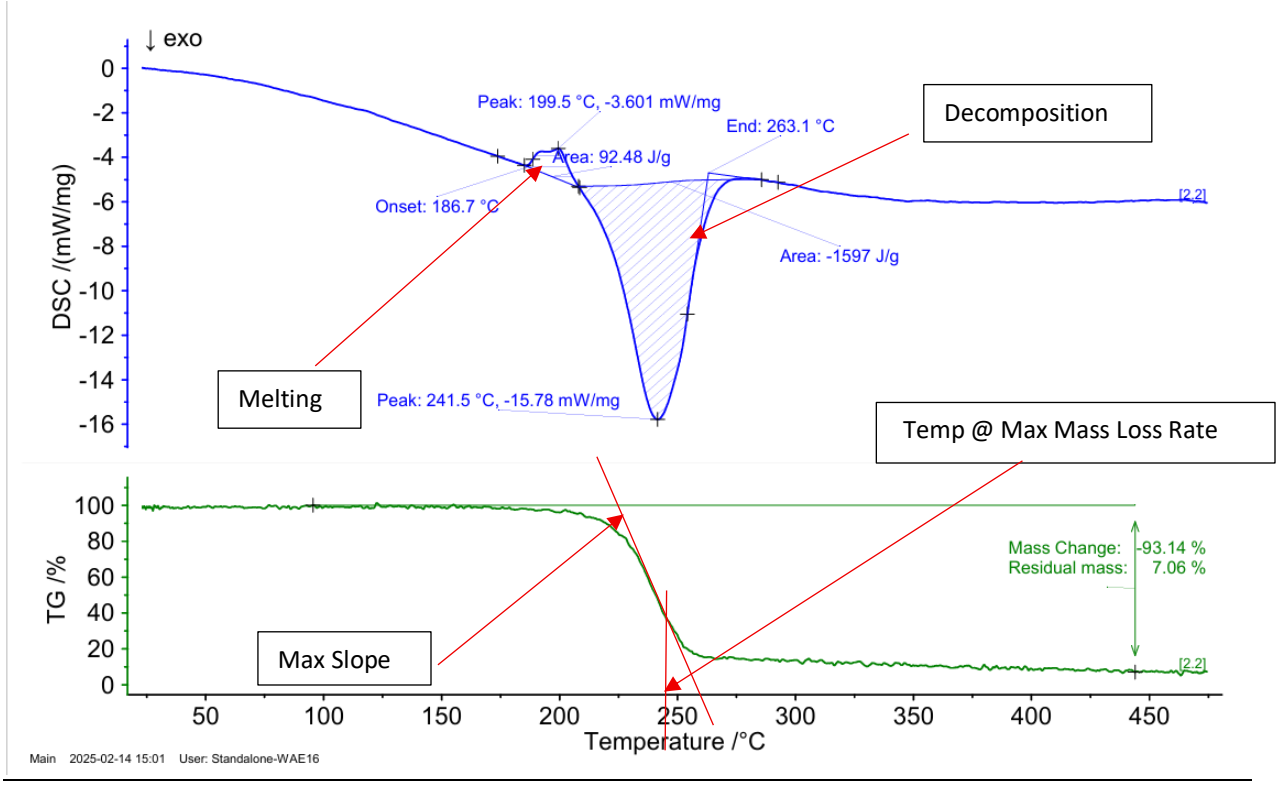

Figure 19. Recent Comp A-3 Thermogram (10 °C/min)

At different heating rates, the temperature at which the maximum rate of mass loss can be estimated by finding the maximum slope on the TGA curve. In Equation 7, ϕ represents the heating rate and T_{max} represents the temperature at which the maximum rate of mass loss occurred, while A and R are constants. A Kissinger kinetic plot can be generated by plotting the $\ln(\frac{\phi}{T_{max}{}^2})$ as a function of $\frac{1}{T_{max}}$. The activation energy, E_a, can be estimated by finding the slope of the best fitted linear line on the plot. (Singh et al, 2019)

The thermal results for the aged and recent TNT samples are summarized in the Table 5. The melting points and decomposition enthalpy from the current study results are in agreement with modern explosive data reported by Weinheimer. However, the decomposition

temperature exhibited a notable difference which both the recent and aged TNT samples have a peak decomposition temperature lower than the expected value.

Table 5. TNT Thermal Results

Sample	Peak Melting Point (°C)	Peak Decomposition Temperature (°C)	Decomposition Enthalpy (J/g)
Aged TNT (10 °C /min)	81.1	195.5	1289
Recent TNT (10 °C /min)	80.9	193.7	1698
Weinheimer	80 - 82	281	1255.2

The Kissinger kinetic plot for the aged TNT sample is shown in Figure 20 and the datum points used for the calculation can be found in Table 6. The activation energy of the aged TNT sample was found to be approximately 174 ± 31 kJ/mol with a R square value of 0.86. The Arrhenius constant (A) was found to be 14.0 ± 1.5 s^{-1}. However, the heating rate of 0.5 and 3.0 °C /min was repeated twice, and they have shown a noticeable difference with respect to the temperature at which the maximum rate of mass loss occurred. The current study result may suggest that the Kissinger assumption is not correct.

Table 6. Aged TNT Sample TGA Kinetic Data

Heating Rate (°C/min)	Temperature at Maximum Mass Loss (°C)
10	237.4
5	240.3
3	228.2
3	222.3
2	221.0
0.5	184.4
0.5	179.4

Notably, as illustrated in Figure 20., the Kissinger linear approximation had shown good approximation results except for Point A. The Point A correlates to the heating rate of 10 °C/min. The R square value could be improved to approximately 0.96 if Point A is discarded from the calculation and resulted in an activation energy of 150 ± 15 kJ/mol. None the less, the current result could be used to indicate a change in the activation energy of TNT in terms of long-term aging impacts. The activation energy calculation in TNT with and without the datum Point A which could represent the alternative views of the process will be further discussed in Chapter 4.

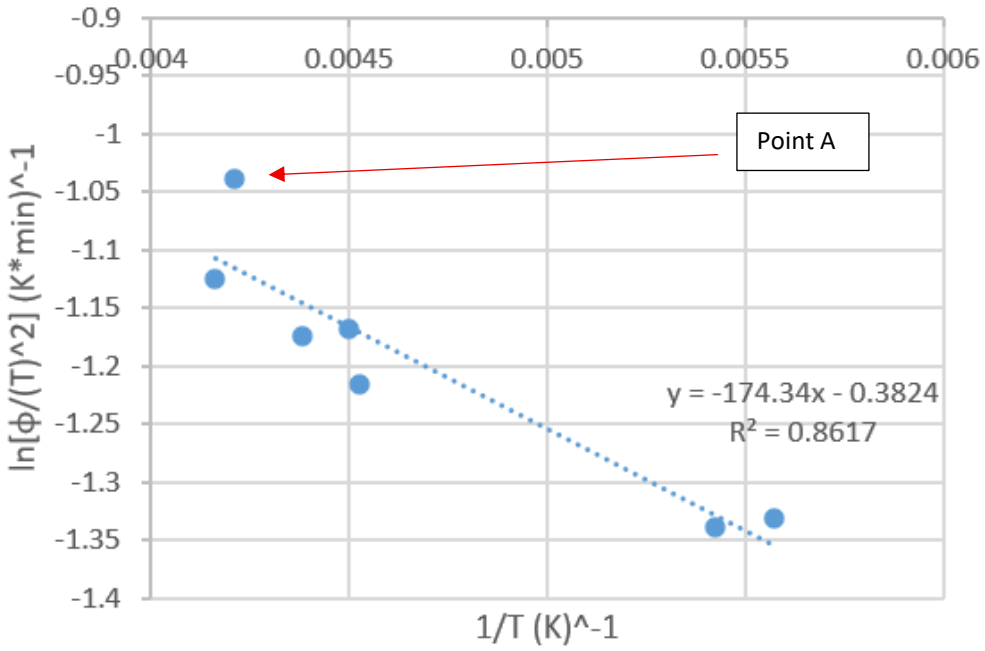

Figure 20. Kissinger Kinetic Plot for Aged TNT Sample

The thermal results for the Comp B samples are presented in the Table 7 below. The melting point from the current results are on agreement with Weinheimer. However, a similar

contradiction noted in the decomposition temperature which both the recent and the aged Comp B samples have lower decomposition temperatures when compared to Weinheimer.

This study only calculated the activation energy for the aged TNT sample using the Kissinger method. The aged Comp B decomposition reaction was found to be non-first order. The TGA thermogram of the aged Comp B sample, shown in Figure 21, revealed the mass loss profile contained different rates which could be used to display different reaction mechanisms. Therefore, the Kissinger assumption could not be applied.

Table 7. Comp B Thermal Results

Sample	Peak Melting Point (°C)	Peak Decomposition Temperature (°C)	Decomposition Enthalpy (J/g)
Aged Comp B (Melted) (10 °C /min)	79.5	239.5	1665
Aged Comp B (Machined) (10 °C /min)	80.4	239.5	1703
Recent Comp B (10 °C /min)	79.9	234.9	1271
Weinheimer	79	255	Not Available

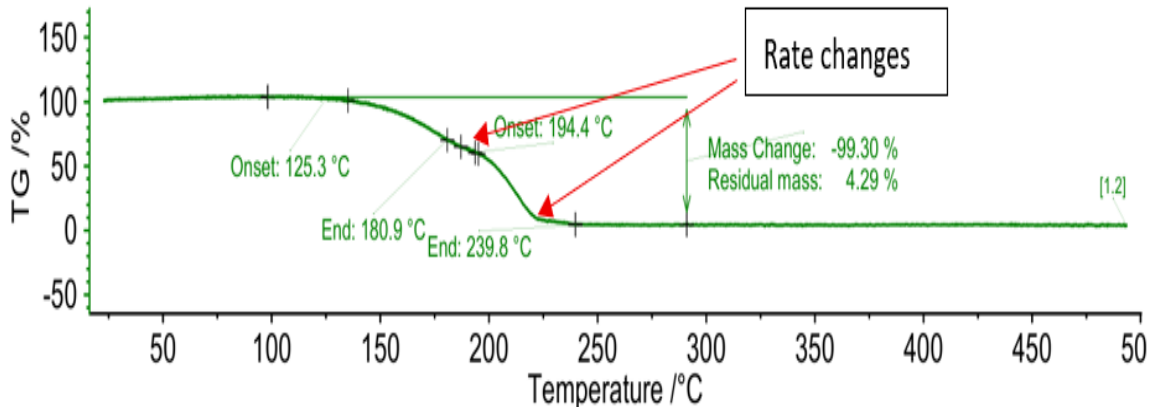

Figure 21. TGA Result of Aged Comp B (Machined) (1 °C /min)

This study postulates that the non-first order reaction mechanics in the Comp B TGA thermogram can be attributed to the composition mixtures of TNT and RDX. The difference of the decomposition enthalpy between the aged Comp B and the recent Comp B samples could be attributed to the different types of RDX crystals that they contain. Thus, the chemical composition of the Comp B and the related aging stability will be further discussed in Chapter 4.

The thermal results for Comp A-3 are presented in the Table 8 below. The melting point and the enthalpy between the samples revealed no significant changes with respect to long-term aging impacts. The Comp A-3 also contained RDX which is presumed to have synthesized using a similar process to Comp B and would contain similar level of RDX impurities as the aged Comp B samples. Thus, the Comp A-3 was believed to contain similar non-linear property as the Comp B. Therefore, this study did not further pursue the determination of the activation energy for other samples using different methods.

Table 8. Comp A-3 Thermal Results

Sample	Peak Melting Point (°C)	Peak Decomposition Temperature (°C)	Decomposition Enthalpy (J/g)
Aged Comp A-3 (10 °C/min)	204.9	237.8	324.6
Aged Comp A-3 (1 °C/min)	204.8	217.2	1682
Recent Comp A-3 (10 °C/min)	199.5	241.5	1597
Weinheimer	200	250	Not Available

The thermal result of the Comp A-3 showed a numerical difference on the peak decomposition temperature of the same sample but at different heating rates. The decomposition enthalpy of the aged Comp A-3 at 324.6 J/g is believed to be an error. A second

run confirmed the decomposition enthalpy of the aged Comp A-3 to be 1682 J/g. Additionally, the aged Comp A-3 had shown a lower peak decomposition temperature when heated at 1 °C/min when compared to the same sample which was heated at 10 °C/min. This is due to the fact that, at the lower heating rates, it will take longer for the sample to reach the decomposition temperature. Such that, there will be more time for slow decomposition pathways to have an effect. Thus, the current study believed there is no significant change in the peak decomposition temperature with respect to aging for the aged Comp A-3 sample.

3.4 Scanning Electron Microscopy

SEM has been used in many disciplines to analyse the surface textures of organic and inorganic materials at nano to micrometer scale. It has higher magnification and deeper penetration when compared to the traditional light or optical microscopy. (Mohammed and Abdullah, 2018) SEM was performed on all samples, as shown in Appendix E. However, the majority of the surface textures of Comp B and Comp A-3 have been distorted by the material extraction process and bear no significant meaning in the current study. In contrast, the aged TNT sample is believed to have preserved at least some of their original surface textures. This is due to the fact that TNT was packed in an aluminium wrapper as a booster package, as shown in Figure 22. Therefore, upon the de-fuzing operation, the booster was easily removed, and the TNT filling was extracted via direct scrapping.

Figure 22. Booster Cavity and TNT Supplemental Charge

Due to the unstable nature of the energetic material, the use of the SEM is limited to the low power magnification and short duration times for image collection. Higher magnification power and longer duration time on the target sample would cause a reaction through which the material surface would change. This is due to the fact that the electron beam from the SEM can impart energy on the material surface leading to formation of localized hotspots. As shown in Figure 23, the same target sample started to react when the electron beam was on the target for less than 1 minute. The reaction caused a distortion on the surface texture which can no longer be interpreted.

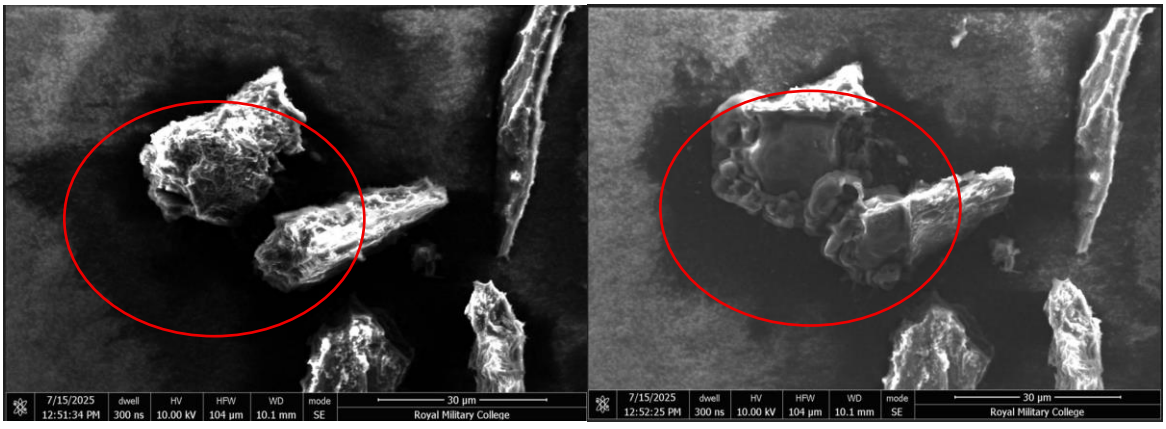

Figure 23. Aged TNT Sample Before (L) and After (R)

The SEM image obtained from the aged TNT sample showed uneven and rough surface texture, as shown in Figure 24. It has visible darker spots on the surface which resemble a dip or hole on the surface of the material. However, there is no visible crack or gap noticed in the aged TNT sample. The current SEM image result is in agreement with previous literature reports by Ahmed et al. and Reinold et al. The cause of the uneven and rough surface textures will be discussed in the following chapter.

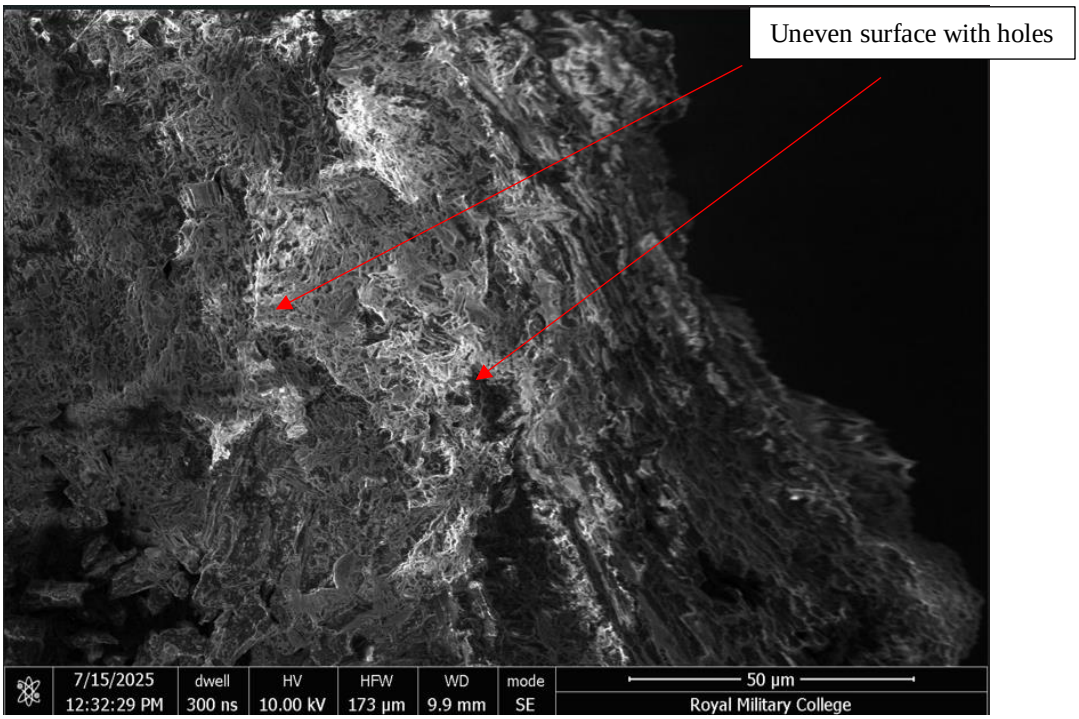

Figure 24. Aged TNT Sample Surface Images

Notably, the changes based on the methods of extraction on the material surface texture can also be seen from the two aged Comp B samples, as shown in Figure 25.

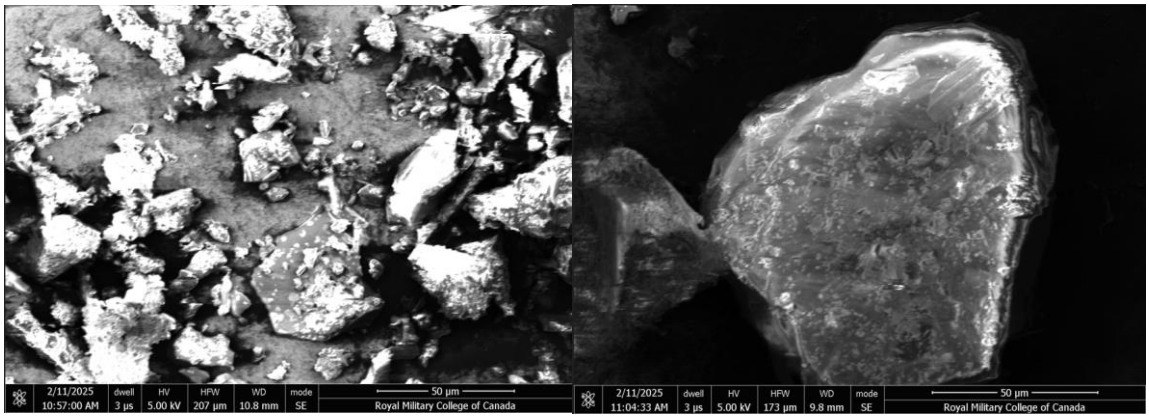

Figure 25. Aged Comp B Surface Images (L: Machined and R: Melted)

While both methods of extraction are known to have distort the surface texture of the sample, the machined sample exhibits far less distortions when compared to the melted sample. The particles are visible, and partial coatings can be recognized from the machined sample SEM images. However, no discernable observation can be made from the melted sample SEM images.

3.5 Gas Chromatography – Mass Spectrometry (GC-MS)

Gas Chromatography – Mass Spectrometry (GC-MS) is a powerful technique which can be used to identify and quantify organic materials. GC can provide separation with high resolution of organic compounds for identification purposes, while the MS can identify the pertinent structural information when compared to a known database for quantification purposes. The combination of GC and MS was developed in the mid 1950s and has been used in various disciplines such as environmental and pharmacology studies. (Hites, 1997) In terms of explosive separation analysis, High Performance Liquid Chromatography (HPLC) is usually a

more favourable technique than GC. This is due to the unstable nature of explosives which may undergo thermal decomposition in the gas phase. (Holmgren, 2005) However, GC has been recognized to be suitable for the analysis of nitro-aromatic compounds due to their high decomposition temperatures such as TNT and it can provide test results rapidly when compared to HPLC. (Bednar et al, 2011)

The identification of the impurity components is achieved using combination of the retention time in the GC and the mass to charge ratio in MS. The standard retention times from a list of known analytes are used as comparison. In addition, the known mass to charge ratio $(\frac{m}{z})$ of the analytes are also used to identify the compounds within the elute. The chemical impurity compounds contained in the aged TNT sample are identified and presented in Table 11 below. Overall, the impurity contained in the aged TNT sample have shown consistent retention times when compared to the reference standard retention time. They can also be correlate to the mass to charge ratio in the MS. Thus, the TNT impurities could be identified using the combination of GC and MS techniques.

The current GC-MS results are presented in the following three tables. The retention time obtained from using the standard analytes and the reference retention time are presented in Table 9. The retention time of the standard analytes were in good agreement with the reference retention times. Notably, the 1,2-DNB, 2,3-DNT and 2,3,4-TNT standard analytes were noted as “absent” in Table 9 which have been excluded from the current GC-MS analysis due to the unavailability of the analytes.

The standard analyte calibration at 100 ppb and 10 ppb results are presented in Table 10. They were compared with a control standard based on the Environmental Protection Agency (EPA) method 8330, Nitroaromatics, Nitramines, and Nitrate Esters by High Performance Liquid Chromatography (HPLC), standard analytes with a concentration of 100 ppb. The results in Table 10 can be used to suggest a linear relationship between the standard calibration peak with concentration at 100 ppb and 10 ppb. Such that, a difference of 10 times in the concentration would result in a difference of 10 times in the detected peak area. The EPA method 8330 analysts were used as control to validate the calibration results which the percentage of recovery is calculated according to the equation below.

$$EPA\ 8330\ Control\ Recovery\ (\%) = \frac{EPA\ 8330\ Peak\ Area\ (100\ ppb)}{Calibration\ Peak\ Area\ (100\ ppb)} * 100$$

Equation 7. EPA Recovery Percentage Calculation

Notably, the standard analytes with 1 ppb concentration did not produce any results. The current study believes that this was due to the aging of the column which was losing the detection sensitivity on the analytes. Despite of the GC-MS system aging impacts, the current study believes that the column could still be used to capture the composition of the aged TNT sample since a linear relationship could be reasonably established between the 10 ppb and 100 ppb standards.

Table 9. GC-MS Calibration Retention Time Results

Analyte	Reference Retention Time (min)	Standard Analyte Retention Time (min)	Mass to Charge Ratio Used for Detection ($\frac{m}{z}$)
Nitrobenzene (NB)	3.56	3.56	123
2-Mononitrotuluene (2-MNT)	3.96	3.94	137
3-Mononitrotuluene (3-MNT)	4.14	4.12	137
4-Mononitrotuluene (4-MNT)	4.21	4.21	137
1,3-Dinitrobezene (1,3-DNB)	5.22	5.21	168
1,2-Dinitrobezene (1,2-DNB)	5.31	absent	168
2,6-Dinitrotoluene (2,6-DNT)	5.27	5.25	165
2,4-Dinitrotoluene (2,4-DNT)	5.56	5.57	165
3,5-Dnitrotoluene (3,5-DNT)	5.64	5.64	165
3,4-Dinitrotoluene (3,4-DNT)	5.78	5.78	165
2,5-Dinitrotoluene (2,5-DNT)	5.45	5.42	165
2,3-Dinitrotoluene (2,3-DNT)	absent	absent	165
2,3,4-Trinitrotoluene (2,3,4-TNT)	6.33	absent	210

Table 10. GC-MS Standard Calibration and Control Results

Analyte	Calibration Peak Area (100 ppb)	Calibration Peak Area (10 ppb)	EPA 8330 Area (100 ppb)	EPA 8330 Recovery (%)
NB	4635	460	4686	101
2-MNT	4733	533	5340	113
3-MNT	3586	338	3104	87
4-MNT	3098	301	3211	104
1,3-DNB	764	56	782	102
1,2-DNB	absent	absent	absent	absent
2,6-DNT	1732	139	1652	95
2,4-DNT	930	93	1176	126
3,5-DNT	613	35	-	-
3,4-DNT	384	-	-	-
2,5-DNT	1000	-	-	-
2,3-DNT	absent	absent	absent	-
2,3,4-TNT	absent	absent	absent	-

Table 11. GC-MS Aged and Recent TNT Sample Results

Analyte	Aged TNT Peak Area (1007 ppm)	Recent TNT Peak Area (1059 ppm)	Aged TNT Conc. in Solid (%)	Recent TNT Conc. in Solid (%)	Previous Work (Voigt) (%)
NB	-	10	-	-	-
2-MNT	20	-	-	-	-
3-MNT	-	-	-	-	-
4-MNT	-	-	-	-	-
1,3-DNB	1338	556	0.017	0.0069	0.02
1,2-DNB	-	-	-	-	-
2,6-DNT	34	51	-	-	0.25
2,4-DNT	10505	2097	0.11	0.021	0.5
3,5-DNT	524	141	0.0085	0.0022	0.01
3,4-DNT	-	-	-	-	0.1
2,5-DNT	-	-	-	-	0.1
2,3-DNT	-	-	-	-	0.05
2,3,4-TNT	-	-	-	-	0.2

The EPA method 8330 recovery percentage illustrated the difference between the expected peak area value of using the EPA method 8330 standard analytes and the analytes used in the current study. Based on the percentage of the recovery difference, this study believes that the setup of the GC-MS was correct since the calibration standards were in similar agreement with the EPA standard analytes. Hence, the study carried out the GC-MS analysis on the aged TNT sample and the results are presented in Table 11.

In Table 11, the aged TNT and recent TNT composition results from the GC-MS along with the impurity levels reported in literature by Voigt are presented. Voigt reported the impurities present in the modern TNT from manufacturing when the samples were subjected to a 70 °C test for a prescribed time. The aged TNT sample had a concentration of 1007 ppm, and the recent TNT sample had a concentration of 1059 ppm. Their corresponding concentration in solution in relation to the detected peak can be calculated in the equation below. In the Equation 8, the calibration concentration was 100 ppb.

$$Conc.\,in\,Sol.\,(ppb) = \frac{Sample\ Peak\ Area}{Cal.\,Peak\ Area} * Cal.\,Conc.\,(ppb)$$

Equation 8. Concentration in Solution Calculation

The concentration in solution can be further calculated to solve for the analyte concentration in the original sample as a percentage according to the equation below where the standard concentration used was 1000 ppb for the calculation.

$$Conc.\,in\,Solid\ (\%) = Conc.\,in\,Sol.\,(ppb) * \frac{Stand.\,Conc.\,(ppb)}{Sample\ Conc.\,(ppm)} * \frac{1\ (ppm)}{1000\ (ppb)} * \frac{100}{1000\ (ppb)}$$

Equation 9. Concentration in Solid Calculation

Notably, the concentration values reported by Voigt represented the maximum possible values and the actual impurity concentrations were expected to be much lower. (Voigt, 1983) Based on the current results, there were three common impurities detected in both the aged and recent TNT samples which were 1,3-DNB, 2,4-DNT and 3,5-DNT. Despite their variance in concentration, they were all below the maximum possible value reported by Voigt. In addition, the detected peak at NB, 2-MNT, and 2,6-DNT were reported as "- "in the concentration in solid of the original samples in Table 11. This was due to the GC-MS detection threshold which, despite of the detected peak area values, the current study considered them as below the detection threshold of 10 ppb and are insignificant to report. In theory, the detected peaks with respect to the analytes of NB, 2-MNT and 2,6-MNT would result in a percentage of the original solid sample. However, due to previous calibration and control results in Table 10, the current GC-MS analysis was identified to be operating at a degraded capacity which it was unable to produce positive results for the standard analytes with 1 ppb concentration. Thus, the current study considers the lower detection limit to be at the reported peak area by the standard analytes at 10 ppb concentration. In addition, other impurities reported by Voigt were believed to have been below the detection threshold in the current study and thus noted in Table 11 as "- ".

Despite the GC-MS method had been a known method to conduct energetic material analysis, the current study had encountered multiple difficulties to obtain the ideal results for interpretation. The GC-MS setup used in the current study was not able to detect the standard analytes with concentration of 1 ppb for the TNT analysis. The component analysis of the Comp B was attempted but it revealed no useful results. The current study believes that the column

used for the GC-MS analysis has been degraded and unable to provide accurate results for component analysis.

In conclusion, the GC-MS results revealed similar impurities between the aged TNT and recent TNT samples. In particular, the current study only identified three common impurities in the samples. These were 1,3-DNB, 2,4-DNT and 3,5-DNT. While the concentration associated with each of the impurity was different between the recent TNT sample and the aged TNT sample, they were below the maximum expected values reported by Voigt. There are no noticeable composition changes. Additionally, the current GC-MS analysis is unable to produce positive results for the Comp B and Comp A-3. The major source of error is believed to be related to the aging of the equipment used in the current study.

Chapter 4 Discussion

The following discussion will be divided into four major sections. They are divided as TNT aging behaviours, Comp A-3 aging behaviours, Comp B aging behaviours, and the influence from manufacturing. Subsections will be used, if necessary, to further amplify or discuss in detail on the particulars related to the aging characteristic of each material and the influence from the manufacturing techniques used.

4.1 TNT Aging Behaviour

As discussed in Chapter 1, TNT is one of the most recognized military explosives in terms of longevity. The longevity of TNT is attributed to the inherent aromatic nature of toluene. However, previous literature studies revealed that the effects of long-term aging on TNT are inconsistent. Current study contained two types of TNT materials. They were used in the TNT booster and in the Comp B mixture within the HE nature projectiles. The current section will be focusing on the TNT drawn from the TNT booster, and the aging behaviour of the Comp B will be discussed separately.

4.1.1 Aged TNT Surface Textures

Due to the unique design of the TNT booster which allowed the ease of extraction without damaging the surface texture of the material, this study believes that the SEM imaging on the TNT booster material contained valuable information on the TNT aging behaviour with regards to their morphology. This section will focus on the results obtained from the SEM images.

The SEM images can reveal the surface texture which could also be part of the microstructure of the material. Notably, the principle of operation in a SEM is the reflection of the scanning electron beam from the sample surface which is subsequently converted to an image by optronics. (Zhou et al, 2007) The advantage of the SEM is the opportunity to detect and examine the defects located on the surface level of the explosive particle. However, there is a limitation on the input energy level used by the electron beam in order to avoid the initiation of the explosive which limits the power of magnification. (Borne et al, 2004)

This study believes that some of the surface texture and the original microstructure in the aged TNT sample have been preserved despite the fact that the extraction might have distorted some of the microstructure features. The current SEM images suggested a surface texture change on the aged TNT samples. The rough surface texture noted on the aged TNT sample image is in agreement with the SEM images from two other studies using naturally aged samples by Ahmad et al. and artificially aged samples by Reinold et al. However, they concluded differently on the cause of the rough surface texture. Ahmad et al. suspected the primary cause was linked to the storage and handling process, in which the sample could have been exposed to hot water spray during the decanting process. Reinold et al. suggested the change in surface texture was because of the prolonged heating during artificial aging simulation but offered no further insight into the detailed cause. In addition, neither study considered the impact of thermal cycling and the material deformation under static environmental stress.

TNT expansion depends on the presence of impurities, particularly in the presence of 2,4-DNT and 2,3,4-TNT. The irreversible growth is driven by the anisotropic thermal expansion. (Parker and Wilson, 1979) While the presence of 2,3,4-TNT was not confirmed in the GC-MS

analysis, the current study confirmed the presence of the 2,4-DNT in both the recent and aged TNT samples, as shown in Table 11. Thus, the growth of the TNT material described by Parker and Wilson could be a possible cause of the uneven surface textures. However, the aluminium packaging wrapper and the TNT booster, as shown in Figure 22., did not reveal any physical deformations or protrusions due to the growth of the TNT. This is in contrary to the results reported by Schimmel and Lowell who reported TNT-based explosives protruded from the burster tubes after artificial aging in 1963. (Schimmel and Lowell, 1963) Although the GC-MS analysis confirmed the presence of impurities, the TGA/DSC result revealed the aged TNT had a melting point of 81.1 °C which could be used to indicate the level of impurities was extremely low. Therefore, this study concludes that the growth of TNT had a negligible effect, if any, on the change of the surface texture of the material.

The current study believes that, in the low temperature environment where the temperature is insufficient to produce ignition of the explosive, the explosive material would experience an annealing effect which could cause a change in the morphology of the material. (Borne et al, 2004) This is demonstrated by Renlund et al. through the examination of thermally degraded energetic materials. Renlund et al. characterized the cause of the rough surface texture as the thermal expansion which was a result of exposure to thermal cycling and coupled with mechanical creep caused by decomposition gas evolution. (Renlund et al, 1997) The heat-affected region in the material can be described as “uneven edges and internal void regions” which reflects the current study observation from the SEM image in Figure 24. (Borne et al, 2004) Therefore, it can be suggested that the rough surface textures on the aged TNT could be due to exposure to thermal stress.

Notably, the degree of thermal exposure is different in the current study when compared to the study by Renlund et al. The current study samples had only been exposed to the ambient environment which could be described by the NATO climatic category as "A3 Intermediate". This category captures the ambient temperature during the summer season and has an average ambient temperature between 28 – 39 °C. (NATO AECTP 230, 2009) Therefore, this study believes that the explosive material would have only experienced mild thermal conditions which are below the melting point of TNT. Thus, the current SEM results could suggest the cause of the surface texture change in the TNT as a result of the thermal exposure of the TNT in the ambient environment.

In summary, the current SEM images are on agreement with other literatures. However, there is no consistent conclusion to the formation of the uneven textures on the TNT material surface. This study believes that the change in the surface textures on the TNT material is a result of thermal exposure in the ambient environment. The growth of the TNT is believed to have negligible effect on the surface texture.

4.1.2 Friction Sensitivity of Aged TNT

The sensitivity of an explosive is a practical problem which involves reliability and safety. The requirement of an explosive is such that it must be functionally reliable when initiated and it must behave safely and remain stable during all stages of transportation and handling. (Macek, 1961) The mechanical sensitivity of an explosive consists of impact, friction and shock. The impact and friction sensitivities can provide the safety assurance in the logistical cycle while the shock sensitivity test provides the functional reliability of the explosive and its risk of sympathetic detonation. In the current study, the functional reliability of the explosive is of a

lesser concern since the aged projectiles will be used as target practice munitions for EOD training by the CAF. Hence the focus of the study will be on the impact and friction sensitivities of the explosives.

All explosive samples were tested for impact and friction initiations. There were no discernable changes in the impact results in relation to long-term aging. The friction and impact results obtained from the current study were based on the highest energy or force at which a response was observed and subsequently no responses following the six consecutive trials at the subsequent lower friction or impact challenge. The individual reaction responses were shown in Table 4 in the previous chapter. The current study found that the aged TNT sample has a friction sensitivity that would be considered as below the standard value. When compared to the standards, TNT typically has a friction sensitivity of approximately 360 N or higher. (Dylong et al, 2022; UN, 2023; NATO STANAG 4025, 1991) The current study has found the friction sensitivity of the aged TNT sample to be 160 N. Although some variation in friction results is expected, there is a notable difference between the sample result and the standard value of friction sensitivity. This is also noted in Dylong et al. study, in which multiple TNT samples ranging from 40 - 60 years old reported a friction sensitivity between 100 – 180 N, irrespective of their age.

According to the current standard, TNT with a solidification point of 80.6°C or higher is considered as “ultra-pure” which is the highest purity level. (NATO STANAG 4025, 1991). The aged TNT sample has a peak melting point at approximately 81.1 °C which suggested it contains low levels of impurities and has a high quality of production. The current result contradicted Dylong et al. study in which they concluded the cause of the low resistance to mechanical

stimuli were attributed to the low manufacturing quality in the TNT material. (Dylong et al, 2022)

Ahmad et al. previously concluded the change in TNT texture, through SEM imaging, would increase the material sensitivity due to the creation of hotspots. (Ahmad et al, 2016) While Ahmad et al. study lacked the evidence to support their theory, the impact and friction initiation of solid explosives can be attributed to the excessive buildup of heat in a localized spot leading to thermal initiation at this location. (Bowden and Gurton, 1949) This is known as the hotspot initiation theory. Field pointed out that, while the hotspot initiation theory encapsulated multiple initiation mechanisms at various conditions, their processes all involve the conversion of mechanical or electrical to thermal energy. (Field, 1992) Notably, the different physical application in the initiation mechanisms between the impact and friction should be distinguished. The impact initiation is caused by the compression of the material (Field, 1992) while the friction initiation is caused by the shear force of the explosives against the test surface. (Bowden and Gurton, 1949) Therefore, it can be suggested that the shearing mechanism had a different effect on the TNT material due to long-term aging.

During the friction test, a solid sample of aged TNT is placed under load against the porcelain test surface. The mechanical force of rubbing is converted into heat at the contact surface which caused the solid TNT to melt and would produce a layer of molten TNT prior to decomposition. (Bowden and Gurton, 1949) Previously discussed, the SEM image on the aged TNT sample has suggested that the prolong exposure of thermal exposure led to the development rough and uneven surface texture on the material. Such that, the surface texture change on the aged TNT surface could have the effect of increasing the area of surface contact

which enhanced the shearing motion force between the solid TNT and the molten TNT on the test surface. Therefore, the overall resistance to friction initiation is reduced.

Evidently, the reasoning above can also be demonstrated using the aged Comp B sample which contains TNT and RDX. There are two different aged Comp B samples: aged (melted) and aged (machined) samples. These two samples came from two different projectiles which the environmental and aging impacts are all identical. The only difference was the method of extraction. The melting extraction was similar to the loading process which the explosive filling was heated to above the melting point of the TNT and poured out by gravity. These two samples should display similar level of friction resistance in theory, if chemical composition alone is responsible for friction sensitivity. However, according to the result in Table 4, the aged (melted) Comp B sample has a friction sensitivity of 120 N while the aged (machined) Comp B sample has a friction sensitivity of 96 N. While both extraction methods are known to distort the original texture of the material, the aged (melted) Comp B sample would have a different surface texture when compared to the aged (machined) Comp B sample, as shown in Figure 25. Melting of the aged (melted) Comp B would at least partially eliminate the previously noted defect of rough surface texture and would have an effect similar to restoring the original morphology due the melting of the TNT. Hence, the aged (melted) Comp B sample has a higher friction resistance when compared to the aged (machined) Comp B sample. This seems to be borne out by the data. Thus, the current study believes that the TNT-based explosives would experience ambient aging behaviour which could negatively impact the friction sensitivity of the material.

In conclusion, the current study noted a decrease in the resistance to friction initiation while the resistance to impact initiation remained unchanged in the aged TNT sample. While all the initiation mechanisms can be traced back to a thermal origin which is known as the hotspot theory, the fundamental difference between the impact and friction initiation has different physical applications. The cause of the reduction in the resistance to friction initiation is believed to be the previously noted surface texture change in TNT due to thermal exposure. The change in the surface texture of the material has an effect similar to increasing the area of contact surface which reduces the friction resistance of TNT. Evidently, the impact of such surface texture change leading to reduction in friction resistance can be demonstrated using the two aged Comp B samples with different methods of extraction. Despite the decrease in friction sensitivity, the current aged TNT sample result still meets the NATO minimum friction sensitivity requirement of above 80 N as a booster explosive. (NATO AOP 7, 2003)

4.1.3 Activation Energy of Aged TNT

Activation energy is known as the energy barrier for a chemical reaction to go from reactants to products. In the application of energetic materials, this can be considered as another important safety parameter as it pertains to the prevention of an undesired decomposition of the material whether in storage or during handling. In general, explosive materials such as TNT and RDX which have an activation energy higher than 40 kcal/mol (170 kJ/mol), their shelf life could be “hundreds of thousands of years” based on the criteria of the time for a mass loss of 0.02 % at 20 °C. (Manelis et al, 2003) Notably, the activation energy depends on the temperature of exposure. Energetic materials, such as NC, can undergo thermal decomposition at temperatures below the auto-ignition temperature at which a spontaneous

and violent reaction may occur. As discussed by Bohn, NC has an activation energy of 146 kJ/mol between the temperature range of 60 – 90 °C and 86 kJ/mol when stored in environments under 60 °C. These correspond to different decomposition mechanisms at different temperature ranges. (Bohn, 2017) Therefore, without understanding the decomposition mechanism, the difference in the activation energy could lead to an overly optimistic life prediction of an energetic material.

The thermal decomposition mechanism of TNT in ambient conditions has been investigated in various studies and over the decades. However, no consistent results or conclusions can be made with regards to the decomposition mechanism as described in Chapter 1. In addition, while the TNT decomposition mechanism remains to be investigated, the effect of long-term ambient aging has also not been taken into consideration in those studies. The established understanding in the aging behaviour of an energetic material is commonly assumed to be an Arrhenius relationship in which the rate of the decomposition reaction is dependent only on the temperature of exposure and the activation energy of the decomposition mechanism. (Sanchirico and Di Sarli, 2024) This assumption forms the basis of artificial aging studies which uses an elevated temperature for a short period of time and linear extrapolation of the temperature data to determine the service life of a material. Many studies have demonstrated that the complicated degradation processes in a material can be modeled by a simple linear Arrhenius relationship. (Celina et al, 2005; Bohn, 2017) The practical application of utilizing the linear Arrhenius relation has been adopted in the NATO AOP 48 to estimate the rate of degradation of NC in storage conditions. Hence the significance of correctly identifying the activation energy which is associated with the degradation mechanism at a

particular temperature condition. In addition, the activation energy of the energetic material can also be viewed as another safety parameter with respect to storage and handling. For energetic materials with an activation energy of decomposition lower than 155 kJ/mol, they could have limited thermal stability which could compromise the storage and handling safety. (Sanchirico and Di Sarli, 2005)

Activation energy is also unique in which it is linked to a particular chemical reaction. However, in the case of the energetic material decomposition, the process is often not a uni-reaction process. Thus, it could be affected by various parameters, such as temperature fluctuation, and the degree of competition between different decomposition reactions could also vary. Despite the multi-reaction mechanism, the aggregated effect of multiple decomposition reactions can still be captured in the overall activation energy for a specific temperature range. (Bohn, 2017) In other words, without the detail knowledge on the decomposition reactions, the Arrhenius method could still be applied for aging prediction if the global activation energy of the decomposition model could be determined with sufficient confidence.

The current study found that, using a linear Arrhenius aging model and applying the Kissinger method, the activation energy of the aged TNT sample is 174 ± 31 kJ/mol with an R square value of 0.86. The aged TNT activation energy was calculated from the line of best fit in the Kissinger kinetic plot, as shown in Figure 20. The current study can be suggested that, under the ambient storage conditions, TNT has a different thermal decomposition reaction mechanism when compared to the standard thermal initiation mechanism with the activation energy of 222 kJ/mol associated with detonation from Table 2.

Notably, as illustrated in Figure 20., the Kissinger linear approximation of the activation energy of the aged TNT sample had an R square value of only 0.86 with majority of the error introduced by the datum point, Point A. The datum points used in the Kissinger method were derived from the TGA thermogram based on the mass loss profile. In particular, Point A was derived from the observed peak temperature at which the maximum rate of mass loss at occurred 237.4 °C with the heating rate of 10 °C/min. As described in Chapter 3, based on the comparison on the R square values, majority of the deviation is believed to be attributed by the single point, Point A, in the activation energy calculation using the Kissinger method.

An alternative solution without the consideration of Point A, shown in Figure 26, with an activation energy of 150 ± 15 kJ/mol and R square value of 0.96 is presented below. Based solely on the R square value, the alternative solution presents a significant improvement on estimation of the activation energy using the Kissinger method. However, the alternative solution only differs by one single point. While the alternative solution has an improved model to the existing data on the Kissinger kinetic plot, the current study postulates that the Kissinger method may not be entirely accurate. The Kissinger method assumes that the reaction is a first order reaction, and the heating rate has a “marked effect” on the temperature at which the kinetic rate of mass loss reaction is at the maximum.

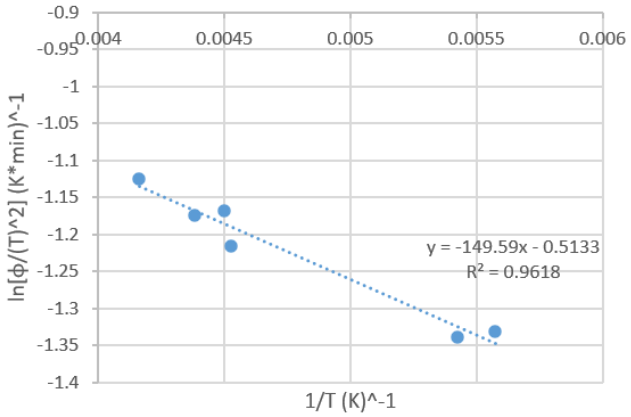

Figure 26. Alternative Aged TNT Kissinger Kinetic Plot

The “marked effect”, as described by Murry and White, referred to the temperature at which the maximum mass loss kinetic reaction rate occurred was tied to a particular heating rate during the thermal analysis. (Murry and White, 1954) However, current study results are suggesting that the Kissinger assumptions may not be accurate, as shown in Table 6. There were two repeated runs at the same heating rate of 3 and 0.5 °C/min. Their respective peak decomposition temperature at the maximum mass rate loss were different from the initial run. The observed difference was more than 5 °C when compared between the initial and the repeated experimental data.

The popularity of the Kissinger method is based on the assumptions that the reaction is a single step kinetic reaction, and the rate of mass loss varies with the heating rate. (Singh et al, 2019) It can be further suggested that without the detail knowledge of a thermal process, the activation energy could be approximated as a single step reaction by using the Kissinger method. (Vyazovkin, 2020) However, the current work believes that the Point A was a valid datum point, and the low R square value could be attributed by the method used. The current

study result is suggesting that there is non-linear property in the kinetic behaviour, illustrated in Figure 20., and discrepancy on the Kissinger assumption, shown in Table 6. Therefore, the current study believes the activation energy of TNT using the Kissinger method to approximate is inaccurate.

In comparison to other literature, the activation energy of TNT was reported to be in the range of 116 - 169 kJ/mol by Long et al. While the current study reported similar value using the Kissinger method when compared to the study by Long et al., they used the isoconversional method to estimate the activation energy of TNT which the reaction rate was based on the conversion factor and the activation energy could vary throughout the reaction. (Long et al, 2001) The conversion factor describes the mass change in relation to the total mass loss during the reaction. Such that, the overall decomposition reaction kinetic could be described by a combination of the Arrhenius equation and a function of the conversion factor. (Vyazovkin, 2008) The current study only undertook the Kissinger method due to its simplicity in application. The difference in the activation energy between Long et al. and the current study is the degradation model used. The current study undertook an assumption that the decomposition kinetic could be simplified to a first order reaction and used the Kissinger method. The Kissinger method can only provide a single value of activation energy with respect to the temperature dependence of the reaction. As point out by Vyazovkin, the Kissinger method was inadequate in considering the physical transformation of the material during a reaction, such as the crystallization behaviour of the material. (Vyazokin, 2020) In addition, the material degradation process can also follow a multiple of competing processes in the long-term aging and lifetime prediction. Celina et al. study further suggested a multi competing

reaction forming a complex reaction process to address the curvature in the Kissinger kinetic plots. (Celina et al, 2005)

Therefore, the current study believes that the aging behaviour of TNT contains multi-mechanisms, and the activation energy could not be simply resolved using the single reaction approach and the Kissinger assumptions. While the safety criteria described by Sanchirico and Di Sarli have not been adopted in Canada, there is no evidence to suggest that the aged TNT sample would compromise safety in storage and during handling.

In summary, the activation energy of an energetic material is often viewed as another safety parameter due to their inherent instability. The activation energy can be used in relation to the aging studies and life predictions of energetic materials. The current aging approach in the energetic material life prediction is the assumption of the Arrhenius behaviour which depends on the activation energy and temperature of exposure with the use of linear extrapolation to interpret the experimental data. However, no consistent conclusion has been accepted or critical parameters defined in the literatures in relation to safe storage and handling based on the activation energy. The current study found the activation energy of the aged TNT sample to be 174 ± 31 kJ/mol with an R square value of 0.86 using the Kissinger method. The activation energy suggested that there is a different degradation process when compared to the standard thermal initiation activation energy at 222 kJ/mol from Table 2. The current study also noted non-linear properties in the Kissinger kinetic plot which could be suggesting multi-mechanism aging behaviour of TNT and the variation of activation energy throughout the reaction. However, there is no evidence to suggest that the aged TNT sample would compromise safety in storage and during handling.

4.2 Comp A-3 Aging Behaviour

Comp A-3 is an earlier version of the Polymer Bonded Explosives (PBX). Its formulation contained 91 % RDX and 9 % inert wax. (NATO AOP 26, 2011) It had only seen a short period of military service between the WWII and the early 1970s. Due to a series of in-bore detonation accidents in naval guns in the late 1960s, Comp A-3 was retired from service and had been replaced by other explosives, such as the Polymer Bonded Explosives Navy (PBXN). (Beauregard, 1971) Despite its brief service history, the aging behaviour of Comp A-3 remains a relevant subject in the current study. The energetic material used in the formulation of Comp A-3 is solely based on RDX which is still in service today and can be used to interpret the aging behaviour of the RDX material.

The current study results suggested that there is minimal measurable change to the energetic material with respect with the ESD and mechanical sensitivity, thermal sensitivity, X-ray imaging and SEM imaging. The X-ray images revealed no void space or crack formation in the explosive filling prior to the material extraction. The ESD sensitivity test confirmed the material is safe for human bare hand contact. The mechanical and thermal sensitivity test results of the aged Comp A-3 sample were at similar level when compared to the recent Comp A-3 sample and published literature results. Therefore, this study concludes that there are no discernable impacts to the Comp A-3 with respect to exposure to the long-term ambient aging environments.

4.3 Comp B Aging Behaviour

Comp B is a well-established military explosive and is in continued service today with the CAF and other militaries. According to the current composition standard, Comp B consists of 59.5 % RDX, 39.5 % TNT and 1 % desensitized inert wax. (NATO AOP 26, 2011) This is often referred to as the 60:40 mix of RDX and TNT. However, the historic composition mixture ratio varies when compared to what is known as the Comp B today. Due to the unique composition nature which it contains both TNT and RDX, the current study believes the aging behaviour of the Comp B could be drawn from the aging behaviours of TNT and Comp A-3.

4.3.1 Friction Sensitivity of Comp B

The mechanical and electro-static sensitivities of the current aged Comp B sample revealed no discernable changes except for the friction sensitivity. The current study found the friction sensitivity of aged Comp B samples at 94 N in the machined sample and 120 N in the melted sample. Sharma et al. reported the fresh Comp B friction sensitivity at 294 N using the BAM friction test method. (Sharma et al, 2023) The difference in the sensitivity level between the melted and the machined sample was believed to be due to the extraction method. Previously, the aging behaviour of TNT was noted to have reduced friction resistance due to thermal exposure resulted in the rough surface textures. The RDX contained within Comp A-3 was noted to have retained the mechanical resistance to initiation. Therefore, the current study believes the reduction in the Comp B friction resistance is attributed by the aging behaviour of the TNT.

It can be suggested that there is a measurable reduction on the Comp B friction resistance due to the thermal exposure which could induce a texture change on the surface level. However, as shown in Figure 25, due to the extraction method used, such surface texture was believed to have been distorted in the sample and unable to provide meaningful justification to the current study. Hence, the current study believes the TNT contained in the Comp B material would experience the similar thermal exposure which would induce a surface texture change and leading to a reduction in friction resistance based on the aging behaviour of TNT. The study further concludes that the aging behaviour of the RDX to have negligible impact on the mechanical sensitivity of the Comp B based on the mechanistic results from the aged Comp A-3 sample. In addition, the relative mechanical sensitivity of the aged Comp B is believed to have a negligible safety impact on the material. Typical primary explosives such as lead azide has a friction resistance of 10 N and PETN, a known sensitive secondary explosive, has a friction resistance of 60 N. (UN, 2023) Therefore, the current study result of 96 N and 120 N on the friction sensitivity is believed to have retained the necessary mechanical resistance as a secondary explosive in the logistical handling and transport environment for the proposed CAF EOD training use.

In summary, Comp B is considered as a TNT-based explosives with the addition of RDX. The mechanical sensitivity results, shown in Table 4, revealed a difference between the two aged Comp B samples. Despite identical exposures, the difference in the friction resistance between the two samples was believed to be attributed by the method of extraction. When compared to the published results of the modern Comp B, both the aged Comp B samples had a lower friction resistance. The current study believes the reduction in the friction resistance is

contributed by the thermal exposure leading to the TNT aging within the composition. Despite the reduction in friction resistance, the current study believes that the aged Comp B has retained the necessary mechanical resistance as a secondary explosive. Hence, there is no safety impact in the logistical handling and transportation environment for the proposed CAF EOD training use.

4.3.2 Comp B Thermal Sensitivity

The thermal behaviour of Comp B can be characterized by its explosive composition and has high similarity when compared to TNT. It has the same melting point as TNT but will remain thermally stable below the auto decomposition temperature. Thus, Comp B is also considered as safe to melt for the purpose of material extraction or cast filling the shells.

From Figure 27, the melting of TNT could be identified by the endothermic peaks at 79.5 °C in the DSC thermogram. When compared to the melting point of 81.1 °C from the TNT booster sample, the current study results revealed that the quality of TNT used in the Comp B was noticeably different. (NATO STANAG 4025, 1991) The current study believes the difference in the melting points between the TNT contained in the aged Comp B sample and the aged TNT sample from the booster represented a difference in the TNT production quality. When compared to known literature, the reported the melting temperature of the TNT contained in the Comp B mixture was 79 °C. (Weinheimei, 2002) The use of lower quality TNT in the application of Comp B had been a known practice. The purpose of the TNT used in the Comp B was as a binding agent while the TNT used in the booster was an exploder which its main purpose was to amplify the shock energy from the primary explosive, as illustrated in Figure 2. Thus, the difference in the TNT quality was applied for different applications. Despite of

different production quality, the TNT used in the Comp B sample had met the NATO STANAG 4025 requirement as an explosive binder.

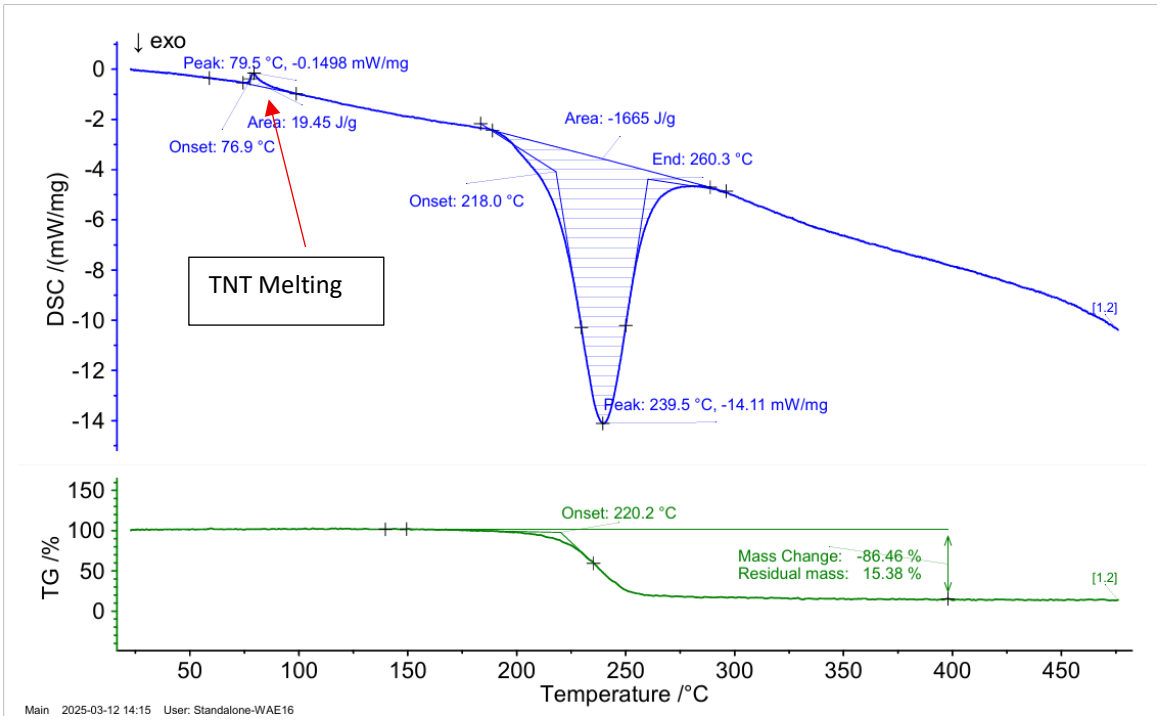

Figure 27. Thermogram of Aged Comp B (Melted) (10 °C/min)

When compared to the known decomposition temperature of Comp B, the peak decomposition temperature of the aged Comp B is lower, as shown in Table 7. (Weinheimer, 2002) This could be used to suggest there was a change in the activation energy of the aged Comp B when compared to the modern Comp B. The current study believes that there is a reduction in the activation energy of the aged Comp B. However, the actual activation energy remains to be determined. The current study has identified multiple rate changes with respect to the mass loss profile which precluded the use of the Kissinger method to estimate the activation energy, as shown in Figure 21. This study believes the rate changes in the mass loss profile could be contributed by the complicated decomposition reactions suggested by Hobbs

et al. Thus, the current study concluded that the Kissinger assumptions could no longer be used to approximate the activation energy of the aged Comp B sample.

Notably, the current study conclusion on the applicability of the Kissinger method contradicted the study by Singh et al. Singh et al. had demonstrated that the Kissinger method could be used to approximate the activation energy of aged Comp B without the detail analysis on the decomposition mechanics. Their results were in agreement with the values obtained from the isoconversion method. (Singh et al, 2019) On the contrary, the current study result revealed a different thermal behaviour when compared to Sing et al. study. As shown in Figure 28 below, an endothermic reaction was noted at 213 °C during the decomposition reaction. The same endothermic reaction was also noted in Figure 29 at 197.7 °C. These endothermic peaks were not observed in the study by Singh et al. which their thermogram was obtained from using similar heating rates. Based on the results from the aged Comp A-3 sample, the melting point of the aged RDX was at approximately 205 °C. However, Hobbs et al. found that the melting

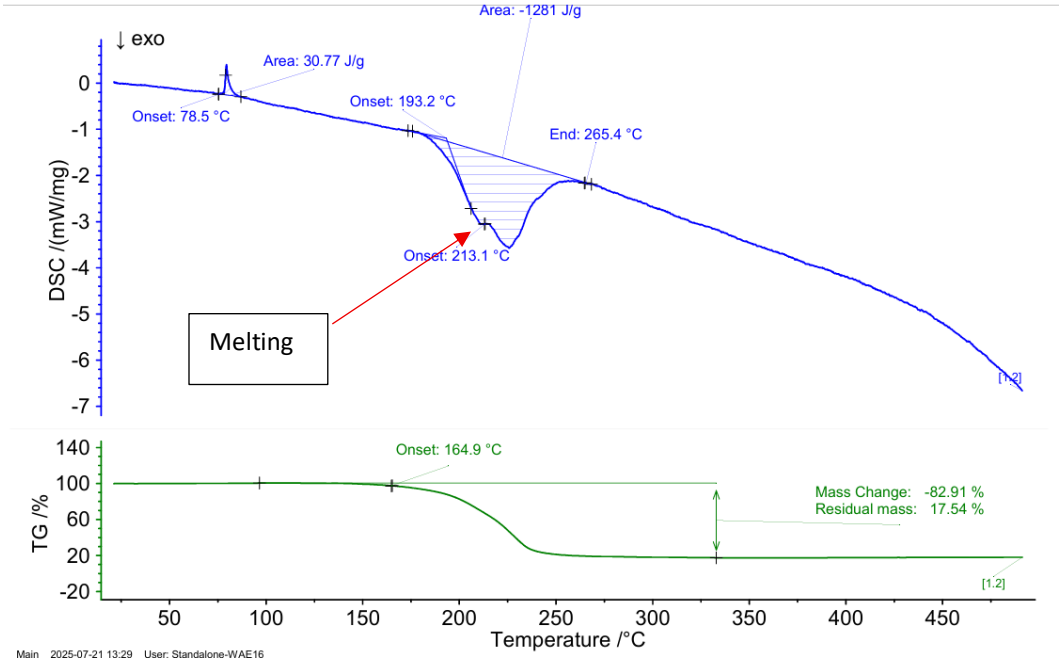

Figure 28. Thermogram of Aged Comp B (Machined) (3 °C/min)

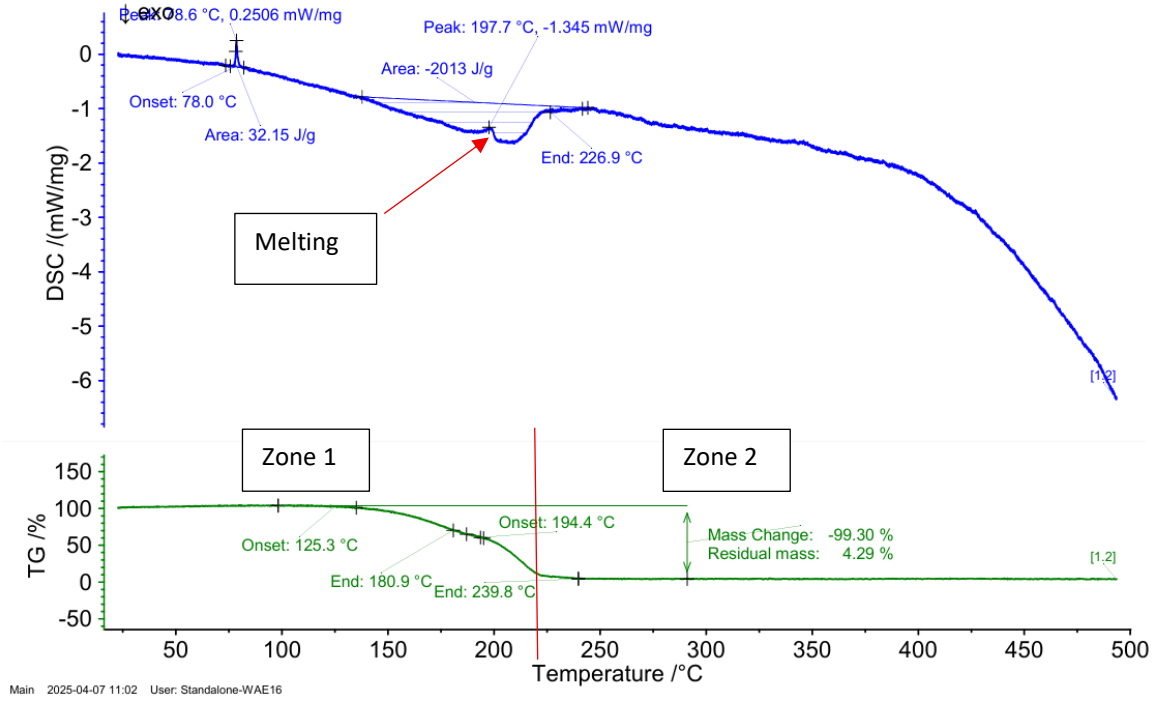

Figure 29. Thermogram of Aged Comp B (Machined) (1 °C/min)

point of RDX contained within the Comp B would be lower, between 127 – 187 °C due to the liquified molten TNT. (Hobbs et al, 2012) Therefore, this study believes that such endothermic reaction could be related to the melting of an unknown composition which had a higher melting point than RDX.

The current study further postulates that the endothermic reaction, shown in Figure 28 and 29, could be due to the melting of a RDX related impurity which later could be used to produce another explosive known as the His Majesty's Explosive or High Melting-point Explosive (HMX). The difference between the current result and the study by Singh et al. could be due to the type of RDX crystals that the aged Comp B contained. According to the current

standard, the type II RDX could contain as much as 17 % of HMX content by weight, while the type I RDX only contained no more than 5 % of HMX content by weight. (NATO AOP 4022, 2023)

The type of RDX crystals contained within the current study sample could be further deduced by using the TGA. The study by Khichar et al. suggested that the last remaining mass of the sample in the TGA which had a different mass loss rate and could correspond to the potential HMX impurity level contained within the Comp B. (Khichar et al, 2019) As illustrated in Figure 29., the TGA of the aged Comp B could be divided into two zones at approximately 220 °C, according to Khichar et al., the Zone 2 mass loss rate was attributed by the HMX content in the sample.

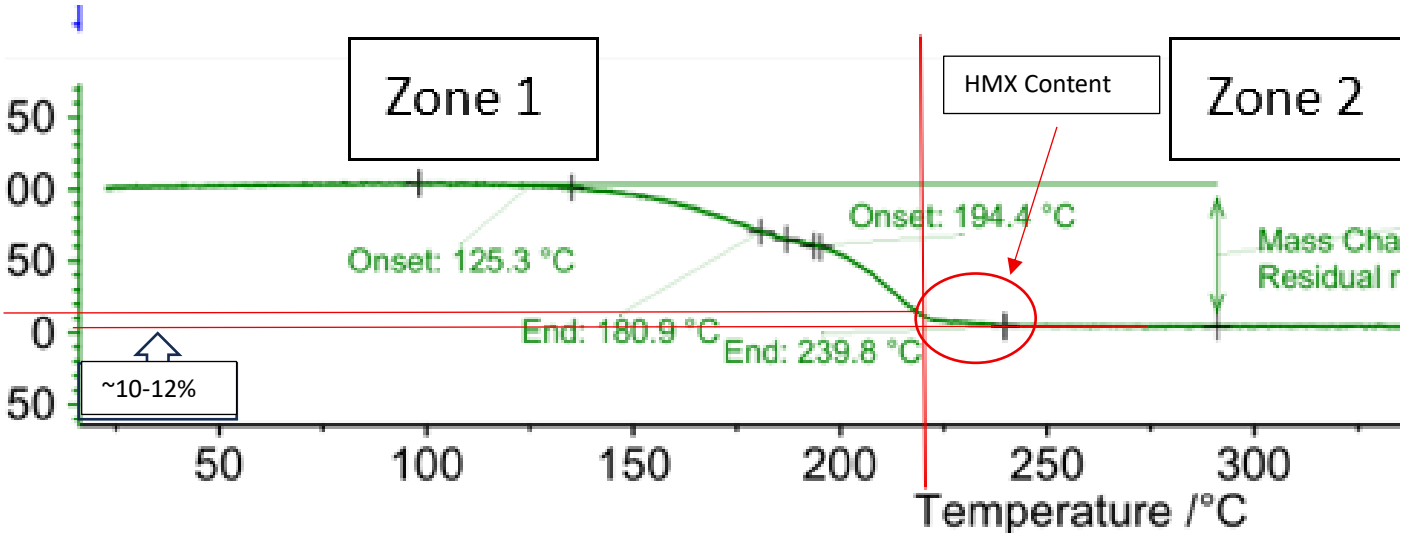

Figure 30. TGA of Aged Comp B (Machined) (1 °C/min)

From Figure 30, the HMX content in the aged Comp B sample could be estimated to be approximately 10 – 12 %. Akhavan pointed out that the impurity level in the RDX is specifically linked to the early manufacturing using the Bachmann process. The RDX produced from the Bachmann process is known to contain impurities between 8 -12 % which this impurity is later

characterized as the HMX. (Akhavan, 2011) Notably, the HMX was first isolated from the RDX impurity in 1942, and the mass production of HMX in military application did not start until the late 1950s. (Homburg, 2017) Hence it is believed that the RDX contained in the current Comp B sample was synthesized using the Bachmann process. Based on the percentage of HMX content it contains, it could be deducted that the RDX is a Type II specification which contains between 4 – 17 % of HMX according to current standard. (NATO AOP 4022, 2023)

Based on the current results, this study concludes that there is no evidence to suggest the aging impact on the Comp B explosive will endanger the CAF for the proposed use. In addition, this study noted that a lower grade of TNT was used for the purpose of explosive binder when compared to the aged TNT found in the booster section. The thermogram of the aged Comp B revealed an unknown endothermic reaction when compared with other literature. The current study further postulates that the endothermic reaction could be due to the HMX content contained in the sample. This study results suggested that the Comp B sample from the 105 mm calibre HE nature projectile contained the Type II RDX which contained approximately 10 – 12 % of HMX content by weight. This is in agreement with the modern defined standard the RDX crystals. Despite of the fact that these munitions were manufactured in 1954, the purity level of the material would still meet the current standard. The percentage of HMX contained in the aged Comp B sample corresponded to the literature reported level for RDX that were synthesized using the Bachmann process.

4.4 Manufacture Defect in the Comp B Filling

Current Canadian defence regulations require a fulsome safety assessment to be completed prior to the introduction of a new ammunition for the CAF use. (DAOD 3002, 2025)

In addition, such a safety assessment is based on the anticipated concept of operation against a known Life Cycle and Environmental Profile (LCEP). As part of the assessment process, the ammunition will be exposed to various environmental stresses such that their robustness in design and material quality can be validated. (NATO AAS3P-11, 2017)

The X-ray photograph results indicated that all HE nature projectiles have a poor quality of production. They contained varying degrees of concentrations of black shadows on the photographs towards the nose section. While these shadows are visually characterized by their appearance and colour scale on the photographs, each of them individually represents a pocket of relatively lower material density when compared to the surrounding explosive materials. They are also known as cavities and are considered as material defects from manufacturing. Such defects are a dangerous phenomenon due to the excessive gun launch setback force which could lead to in-bore detonation accidents. (Baker, 2018) Therefore, the appearance of these cavities in the HE nature of the 105 mm recoilless ammunition would pose a major safety risk for the gun crew, and they would have been rejected for service due to such defects according to the current standard.

As early as 1924, the problem of cavities in the upper portion of the projectile was recognized as the temperature differentials on the solidification of TNT would produce occluded air and shrinkage. (Hawkes, 1924) Hawkes found that the cavities were primarily made up of air in the case of TNT casting shells and could be prevented by using remediations such as heating up the shell to reduce the temperature differential and the use of risers for the air pocket to escape. (Hawkes, 1924) The current subject munition contained the Comp B filling which was a TNT-base casting explosive, and it consisted of TNT and RDX. The problem of TNT

cavities had been well researched and understood as early as 1924 by Hawkes. Therefore, the appearance of such defect in the current study, which was 30 years after Hawkes work, was an unusual occurrence.

According to Kuranda et al., the ammunition manufacturing process in the US during the Korean conflict was largely unchanged from what was known as the melt-load process used in the WWII. The Comp B explosive was heated to slightly above the melting point of TNT, and then the hot liquid explosive mixture was poured into empty projectile shells by gravity. The cooling and solidification of the liquid explosive was by natural conditions. (Kuranda et al, 2009) Since the cooling was provided by the ambient temperature, the material solidification would start from the outer layer which was in contact with the inner surface of the shell body. Such that, there existed a temperature gradient between the material at the core of the shell and the material solidified at the outer layer. Due to the uncontrolled ambient thermal cycling, the outer layer temperature of the filled shell was solidified first, and the warm explosive materials and air would be trapped inside the core of the projectile. Thus, forming cavities. (Kumar and Rao, 2014)

The current X-ray images revealed no break or gap between the fillings which could be suggested that the manufacturer used the single pour filling technique which all the explosive filling was poured in at the same time. The cavities were noted in the upper region of the projectile which is on agreement with the modelling simulation conducted by Kuman and Rao. Therefore, this study believes the formation of cavities in the current 105 mm calibre HE munitions was due to the temperature differential between the hot Comp B explosives and the uncontrolled ambient cooling during the solidification process. Additionally, the current subject

munitions are believed to be one of the last remaining munitions that were produced by the melt-load process and thus contain the cavity defect. The new process which was known as the Single Pour Controlled Cooling (SPCC) method was adopted in the late 1956 in the US. The SPCC pre-heats the shells prior to loading which eliminates the temperature differential between the shell and the explosive during solidification and therefore improves the quality of production. (Kuranda et al, 2009)

Despite the cavity defect in the HE munitions, they were believed to have functioned safely. While the exact material specification can not be located, Baker pointed out that, the acceptable criterion from a radiographic examination is often based on historical precedent with unknown methodology. (Baker, 2018) Considering the main design advantage of the recoilless weapon was to reduce the gun launch setback and to increase its mobility on the battlefield (Olcer and Levin, 1976), it is believed that these cavities would not have caused in-bore detonation accidents due to the open chamber weapon design. Part of the gun launch pressure from the propellant is re-directed to the rear to achieve the recoilless effect of the weapon system. (Olcer and Levin, 1976) These cavities are concentrated in the nose section which would experience relatively less setback force when compared to the cavities formed at the base of the projectile. (Baker, 2018) According to CNR, the ammunition was in used until 2015. (Evens, 2024) Although, there were known accidents related to the use of the recoilless ammunition in the late 1990s and in the early 2000s during the avalanche control service; the accidents were attributed to the defect at the base of the projectile, not the cavity in question. (Abromeit, 2004) In addition, historical records revealed that the US ammunition supply program was experiencing a major shortage in 105 mm recoilless munitions throughout the

Korean conflict. The shortage was caused by the demilitarization of WWII-era munitions and increased demand from the production of new munition types such as the recoilless munitions. (Joint Munition Command, 2010) Thus, the quality of production is believed to have relaxed at the time of manufacturing to allow the cavities to remain in the Comp B fillings for the HE nature recoilless munitions.

To summarize, the cause of the cavities in the HE nature munitions are due to the temperature differential between the Comp B fillings and the uncontrolled ambient cooling. These HE nature munitions were manufactured using the WWII melt-load process which predates the temperature controlled SPCC method in the US. Despite the manufacture defect, these munitions were believed to have functioned safely due to the weapon design and the location of the cavitations where they would experience relatively less gun launch force. Coupling with the wartime ammunition shortage, the product quality is believed to have been relaxed in order to accept the defective munitions into active service.

Chapter 5 Conclusion and Future Studies

In the current study, the chemical aging effects and the influence on manufacturing of high explosives has been investigated using live aging samples from the Korean war era surplus. These munitions have been in storage conditions in excess of 70 years. Due to safety concerns, the propellants were immediately disposed at CFAD Dundurn upon arrival. However, the CAF proposed to reuse the projectiles containing high explosives and the fuze element for EOD training. Based on the results, the current study concludes that, despite of its age and minimal visible signs of aging deteriorations, the explosive contents remain chemically stable. There is no evidence to suggest these materials would endanger the personnel with the proposed use as EOD target training munitions by CAF.

The aged TNT was found to have shown signs of thermal damaging on the surface by SEM imaging, such that, the friction resistance of the TNT was reduced when compared to the modern TNT. The activation energy of the aged TNT sample was found to be 174 ± 31 kJ/mol with an R square value of 0.86 using the Kissinger method. However, non-linear properties were noted which could contributed to the low R square value. The aged TNT composition analysis using the GC-MS revealed low content of impurities. The aged Comp A-3 was found to contain minimal measurable differences with respect to aging in the ambient conditions while the aging of TNT within the Comp B had a predominant effect on the aging behaviour of the Comp B.

The actual performance of the materials has not been evaluated with respect to long-term aging impacts, such as measuring the velocity of detonation or pressure. The method of research in the current study has focused on the chemical and physical stability of the explosive

materials with reference to the application of explosive inventory and safety management. While this study revealed notable sensitivity variations as a result of the aging in the ambient conditions, the impact to the explosive performance and their related properties have not been investigated. Further studies should investigate the impact on the performance of the explosives with respect to long-term ambient aging and conduct composition analysis using a different method such as the HPLC to improve accuracy on the results.

Driven by cost-saving measures, limiting environmental contamination initiatives, or wartime shortage, the concept of energetic material re-utilization or ammunition life extension has always been a subject of interest within the ammunition and explosive community. The current ammunition management assigns the shelf life based on the weakest component within the ammunition. While the current work has found no evidence to suggest any comprises in the safe storage and handling of the aged explosives, future work should continue the investigation to integrate the current knowledge into the lifecycle management of other aged munitions and the potential re-utilization of the energetic materials.

In conclusion, the current study revealed serval notable sensitivity variations to the high explosives exposed in the ambient aging environment. Further studies are recommended to continue in the investigation of the aging related impacts on the explosive performance and the integration of current knowledge into the CAF lifecycle management and potential re-utilization of the energetic materials.

Chapter 6 References

Abromeit, D. (2004), *Military Weapons for Avalanche Control Program*, USDA Forest Service National Avalanche Center, https://arc.lib.montana.edu/snow-science/objects/issw-1990-167-174.pdf

Agrawal, J.P. (2010), *High Energy Materials: Propellants, Explosives and Pyrotechnics*, Wiley-VCH

Ahmad et al. (2016), *Thermal Decomposition and Kinetic Evaluation of Decated 2,4,6-Trinitrotoluene (TNT) for Reutilization as Composite Material*, IOP Conference Series: Materials Science and Engineering, DOI:10.1088/1757-899X/146/1/012032

Akhavan, J. (2011), *The Chemistry of Explosive*, 3rd Ed, RSC Publishing

Armourguy (2018), 1/6th Scale M27 Recoilless Rifle Project, Fine Scale Modeler, https://forum.finescale.com/t/1-6th-scale-m27-recoilless-rifle-project/248567

Bachmann, W.E. and Sheehan, J.C., (1949). A new method of preparing the high explosive RDX. *Journal of the American Chemical Society*, *71*(5), pp.1842-1845. doi: 10.1021/ja01173a092

Baker et al. (2020), *TNT Exudation, Crystal Growth, and Aging*, Munition Safety Information Analysis Center (MSIAC)

Baker, E. (2018), *Laboratory Setback Activators and Explosive Suitability for Gun Launch*, MSIAC, DOI:10.5604/01.3001.0013.0793

Batten, J.J. & Murdie, D.C. (1969), *The Thermal Decomposition of RDX at Temperatures Below the Melting Point: I. Comments on the Mechanism*, CSIRO Publishing, https://doi.org/10.1071/CH9700737

Batten, J.J. & Murdie, D.C. (1969), *The Thermal Decomposition of RDX at Temperatures Below the Melting Point: II. Activation Energy,* CSIRO Publishing, https://doi.org/10.1071/CH9700749

Batten, J.J. (1971), *The Thermal Decomposition of RDX at Temperatures Below the Melting Point: III. Towards the Elucidation of the Mechanism*, CSIRO Publishing, https://doi.org/10.1071/CH9710945

Batten, J.J. (1971), *The Thermal Decomposition of RDX at Temperatures Below the Melting Point: IV. Catalysis of the Decomposition by Formaldehyde*, CSIRO Publishing, https://doi.org/10.1071/CH9712025

Batten, J.J. (1972), *The Thermal Decomposition of RDX at Temperatures Below the Melting Point: V. The Evolution of Occluded Volatile Matter Prior to the Decomposition, and the Influence of Past History of the Sample on the Rate of Decomposition*, CSIRO Publishing, https://doi.org/10.1071/CH9722337

Bednar et al. (2011), *Analysis of Munitions Constituents in Groundwater using a Field-Portable GC-MS*, Elsevier, doi:10.1016/j.chemosphere.2012.01.042

Beauregard, R.L. (1971), In Bore Detonation of Projectiles in Navy Large Calibre Guns, The History of Insensitive Munitions, https://www.insensitivemunitions.org/history/in-bore-premature-detonation-of-projectiles-in-navy-large-caliber-guns/

Blaine, R.L. and Kissinger H.E. (2012), *Hommer Kissinger and the Kissinger Equation*, Thermochnimica Acta, https://doi.org/10.1016/j.tca.2012.04.008

Brassard, M. (2024), Personal Communication

Brady et al. (2017), *Polymorphic Phase Control of RDX-Based Explosives*, Applied Spectroscopy, DOI: 10.1177/0003702817712259

Brill, T.B. and James, K.J. (1993), Thermal Decomposition of Energetic Materials. 62. Reconciliation of the Kinetics and Mechanisms of TNT on the Time Scale from Microseconds to Hours, ACS Publications, doi: 10.1021/j100136a018

Bohn, M.A. (2017), *Principles of Aging of Double Base Propellants and Its Assessment by Several Methods Following Propellant Properties*, Fraunhofer Institute of Chemical Institute, NATO

Borne et al. (2004), Energetic Materials: Particle Processing and Characterization, Chapter 9 Microstructure and Morphology, https://doi.org/10.1002/3527603921.ch9

Bowden, F.P. and Gurton, O.A. (1949), Initiation of Solid Explosives by Impact and Friction: the Influence of Grit, Royal Society of London, https://doi.org/10.1098/rspa.1949.0105

Canadian Joint Operational Command (CJOC) (2019), *Briefing Note to Comd CJOC Ref CN Rail Requesting for CAF Support in Disposing of Ammunition*, CAF

Celina et al. (2005), *Accelerated Aging and Lifetime Prediction: Review of non-Arrhenius Behaviour due to Two Competing Processes*, Elsevier, https://doi.org/10.1016/j.polymdegradstab.2005.05.004

Cline, C. (2024), Personal Communication

Cohen et al. (2007), *Mechanism of Thermal Unimolecular Decomposition of TNT (2.4.6-Trinitrotoluene): A DFT Study*, Journal of Phys. Chem., doi: 10.1021/jp072121s

Cooper, P.W. (1996), *Explosives Engineering*, Wiley-VCH

Cooper, P.W. & Kurowski, S.R. (1996), *Introduction to the Technology of Explosives*, Wiley-VCH

Dattelbaum et al. (2013), Chemical Stability of Molten 2,4,6-Trinitrotoluene at High Pressure, Applied Physics Letters 104, https://doi.org/10.1063/1.4860395

Defence Administrative Orders and Directives (DAOD) 3002, *Ammunition and Explosives*

Druet, L. & Asselin, M. (1988), *A review of stability test methods for gun and mortar propellants*, *the chemistry of propellant ageing*, Journal of Energetic Materials, 6:1-2, 27-43, DOI: 10.1080/07370658808017235

Druet. L. & Asselin, M. (1988), *A review of stability test methods for gun and mortar propellants, II: Stability testing and surveillance*, Journal of Energetic Materials, 6:3-4, 215-254, DOI: 10.1080/07370658808012555

Dylong et al. (2022), *Impact of TNT Storage Time on Its Physiochemical and Explosive Properties*, Materials Research Proceedings, https://doi.org/10.21741/9781644902059-21

Edward, J.T. (1942), *The Preparation of R.D.X. by the McGill Process*, McGill University, https://escholarship.mcgill.ca/concern/theses/8623j214t

Environmental Protection Agency (EPA) Method 8330B, *Nitroaromatics, Nitramines, and Nitrate Esters by High Performance Liquid Chromatography (HPLC)*

Evens, T. (2024), Personal Communication

Eyster, E.H. & Weltman, C.A. (1945), *The Preparation and Properties of RDX-Composition A*, National Defence Research Committee of the Office of Scientific Research and Development, https://apps.dtic.mil/sti/citations/tr/ADB279221

Field, J.E. (1992), *Hot Spot Ignition Mechanisms for Explosives*, ACS Publications, doi: 10.1021/ar00023a002

Fisher, R.J. (1989), *A Severe Human ESD Model for Safety and High Reliability System Qualification Testing*, Sandia National Laboratory, https://www.jpyro.co.uk/wp-content/uploads/j06_FULL_rnrn.pdf#page=59

Furman et al. (2014), *Decomposition of Condensed Phase Energetic Materials: Interplay between Uni- and Bimolecular Mechanisms*, ACS Publications, doi: 10.1021/ja410020f

Gawrysiak, E. & Jarosz, T. (2021), *2,4,6-Trinitrotoluene: Review of Production Methods and Applications*, Silesian University of Technology, Gliwice, Poland, https://essuir.sumdu.edu.ua/bitstream-download/123456789/98602/1/Gawrysiak_trinitrotoluene.pdf;jsessionid=6D4F3DDF5B4F9C343946A94665A71CFE

Gershanik et al. (2010), *Sublimation Rate of Energetic Materials in Air: RDX and PETN*, Journal of Physical Chemistry, Israel, https://doi.org/10.1002/prep.201100038

Geneva International Centre for Humanitarian Demining (2019), *Vietnam Ageing Study Management of Explosive Remnants of War (MORE)*, Global CWD Repository 1235, https://commons.lib.jmu.edu/cisr-globalcwd/1235

Gillespie et al. (1948), *Aromatic Nitration*, Quarterly Reviews, Chemical Society, https://doi.org/10.1039/QR9480200277

Gorzynski, C.S. and Maycock, J.N. (1974), *Explosives and Pyrotechnic Propellants for Use in Long Term Deep Space Missions*, Martin Marietta Laboratories, Baltimore, Maryland, https://doi.org/10.2514/3.62044

Hariri et al. (2019), *Purification of 2,4,6-Trinitrotoluene by Digestion with Sodium Sulfite and Determination of its Impurities by Gas Chromatography – Electron Capture Detector (GC-ECD)*, Journal of the Iranian Chemical Society, https://doi.org/10.1007/s13738-019-01709-z

Harris, D.C. (2010), *Quantitative Chemical Analysis*, 8th Ed, W.H. Freeman and Company, New York

Hawkes, F. (1924), *The Malfunctioning of Ammunition*, National Defense Industrial Association, https://www.jstor.org/stable/45481237

Hites, R.A. (1997), *Gas Chromatography Mass Spectrometry*, Handbook of Instrumental Techniques for Analytical Chemistry, https://diverdi.colostate.edu/all_courses/handbook%20of%20instrumental%20techniques%20for%20analysis/ch31.pdf

Hobbs et al. (2012), *Cookoff of a Melt-Castable Explosive (Comp-B)*, Sandia National Laboratories, https://www.osti.gov/servlets/purl/1116169

Hobbs et al. (2019), *RDX Solubility in TNT at High Temperatures*, Sandia National Laboratories, https://www.osti.gov/servlets/purl/1574437

Holmgren et al. (2005), *Determination and Characterization of Organic Explosives using Porous Graphitic Carbon and Liquid Chromatography – Atmospheric Pressure Chemical Ionization Mass Spectrometry*, Elsevier, https://doi.org/10.1016/j.chroma.2005.08.088

Homburg, A. (2017), *Remarks on the Evolution of Explosives*, Prop., Explos., Pyrotech., 42: 851-853. https://doi.org/10.1002/prep.201780831

Hopewell, S. & Betts, P. (2000), *Reutilization of Downloaded Supplementary Charges for the Production of 155mm HE M795, M107 Projectiles and Other High Explosive (HE) Loaded Projectiles*, US Army Armament Research Development Center, https://apps.dtic.mil/sti/citations/tr/ADA532587

James, E. (1965), *The Development of Plastic Bonded Explosives*, Lawrence Radiation Laboratory, University of California, https://www.osti.gov/servlets/purl/4612485

Joint Munitions Command (2010), *History of the Ammunition Industrial Base*, https://www.jmc.army.mil/Docs/History/History_of_the_Ammunition_Industrial.pdf

Kelly, J. (2004), *Gunpowder - Alchemy, Bombards, & Pyrotechnics: The History of the Explosive that Changed the World*, Basic Books

Kennedy, J.E. (2010), *Spark and Laser Ignition*, Shock Wave Science and Technology Reference Library, DOI 10.1007/978-3-540-87953-4_11

Khichar et al. (2019), *Comparative Analysis of Vaporization and Thermal Decomposition of Cyclotrimethylenetrinitramine (RDX)*, Journal of Propulsion and Power, https://doi.org/10.2514/1.B37643

Kirchner et al. (1993), *Occupational Health: The Soldier and the Industrial Base*, Chapter 10 Combustion Products of Propellants and Ammunition, US Department of the Army

Kirshenbaum, M.S. & Avrami, L. (1984), *The Effect of Aging on the Properties of Composition B*, US Army Armament Research and Development Center, https://apps.dtic.mil/sti/pdfs/ADA139611.pdf

Kogelbauer et al. (2000), *Solid Acids as Substitutes for Sulfuric Acid in the Liquid Phase Nitration of Toluene to Nitrotoluene and Dinitrotoluene*, Elsevier, https://doi.org/10.1016/S0920-5861(99)00234-5

Kroger, M. & Fels, G. (2000), *C-TNT Synthesis Revisited*, Journal of Labelled Compounds and Radiopharmaceuticals, Paderborn, Germany, https://doi.org/10.1002/(SICI)1099-1344(20000315)43:3<217::AID-JLCR305>3.0.CO;2-U

Kumar, A.S. and Rao, V.D., (2014), Modeling of Cooling and Solidification of TNT Based Case High Explosive Charges, Naval Science and Technology Laboratory, India, DOI : 10.14429/dsj.64.4673

Kuranda et al. (2009), Army Ammunition Production During the Cold War (1946 – 1989), US Army Environmental Command, https://aec.army.mil/Portals/115/CR_Army_Ammo_Prod_During_Cold_War_1946-1989.pdf?ver=o4qC_4pp_1VM0oYqJaRIjA%3d%3d

Lussier, L.S. & Gagnon, H. (1996), *Development of Modern Methods for Determination of Stabilizers in Propellants*, Defence Research Establishment Valcartier, Quebec, https://apps.dtic.mil/sti/tr/pdf/ADA637697.pdf

Long et al. (2001), *Autocatalytic Thermal Decomposition Kinetics of TNT*, Elsevier, https://doi.org/10.1016/S0040-6031(02)00031-X

Macek, A. (1961), *Sensitivity of Explosives*, Atlantic Research Corporation and US Naval Ordnance Laboratory, doi: 10.1021/cr60215a003

Maksacheff, M. and Whelan, D.J. (1986), *Thermochemistry of Normal and Basic Lead Styphnates using Differential Scanning Calorimetry*, Defence Science and Technology Organization, Melbourne, Victoria, https://apps.dtic.mil/sti/pdfs/ADA174717.pdf

Manelis et al. (2003), *Thermal Decomposition and Combustion of Explosives and Propellants*, Taylor and Francis

May et al. (1969), *A Glass Transition in Trinitrotoluene*, Australia Defence Scientific Service, https://doi.org/10.1016/0022-0248(69)90063-3

Miles, K. K. (1972). *The thermal decomposition of RDX* (Doctoral dissertation, Monterey, California. Naval Postgraduate School), https://calhoun.nps.edu/server/api/core/bitstreams/620e2ae6-91a6-4794-b457-ce994d4f36f0/content

Mohammed, A. and Abdullah, A. (2018), *Scanning Electron Microscopy (SEM): A Review*, Proceedings of the 2018 International Conference on Hydraulics and Pneumatics, https://fluidas.ro/hervex/proceedings2018/77-85.pdf

Munition Safety Information Analysis Center (MSIAC) Accident Database Exchange (MADx) (1998), Accident 8981, Marion, Illinois

Murry, P. and White, J. (1954), *Kinetics of Clay Dehydration*, Atomic Energy Research Establishment, Harwell, https://web.archive.org/web/20160527093346id_/http://www.minersoc.org/pages/Archive-CM/Volume_2/2-13-255.pdf

MSIAC (2020), High Explosive (TNT, Comp A3, Tetryl) Aging Effects

MSIAC MADx (2007), *Accident 10482*, Milan, Tennessee

MSM Group (2025), *Image: 105mm HE R-105-60*, https://www.msm.sk/en/produkt/105-mm-he-r-105-60-en/

Muraour, H. & Munroe, C. (1924), *The Purification of TNT*, National Defense Industrial Association, https://www.jstor.org/stable/45484735

Mundy, R.A. & Spencer, J.R. (1981), *TNT Purification Studies*, US Army Armament Research and Development Command, DOI: 10.21236/ADA109719

Narang et al. (1993), *Storage Life of an Aluminised HE Composition*, Explosive Research and Development Laboratory, https://pdfs.semanticscholar.org/b160/243640e03e25db21b44310fd3f7de7d10cc9.pdf

NATO AAS3P-11 (2017), *Safety and Suitability for Service Assessment Testing for Surface and Underwater Launched Munitions*, Edition A Version 1

NATO (2009), *Allied Environmental Conditions and Test Publication (AECTP) 230, Climatic Conditions*, 1st Ed

NATO (2003), *Allied Ordnance Publication (AOP) 7, Manual of Data Requirements and Tests for the Qualification of Explosive Materials for Military Use*, 2nd Ed

NATO (2011), *Allied Ordnance Publication (AOP) 26, NATO Catalog of Qualified Explosives*, 3rd Ed Rev 1

NATO (2022), *Allied Ordnance Publication (AOP) 46, The Scientific Basis For the Whole Life Assessment of Munitions*, Edition B, Version 1

NATO (2008), *Allied Ordnance Publication (AOP) 48, Explosives, Nitrocellulose-Based Propellants, Stability Test Procedures and Requirements Using Stabilizer Depletion*

NATO (2023), *AOP-4022, Energetic Materials, Specification for RDX (Cyclotrimethylenetrinitramine)*

NATO (1991), *Standardization Agreement (STANAG) 4025, Specification For TNT (Tolite) For Deliveries From One NATO Nation to Another*, 3rd Ed

NATO (2009), *Standardization Agreement (STANAG) 4487, Explosive, Friction Sensitivity Tests*, 2nd Ed

NATO (2007), *Standardization Agreement (STANAG) 4582, Explosives, Nitrocellulose Based Propellants, Stability Test Procedure and Requirements Using Heat Flow Calorimetry*

Netherland Public Prosecution Office (2020), *Report Concerning 60mm Mortar Accident Investigations*, https://www.onderzoeksraad.nl/wp-content/uploads/2023/11/bijlage_c_expert_report_heropend_onderzoek_2022_mortierongeval_mali.pdf

Novik, G. and Christensen, D. (2024), *Increased Impact Sensitivity in Ageing High Explosives; Analysis of Amatol Extracted from Explosive Remnants of War*, Royal Society Open Science, https://doi.org/10.1098/rsos.231344

Olah, G. (1970), *Mechanism of Electrophilic Aromatic Substitutions*, Case Western Reserve University, Cleveland, Ohio, doi: 10.1021/ar50043a002

Olcer N.Y. and Levin, S. (1976), *Engineering Design Handbook: Recoilless Rifle Weapon Systems*, Army Material Command, https://apps.dtic.mil/sti/citations/tr/ADA023513

Perla, R. (1976), *High Explosive and Artillery in Avalanche Control, Montana State University*, https://arc.lib.montana.edu/snow-science/objects/issw-1976-042-049.pdf

Parker, R.P. and Wilson, W.S. (1979), *Dimensional Instability of Creamed TNT*, Elsevier, https://doi.org/10.1016/0022-0248(79)90152-0

Payne, C. (2010), *Principles of Naval Weapon Systems*, 2nd Ed, Naval Institute Press

Pimbley, G.H. & Marshall, E.F. (1980), *The Premature Detonation Problem*, Los Alamos Scientific Laboratory, https://doi.org/10.2172/5376921

Pouretedal et al. (2017), *The Kinetic of Mass Loss of Grades A and B of Melted TNT by Isothermal and Non-Isothermal Gravimetric Methods*, Elsevier, https://doi.org/10.1016/j.dt.2017.11.007

Rae, P.J. & Dickson, P.M. (2020), *Some Observations About the Drop-Weight Explosive Sensitivity Test*, Journal of Dynamic Behaviour of Materials, https://doi.org/10.1007/s40870-020-00276-2

Rahaman et al. (2009), *Nitration of Nitrobenzene at High-Concentrations of Sulfuric Acid: Mass Transfer and Kinetic Aspects*, Wiley InterScience, DOI 10.1002/aic.11989

Reinold et al. (2023), *TNT in ammunition shells: an investigation of chemical integrity after artificial aging using Fourier-transform infrared spectroscopy and gas chromatography–mass spectrometry,* Europe PMC, https://doi.org/10.22541/au.168009486.67202787/v1

Renlund et al. (1997), Characterization of Thermally Degraded Energetic Materials, Sandia National Laboratory, https://doi.org/10.2172/629380

Saw, C.K. (2002), *Kinetics of HMX and Phase Transitions: Effects of Grain Size at Elevated Temperature*, University of California, https://www.osti.gov/servlets/purl/15005534

Sanchirico R. and Di Sarli, V. (2024), *Predicting the Shelf Life of Energetic Materials via Kinetic Analysis of Decomposition Data Gathered by Using Thermal Analysis Techniques*, Chemical Engineering Transactions, DOI: 10.3303/CET24111062

Schimmel R.T. and Lowell, S.J. (1963), *Growth of Composition B Type Charges*, Picatinny Arsenal, https://apps.dtic.mil/sti/tr/pdf/AD0404310.pdf

Schleiss, V.G. (1989), *Rogers Pass Snow Avalanche Control – A Summary*, Environment Canada, Canadian Parks Service, http://parkscanadahistory.com/publications/rogers/rogers-pass-snow-avalanche-control.pdf

Sharma et al. (2023), *Effect of Natural Aging on the Safety Parameters and Performance of TNT-based Melt Cast RDX/TNT Compositions*, Central European Journal of Energetic Materials, DOI 10.22211/cejem/168579

Simoens, B. &Lefebvre, M.H. (2024), *Study of the Properties of 100 Years-Old Aged Explosive Compounds*, Journal of Energetic Materials, 42:1, 15-30, DOI: 10.1080/07370652.2021.2017077

Singh et al. (2019), *Thermal Degradation Behaviour and Kinetics of Aged TNT-Based Melt Cast Composition B*, Central European Journal of Energetic Materials, DOI 10.22211/cejem/112234

Spice, J.E. (1964), *Chemical Binding and Structure*, Pergamon Press

Szala, M. (2021), *Polymer-Bonded Secondary Explosives*, Military University of Technology, DOI 10.22211/matwys/0213

Szala, M. (2022), *Natural and Synthetic Waxes in Explosives – A Review*, Military University of Technology, DOI 10.22211/matwys/0225

Todd, S.N. (2020), *Energetic Materials Fundamentals and Applications* [Presentation], Sandia National Lab, https://www.osti.gov/servlets/purl/1766699

Tro, N. (2008), *Chemistry: A Molecular Approach*, 2nd Ed, Prentice Hall

Trzciński et al. (2014), *A Comparison of the Sensitivity and Performance Characteristics of Melt-pour Explosives with TNT and DNAN Binder,* Central European Journal of Energetic Materials, 11(3), 443–455

United Nations (2023), *Manual of Tests and Criteria*, 8th Ed

University of Bristol, *TNT*, https://www.chm.bris.ac.uk/~paulmay/webprojects2001/moorcraft/TNT.htm

US Technical Manual (TM) (1977), TM 43-0001-28, *Artillery Ammunition Guns, Howitzers, Mortars, Recoilless Rifles, Grenade Launchers, and Artillery Fuzes*, Army Ammunition Data Sheets

Voigt, H.W. (1983), *Exudation Test for TNT Explosives under Confinement: Exudation Control and Proposed Standards*, US Army Armament Research and Development Center, https://apps.dtic.mil/sti/citations/tr/ADA125476

Vroom, A.H. (1945), *War Research: The Mechanism of Direct Nitrolysis of Hexamine*, McGill University, https://escholarship.mcgill.ca/concern/theses/2n49t5316

Vyazovkin, S (2008), *Chapter 13 Isoconversional Kinetics*, Handbook of Thermal Analysis and Calorimetry, Elsevier, https://doi.org/10.1016/S1573-4374(08)80016-7

Vyazovkin, S (2020), *Kissinger Method in Kinetics of Materials: Things to Beware and Be Aware of*, MDPI, https://doi.org/10.3390/molecules25122813

Weinheimer, R. (2002), *Properties of Selected High Explosives*, https://www.academia.edu/34451320/Properties_of_Selected_High_Explosives?sm=b

Westheimer, F.H. & Kharasch, M.S. (1946), *The Kinetics of Nitration of Aromatic Nitro Compounds in Sulfuric Acid*, Journal of the American Chemical Society, doi: 10.1021/ja01214a001

Whistler Museum (2016), *The Origins of Avalanche Control on Whistler Mountain*, Whistler Museum and Archives Society, https://whistlermuseum.org/2016/02/13/the-origins-of-avalanche-control-on-whistler-mountain/

Wikipedia (2025), *TNT*, https://en.wikipedia.org/wiki/TNT

Wikipedia (2025), *RDX*, https://en.wikipedia.org/wiki/RDX

Wilson, W.S. (1981), *The Effect of Crystal Orientation on Growth on Polycrystalline TNT*, Defence Science and Technology Organization Materials Research Laboratories, Melbourne, Victoria, https://apps.dtic.mil/sti/tr/pdf/ADA096591.pdf

Wilson, W.S. (1985), *The Effect of Impurities and Additives on the Growth of Polycrystalline TNT*, Defence Science and Technology Organization Materials Research Laboratories, Melbourne, Victoria, https://apps.dtic.mil/sti/tr/pdf/ADA149085.pdf

Yeager et al. (2013), *Microstructural Effects of Processing in the Plastic-Bonded Explosive Composition A-3*, Elsevier, https://doi.org/10.1016/j.matchemphys.2013.01.041

Zhang et al. (2018), Production of High Purity Metals: A Review on Zone Refining Process, Journal of Crystallization Process and Technology, DOI: 10.4236/jcpt.2018.81003

Zhang et al. (2024*), Effects of Aging on Mechanical Sensitivity Threshold and Thermal Decomposition Characteristics of RDX/HMX*, ScienceDirect, https://doi.org/10.1016/j.dt.2024.10.011

Zhou et al. (2007), *Fundamentals of Scanning Electron Microscopy (SEM)*, Spinger, New York, https://doi.org/10.1007/978-0-387-39620-0_1

Appendix A. X-Ray Photography

The following X-ray images are obtained from the 105 mm calibre HE nature projectiles. There are 5 samples in total. The method of imaging is described in Chapter 2.

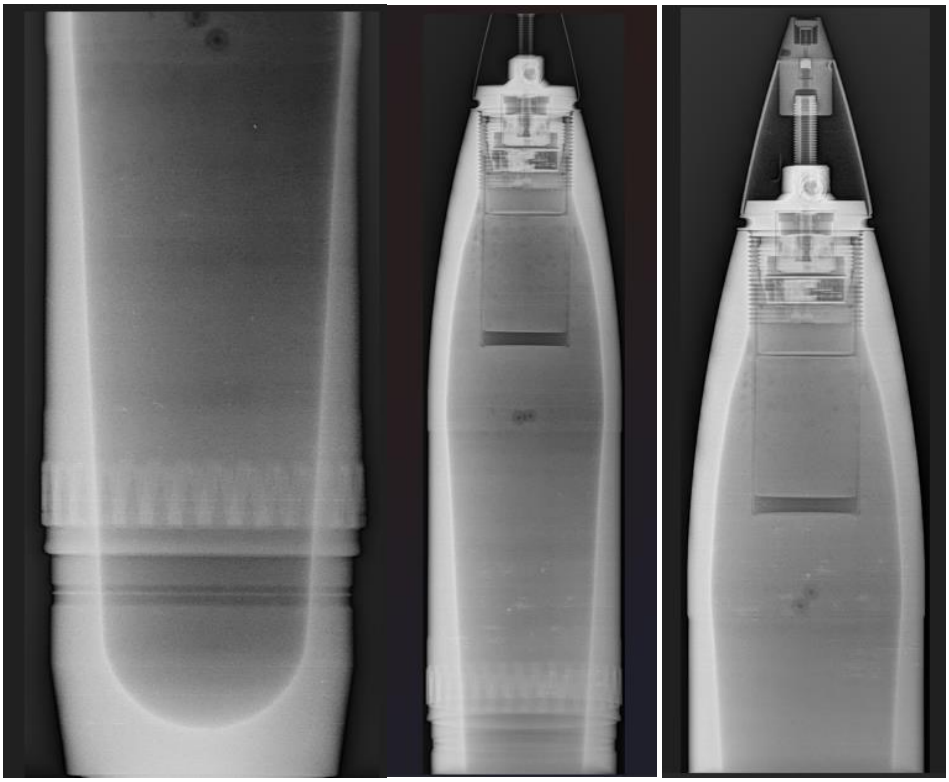

Figure A-1. Sample 1 0° X-Ray Images

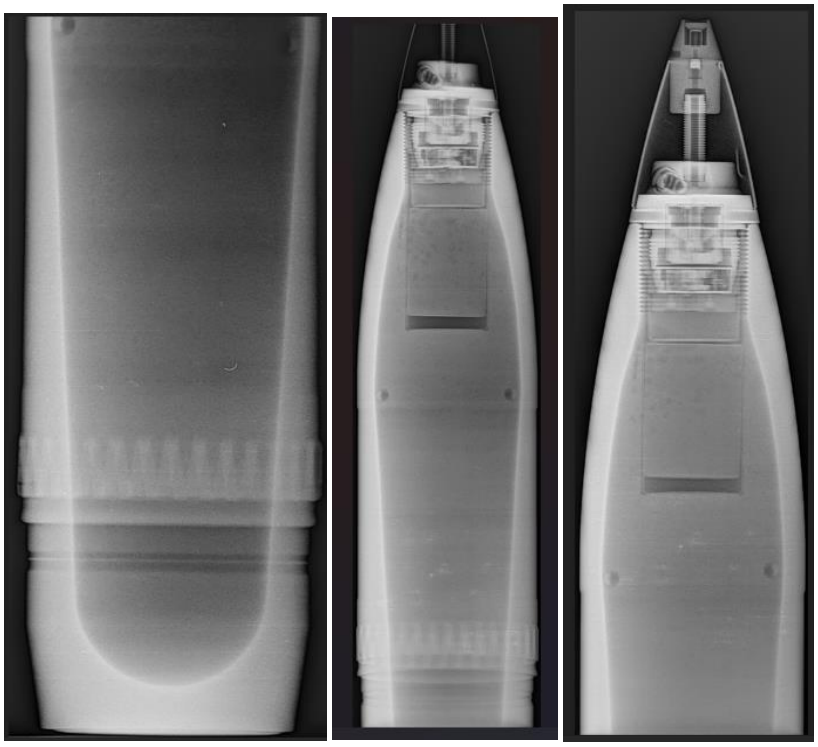

Figure A-2. Sample 1 45° X-Ray Images

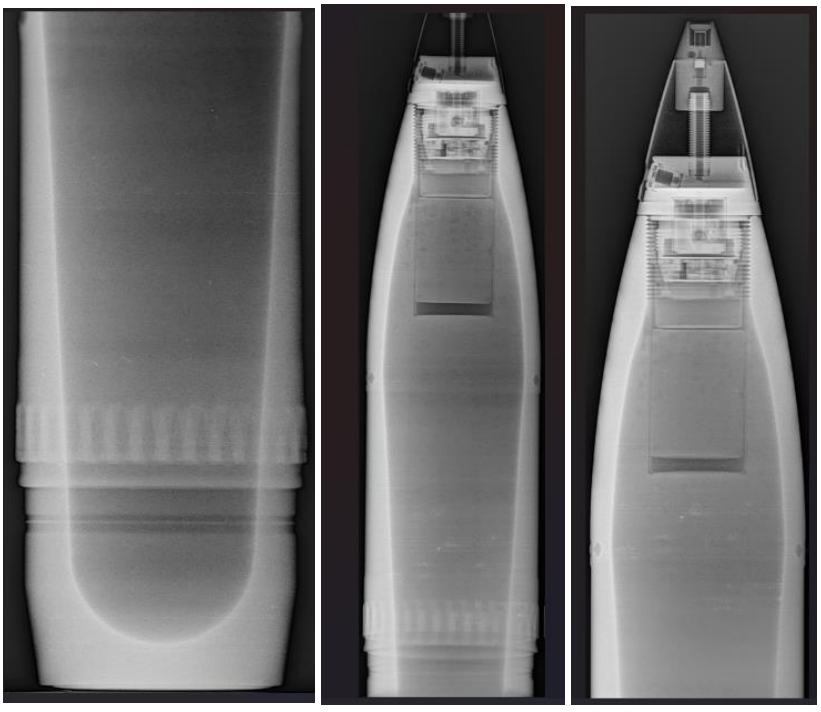

Figure A-3. Sample 1 90° X-Ray Images

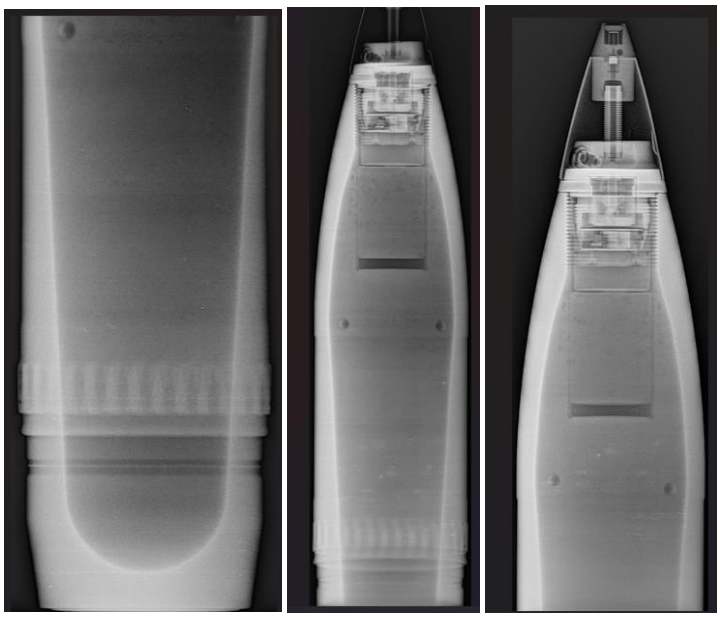

Figure A-4. Sample 1 135° X-Ray Images

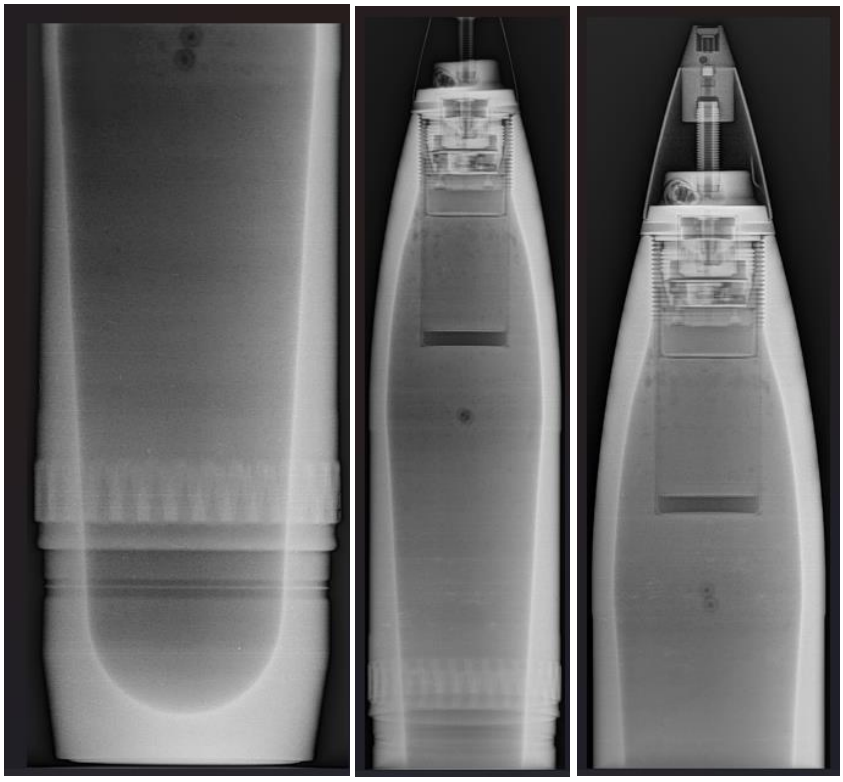

Figure A-5. Sample 2 0° X-Ray Images

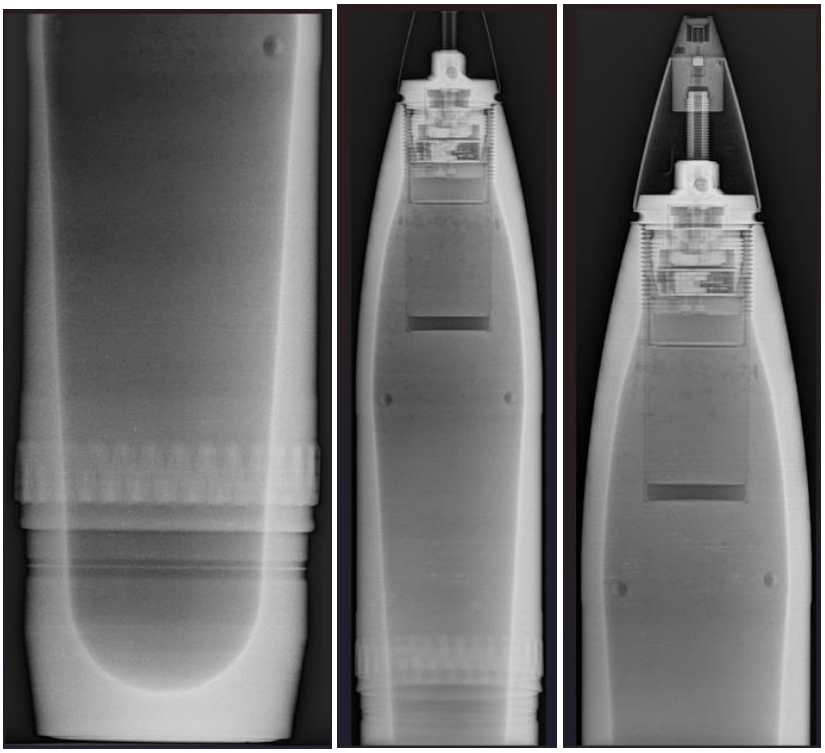

Figure A-6. Sample 2 45° X-Ray Images

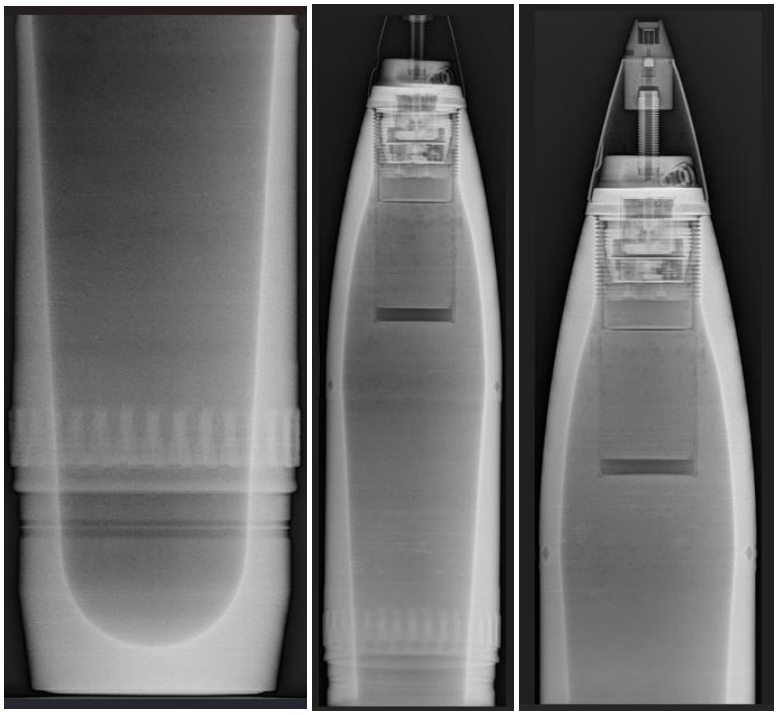

Figure A-7. Sample 2 90° X-Ray Images

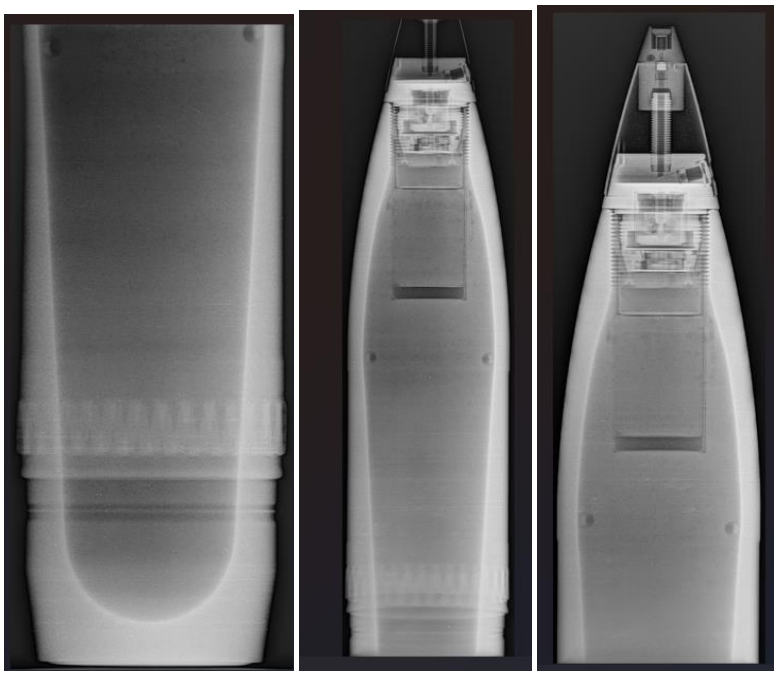

Figure A-8. Sample 2 135° X-Ray Images

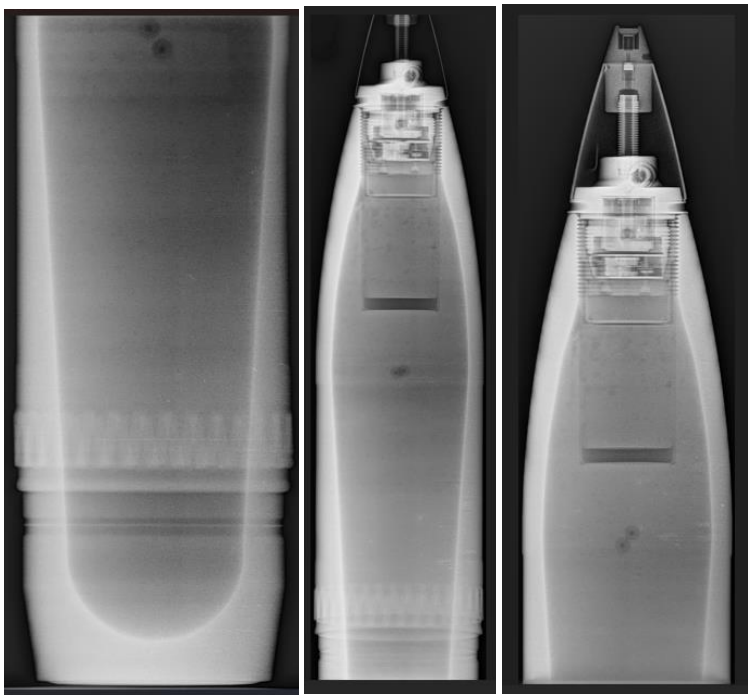

Figure A-9. Sample 3 0° X-Ray Images

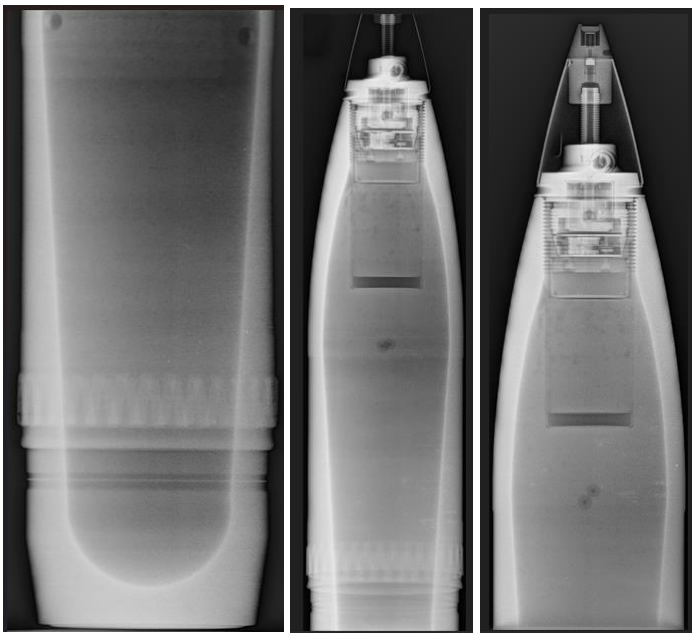

Figure A-10. Sample 3 45° X-Ray Images

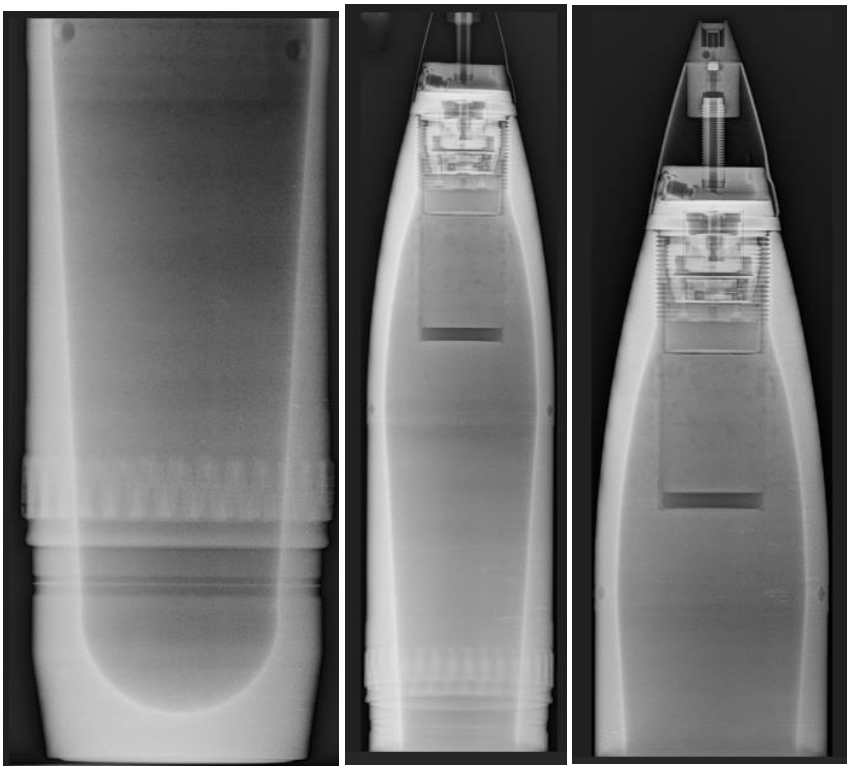

Figure A-11. Sample 3 90° X-Ray Images

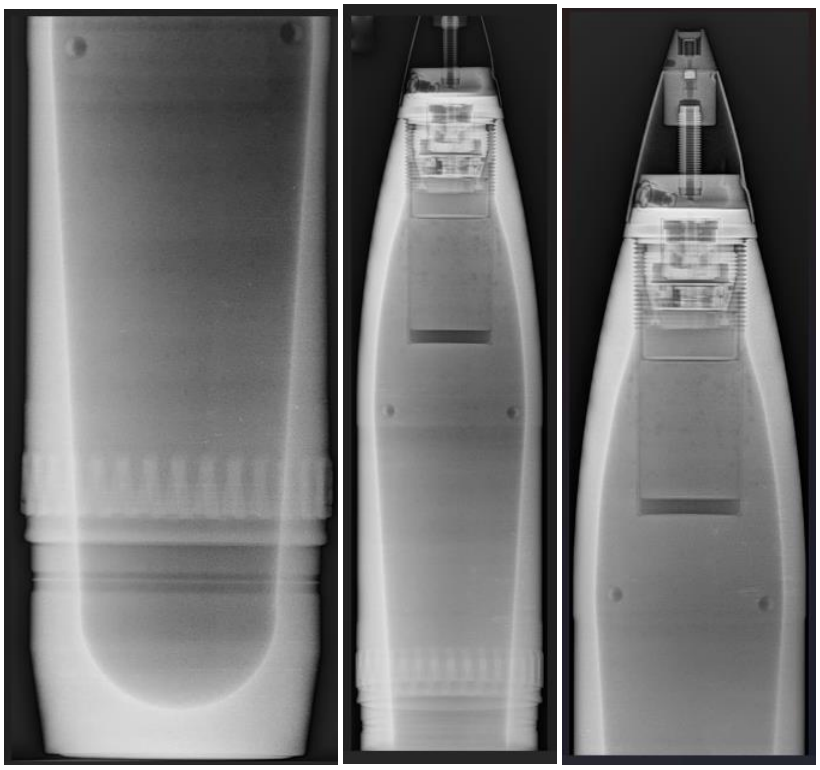

Figure A-12. Sample 3 135° X-Ray Images

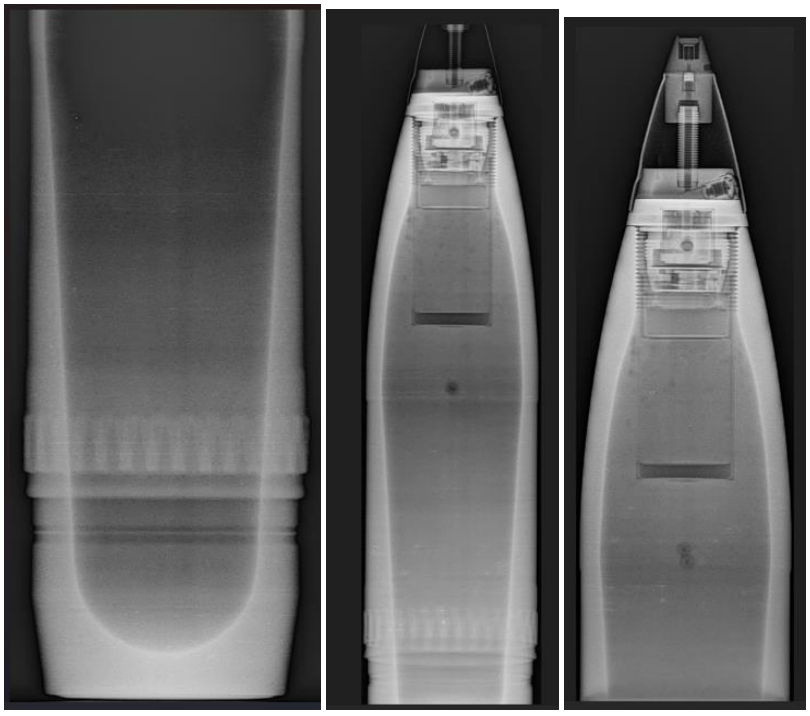

Figure A-13. Sample 4 0° X-Ray Images

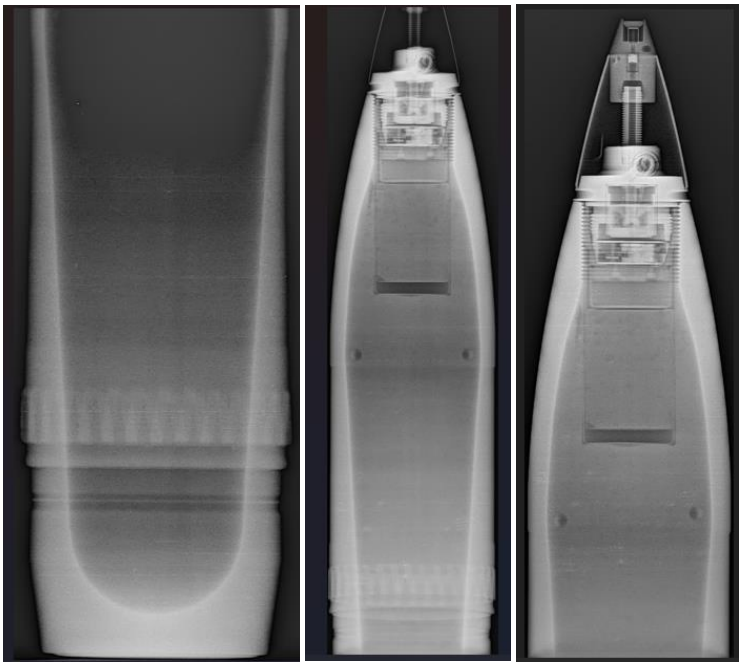

Figure A-14. Sample 4 45° X-Ray Images

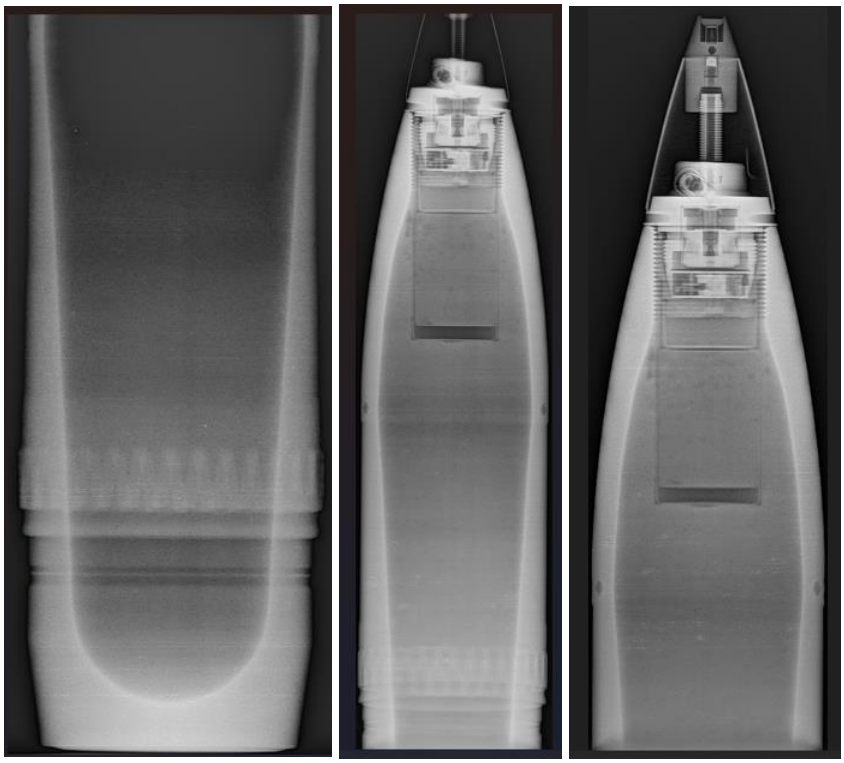

Figure A-15. Sample 4 90° X-Ray Images

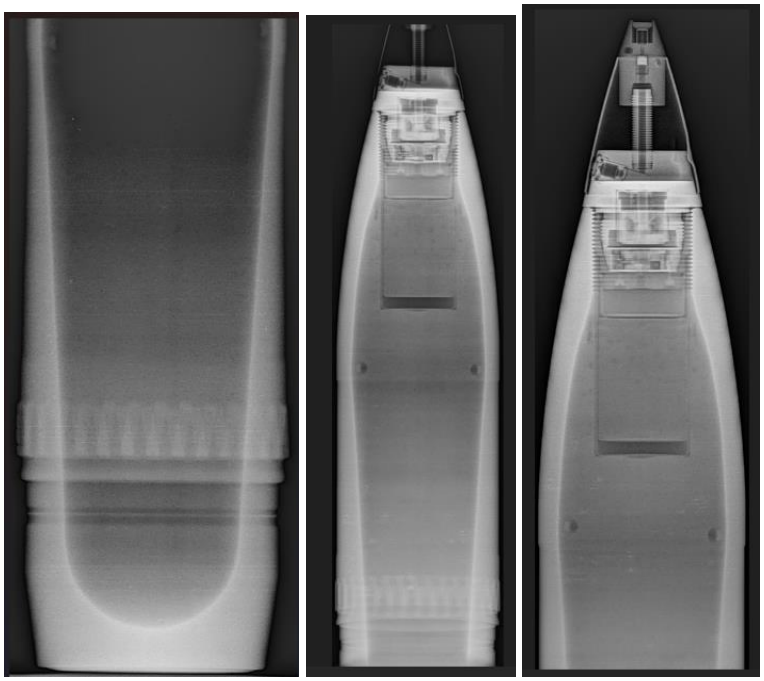

Figure A-16. Sample 4 135° X-Ray Images

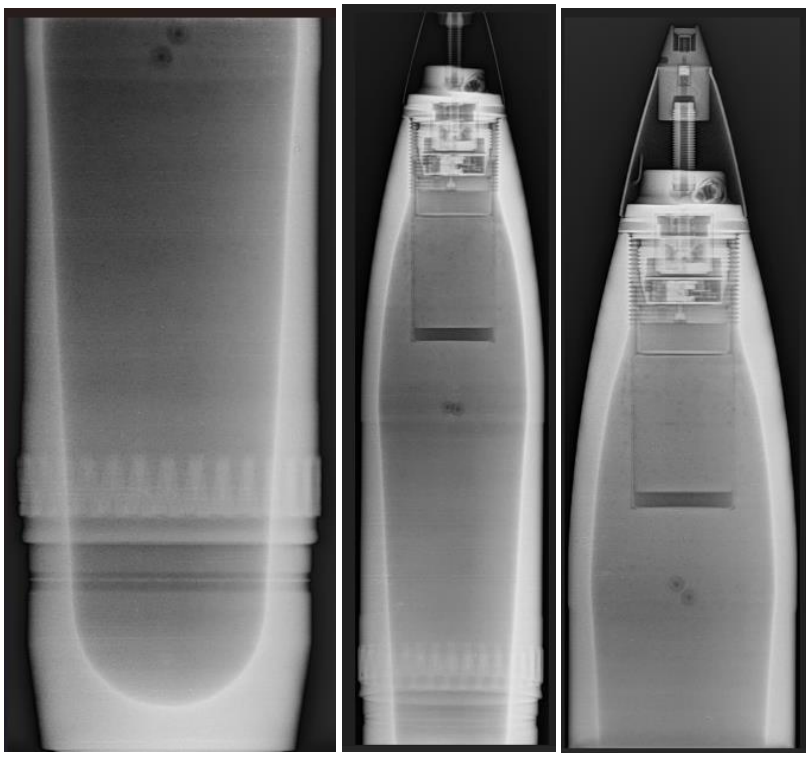

Figure A-17. Sample 5 0° X-Ray Images

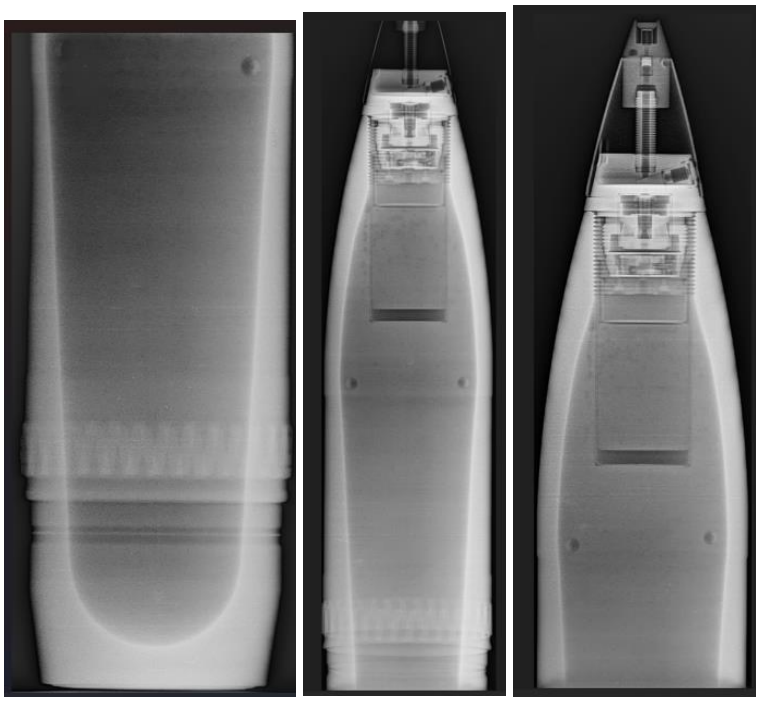

Figure A-18. Sample 5 45° X-Ray Images

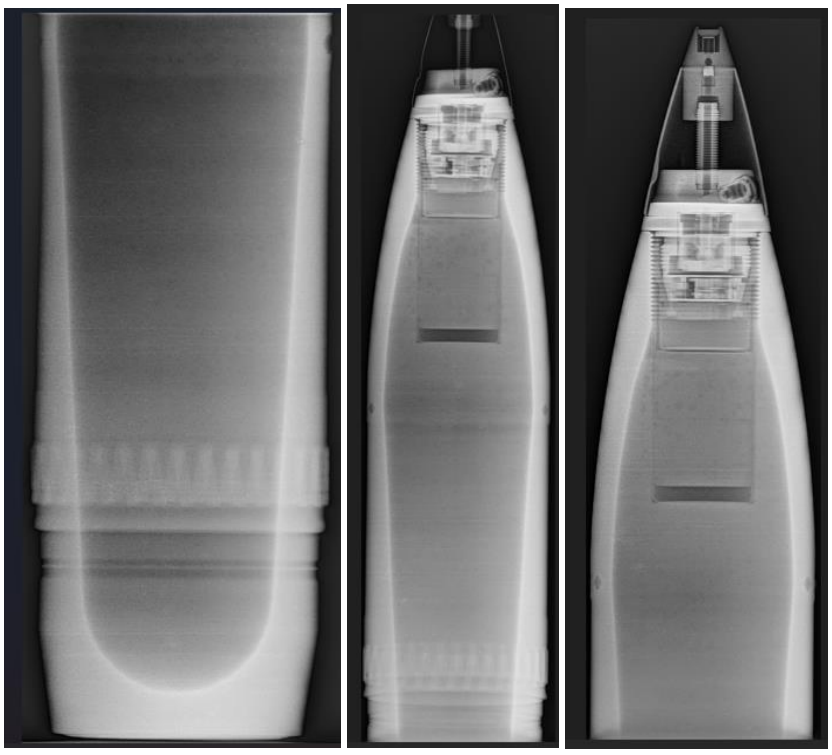

Figure A-19. Sample 5 90° X-Ray Images

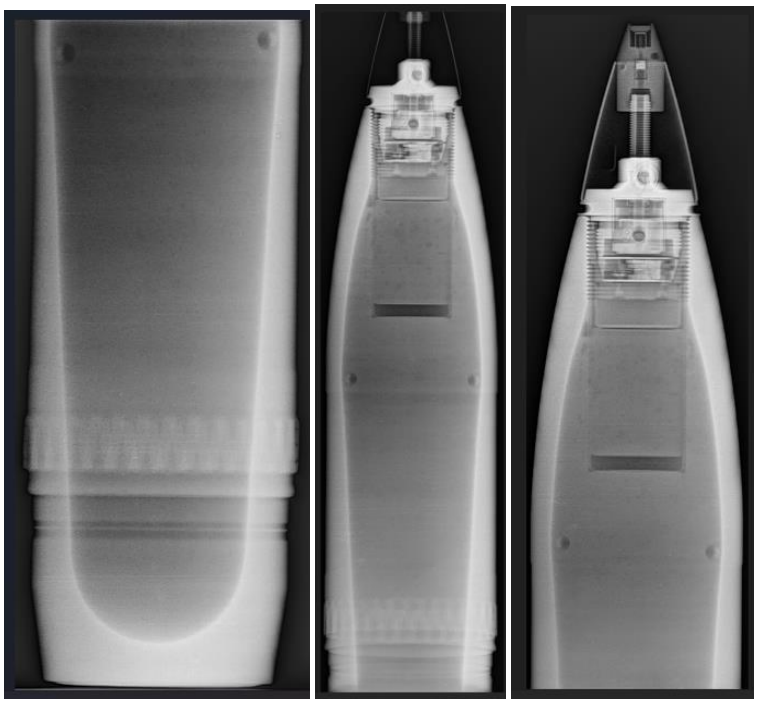

Figure A-20. Sample 5 135° X-Ray Images

The following X-ray images are obtained from the 105 mm calibre HEP-T nature projectiles. The method of imaging is described in Chapter 2.

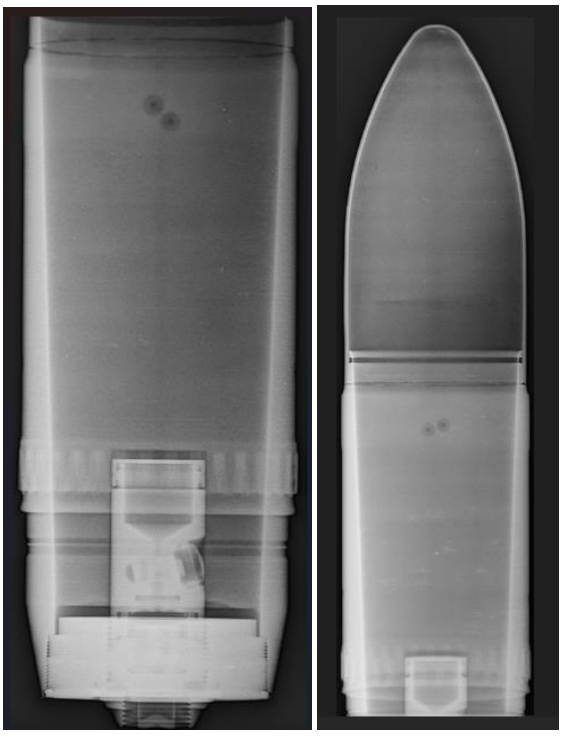

Figure A-21. Sample 6 0° X-Ray Images

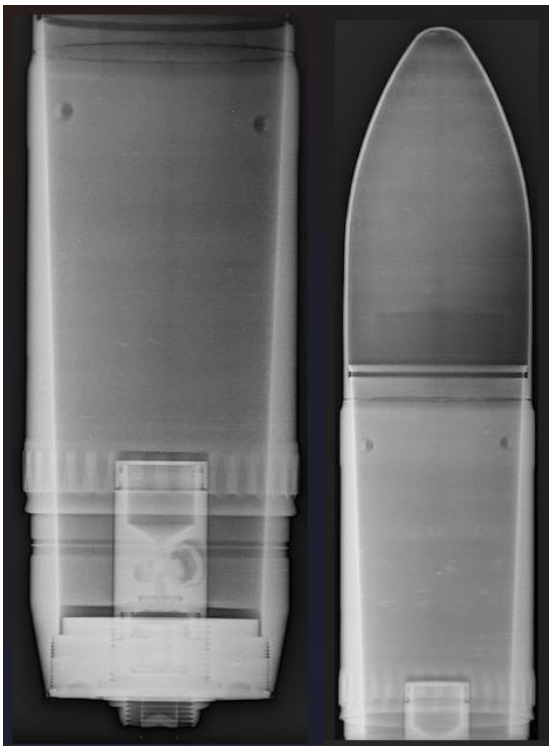

Figure A-22. Sample 6 45° X-Ray Images

Figure A-23. Sample 6 90° X-Ray Images

Figure A-24. Sample 6 135° X-Ray Images

Figure A-25. Sample 7 0° X-Ray Images

Figure A-26. Sample 7 45° X-Ray Images

Figure A-27. Sample 7 90° X-Ray Images

Figure A-28. Sample 7 135° X-Ray Images

Figure A-29. Sample 8 0° X-Ray Images

Figure A-30. Sample 8 45° X-Ray Images

Figure A-31. Sample 8 90° X-Ray Images

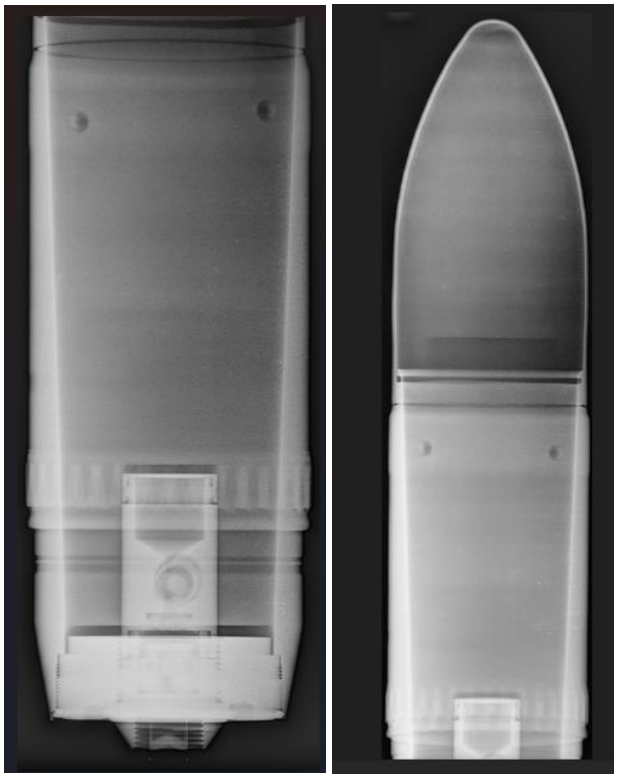

Figure A-32. Sample 8 135° X-Ray Images

Figure A-33. Sample 9 0° X-Ray Images

Figure A-34. Sample 9 45° X-Ray Images

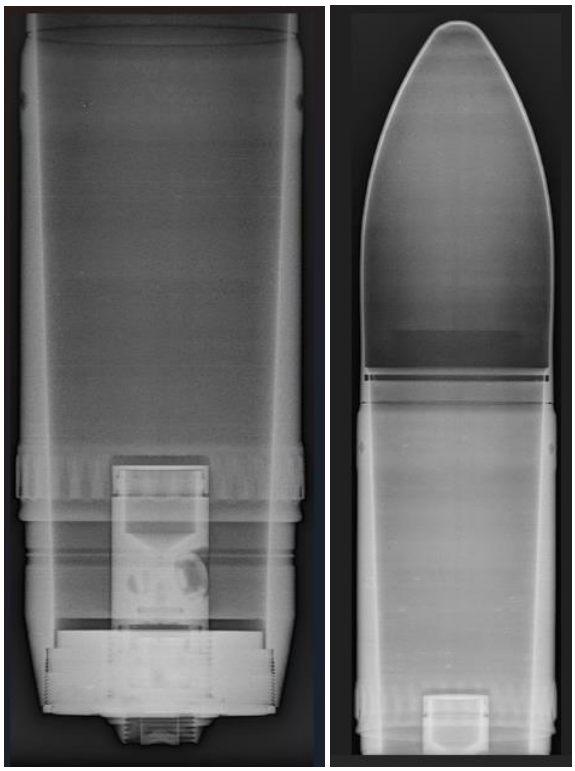

Figure A-35. Sample 9 90° X-Ray Images

Figure A-36. Sample 9 135° X-Ray Images

Figure A-37. Sample 10 0° X-Ray Images

Figure A-38. Sample 10 45° X-Ray Images

Figure A-39. Sample 10 90° X-Ray Images

Figure A-40. Sample 10 135° X-Ray Images

Appendix B. ESD Sensitivity Test Results

The following tables are the results from ESD sensitivity tests for each sample in the current study. The method of testing is described in Chapter 2.

Table B-1. Recent Comp A-3 ESD Results

SENSITIVITY OF SUBSTANCES TO ELECTROSTATIC DISCHARGE

Sample	A3 (pastille écrasée) recent
Sample preparation :	RD-grenade-01

Temperature °C: 25.3

Relative humidity %: 48%

Capacitance (pF): 2000

Sealed Sample Cell: ☐ Open Sample Cell: X

Air Gap (mm): 0.5

Voltage kV	Energy J	TRIAL 1	2	3	4	5	6	7	8	9	10	REACTION	Total
25	0.625	N	N	N	N	N	N	N	N	N	N	N	
20	0.400												
15	0.225												
10	0.100												
5	0.025												
2	0.004												

N = No Reaction I = Ignition D = Detonation

Limiting Energy : >0.625

Sensitivity to Electrostatic Discharge (Y/N) ? N

Operators: Jeremy Hebert, Frederic Lirette Date: 22/08/2024

Table B-2. Aged Comp A-3 ESD Results

SENSITIVITY OF SUBSTANCES TO ELECTROSTATIC DISCHARGE

Sample	A3 usiné
Sample preparation :	obus #7 105R Hep-T M326

Temperature °C: 25.3

Relative humidity %: 48%

Capacitance (pF): 2000

Sealed Sample Cell: [ ] Open Sample Cell: [X]

Air Gap (mm): 0.5

Voltage kV	Energy J	TRIAL 1	2	3	4	5	6	7	8	9	10	REACTION	Total
25	0.625	N	N	N	N	N	N	N	N	N	N	N	
20	0.400												
15	0.225												
10	0.100												
5	0.025												
2	0.004												

N = No Reaction I = Ignition D = Detonation

Limiting Energy : >0.625

Sensitivity to Electrostatic Discharge (Y/N) ? N

Operators: Jeremy Hebert, Frederic Lirette Date: 22/08/2024

Table B-3. Aged Comp B (Melted) ESD Results

SENSITIVITY OF SUBSTANCES TO ELECTROSTATIC DISCHARGE

Sample	**Composition B fondue**
Sample preparation :	#lot: 1315-20-a0w-0662 onus#2 105 mm He M323

Temperature °C: 25.3

Relative humidity %: 48%

Capacitance (pF): 2000

Sealed Sample Cell: [ ] Open Sample Cell: [X]

Air Gap (mm): 0.5

Voltage kV	Energy J	TRIAL 1	2	3	4	5	6	7	8	9	10	REACTION	Total
25	0.625	N	N	N	N	N	N	N	N	N	N	N	
20	0.400												
15	0.225												
10	0.100												
5	0.025												
2	0.004												

N = No Reaction I = Ignition D = Detonation

Limiting Energy : >0.625

Sensitivity to Electrostatic Discharge (Y/N) ? N

Operators: Jeremy Hebert, Frederic Lirette Date: 22/08/2024

Table B-4. Aged Comp B (Machined) ESD Results

SENSITIVITY OF SUBSTANCES TO ELECTROSTATIC DISCHARGE

Sample	**Composition B usiné**
Sample preparation :	105 mm M323 obus#5

Temperature °C: 25.3

Relative humidity %: 48%

Capacitance (pF): 2000

Sealed Sample Cell: [ ] Open Sample Cell: [X]

Air Gap (mm): 0.5

Voltage kV	Energy J	TRIAL 1	2	3	4	5	6	7	8	9	10	REACTION	Total
25	0.625	N	N	N	N	N	N	N	N	N	N	N	
20	0.400												
15	0.225												
10	0.100												
5	0.025												
2	0.004												

N = No Reaction I = Ignition D = Detonation

Limiting Energy : >0.625

Sensitivity to Electrostatic Discharge (Y/N) ? N

Operators: Jeremy Hebert, Frederic Lirette Date: 22/08/2024

Table B-5. Recent Comp B ESD Results

SENSITIVITY OF SUBSTANCES TO ELECTROSTATIC DISCHARGE

Sample	**Composition B recent**
Sample preparation :	Ddp05L008-012

Temperature °C: 25.3

Relative humidity %: 48%

Capacitance (pF): 2000

Sealed Sample Cell: [ ] Open Sample Cell: [X]

Air Gap (mm): 0.5

Voltage kV	Energy J	TRIAL 1	2	3	4	5	6	7	8	9	10	REACTION	Total
25	0.625	N	N	N	N	N	N	N	N	N	N	N	
20	0.400												
15	0.225												
10	0.100												
5	0.025												
2	0.004												

N = No Reaction I = Ignition D = Detonation

Limiting Energy : >0.625

Sensitivity to Electrostatic Discharge (Y/N) ? N

Operators: Jeremy Hebert, Frederic Lirette Date: 22/08/2024

Table B-6. Aged TNT ESD Results

SENSITIVITY OF SUBSTANCES TO ELECTROSTATIC DISCHARGE

Sample	**TNT Booster charge**
Sample preparation :	Provient de l'obus #5

Temperature °C: 25.3

Relative humidity %: 48%

Capacitance (pF): 2000

Sealed Sample Cell: [ ] Open Sample Cell: [X]

Air Gap (mm): 0.5

Voltage kV	Energy J	TRIAL 1	2	3	4	5	6	7	8	9	10	REACTION	Total
25	0.625	N	N	N	N	N	N	N	N	N	N	N	
20	0.400												
15	0.225												
10	0.100												
5	0.025												
2	0.004												

N = No Reaction I = Ignition D = Detonation

Limiting Energy : >0.625

Sensitivity to Electrostatic Discharge (Y/N) ? N

Operators: Jeremy Hebert, Frederic Lirette Date: 22/08/2024

Table B-7. Recent TNT ESD Results

SENSITIVITY OF SUBSTANCES TO ELECTROSTATIC DISCHARGE

Sample	TNT Broyer recent

Sample preparation :	Lot: 1104

Temperature °C: 25.3

Relative humidity %: 48%

Capacitance (pF): 2000

Sealed Sample Cell: [ ] Open Sample Cell: [X]

Air Gap (mm): 0.5

Voltage kV	Energy J	TRIAL 1	2	3	4	5	6	7	8	9	10	REACTION	Total
25	0.625	N	N	N	N	N	N	N	N	N	N	N	
20	0.400												
15	0.225												
10	0.100												
5	0.025												
2	0.004												

N = No Reaction **I = Ignition** **D = Detonation**

Limiting Energy : >0.625J

Sensitivity to Electrostatic Discharge (Y/N) ? N

Operators: Jeremy Hebert

Frederic Lirette

Date: 22/08/2024

Appendix C. BAM Friction Sensitivity

ESSAI DE SENSIBILITÉ À LA FRICTION BAM

MATÉRIEL ÉVALUÉ (plus une brève description de l'état physique)	DATE jj/mm/aa	POIDS UTILISÉ						POSITION DU POIDS UTILISÉ						TYPE DE RÉACTION N, D, I, C, E						RESULTATS (NEWTON)
		1	2	3	4	5	6	1	2	3	4	5	6	1	2	3	4	5	6	
PETN classe 4	20/08/2024	6	6	6	6	6	5	4	6	4	4	4	6	N	C	N	N	C	N	**96N**
		5	5	5	5	5		6	6	6	6	6		N	N	N	N	N		
TNT Booster	20/08/2024	7	6	6	6	6	6	6	6	6	6	6	6	D	N	N	N	N	N	**160N**
		6						6						N						
TNT broyé ''récent''	20/08/2024	9	8	7	6	6	6	6	6	6	6	4	4	I	I	I	I	N	N	**120N**
		6	6	6	6			4	4	4	4			N	N	N	N	N		
A3 ''récent''	20/08/2024	9	8	7	7	7	7	6	6	6	6	6	6	I	I	N	N	N	N	**240N**
		7	7					6	6					N	N					
A3 usiné	20/08/2024	9	8	7	6	6	6	6	6	6	6	6	6	C	I	I	N	N	N	**160N**
		6	6	6				6	6	6				N	N	N				
Composition B usiné	20/08/2024	7	6	6	5	5	5	6	6	4	6	6	6	I	I	I	N	N	N	**96N**
		5	5	5				6	6	6				N	N	N				
Composition B ''récent''	20/08/2024	7	6	6	6	6	6	6	6	6	6	6	6	I	N	N	N	N	N	**160N**
		6						6						N						
Composition B fondu	20/08/2024	9	8	7	6	6	6	6	6	6	6	6	6	I	I	I	N	N	N	
		6	6	6	6	6	6	6	6	4	4	4	4	N	D	N	N	N	N	**120N**
		6	6					4	4					N	N					

Le produit était collant

NOTE: LES TYPES DE RÉACTIONS SONT:

N = NO RÉACTION D = DÉCOMPOSITION I = IGNITION
C = CRAQUEMENT E = EXPLOSION

TECHNICIENS : Jérémy Hébert, Frédéric Lirette, Janyce Lavoie

COMBINAISON À ÊTRE UTILISÉES					
POIDS	POSITION	CHARGE	POIDS	POSITION	CHARGE
1	1	5	4	6	60
1	3	7	5	6	80
1	6	10	6	4	96
2	6	20	6	6	120
4	1	30	7	6	160
3	6	40	8	6	240
			9	6	360

Appendix D. BAM Impact Sensitivity

ESSAI DE SENSIBILITÉ À L'IMPACT BAM

MATÉRIEL ÉVALUÉ (plus une brève description de l'état physique)	DATE jj/mm/aa	RÉSULTATS (joules)	RÉACTION	1 Kg					5 Kg					10 Kg			20 Kg	
				10	20	30	40	50	15	20	30	40	50	30	40	50	30	40
RDX Classe 5 type II	20/08/2024	5J	N = NON D = DÉCOMPOSITION E = EXPLOSION				NN NN NN	NN NE	E	NE	NE	E						
TNT Booster	20/08/2024	>80J	N = NON D = DÉCOMPOSITION E = EXPLOSION											NN	N	N	N	NN NN NN
TNT ''récent''	20/08/2024	7,5J	N = NON D = DÉCOMPOSITION E = EXPLOSION					NN NN NN	ND	NN D	NN D	D	NN NN ND	ND	D	NN ND	NN ND	E
Composition B ''récent''	20/08/2024	15J	N = NON D = DÉCOMPOSITION E = EXPLOSION							NN NN NN	NE	E	NE	E	E			
Composition B usiné	20/08/2024	15J	N = NON D = DÉCOMPOSITION E = EXPLOSION							NN NN NN	NN NN N D*	N D*	NN NN N D*	D*				
Composition B fondu	20/08/2024	20J	N = NON D = DÉCOMPOSITION E = EXPLOSION								NN NN NN	E						
A3 ''récent''	20/08/2024	15J	N = NON D = DÉCOMPOSITION E = EXPLOSION							NN NN NN	D*	D*	D*					
A3 usiné	20/08/2024	20J	N = NON D = DÉCOMPOSITION E = EXPLOSION								NN NN NN	D	ND	E	NN N D*	NN NE	D*	

	JOULES	1	2	3	4	5	7.5	10	15	20	25	30	40	50	60	80

* Décomposition partielle

TECHNICIENS : Jérémy Hébert, Frédéric Lirette, Janyce Lavoie

Appendix E. SEM Images

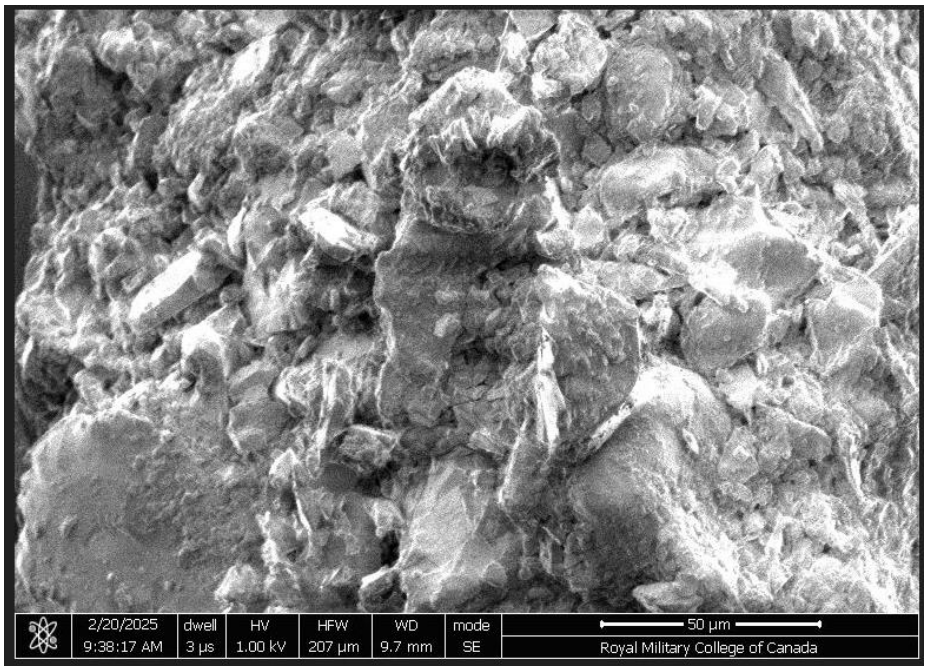

Figure E-1. Aged Comp A-3 SEM Image

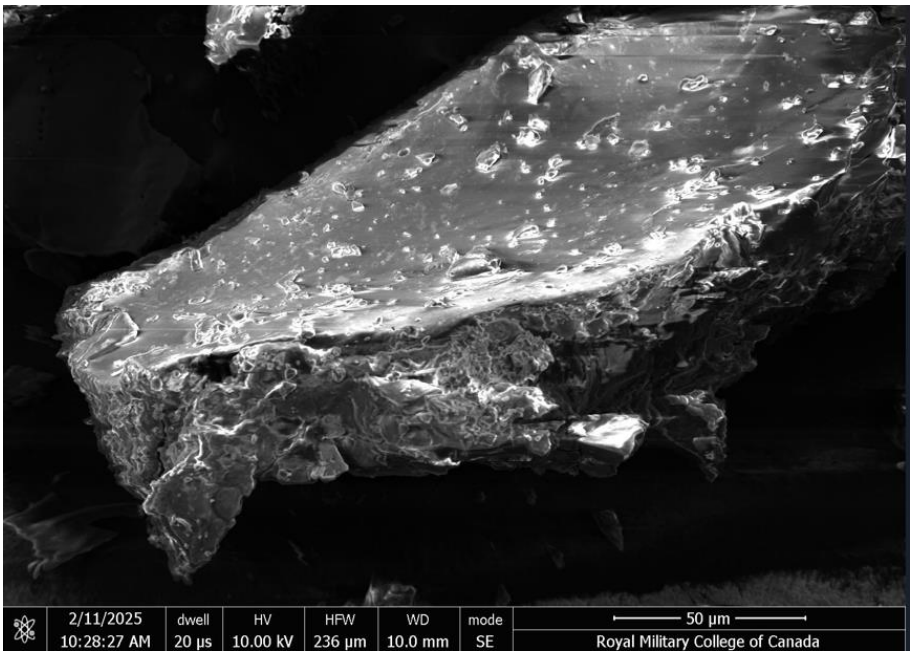

Figure E-2. Recent Comp A-3 SEM Image

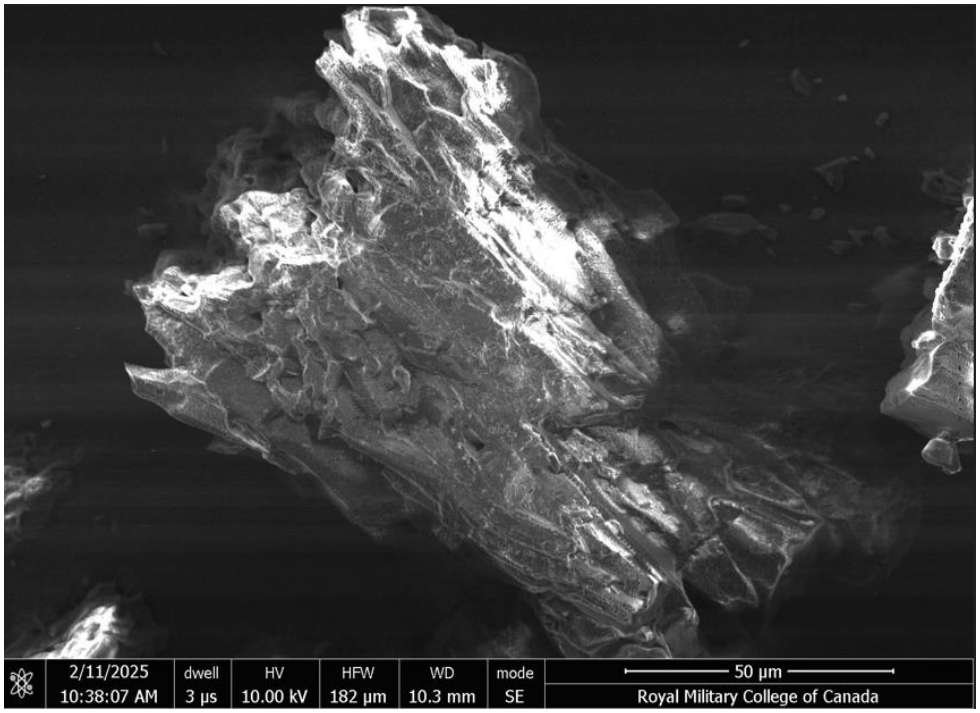

Figure E-3. Recent TNT SEM Image

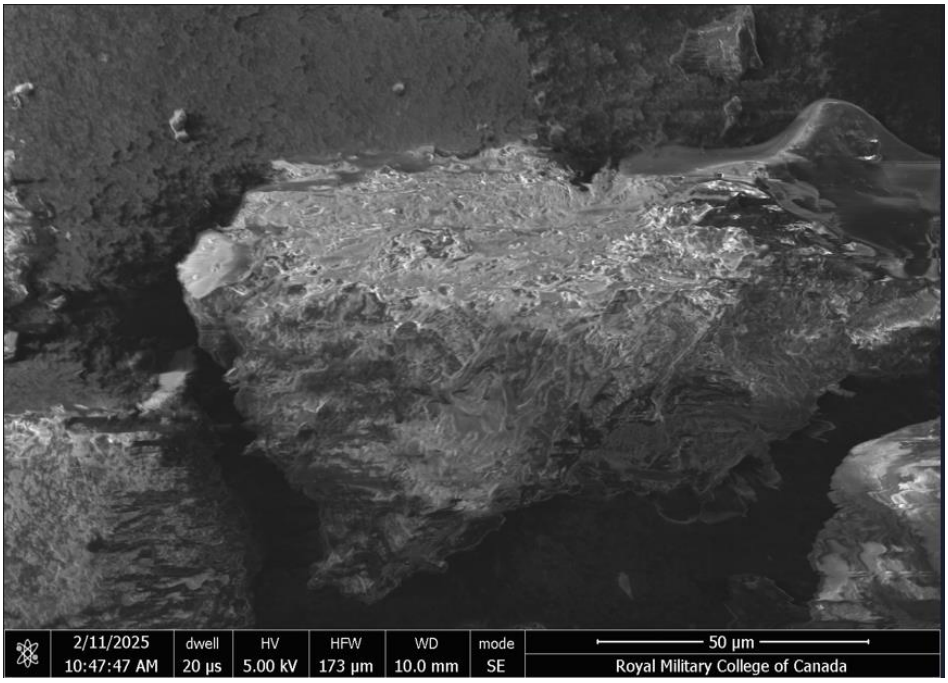

Figure E-4. Recent Comp B SEM Image

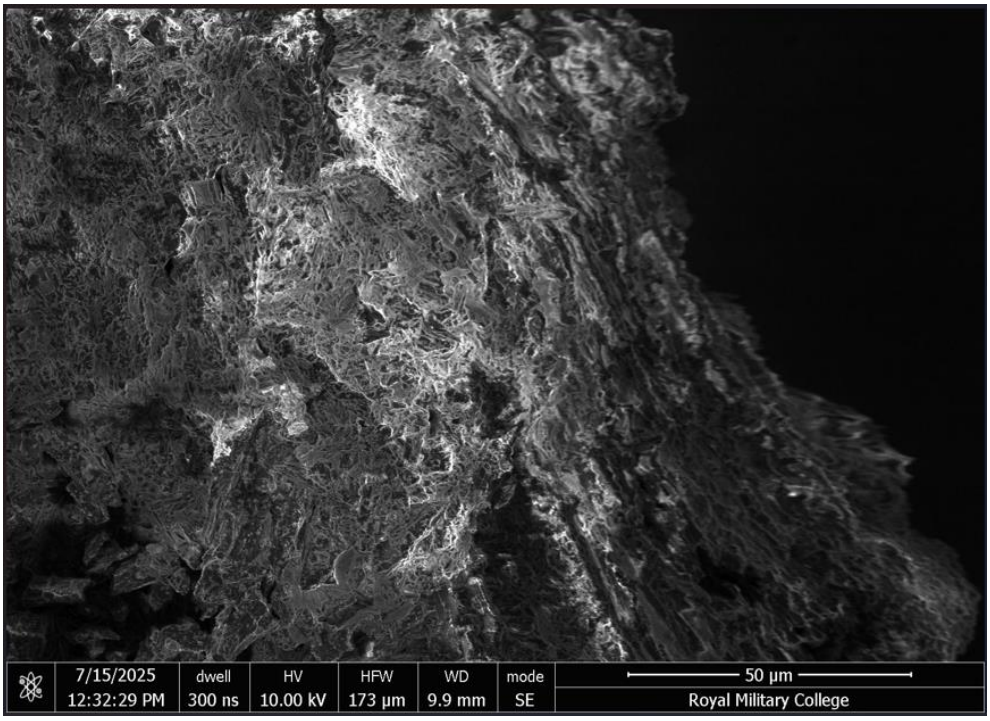

Figure E-5. Aged TNT SEM Image

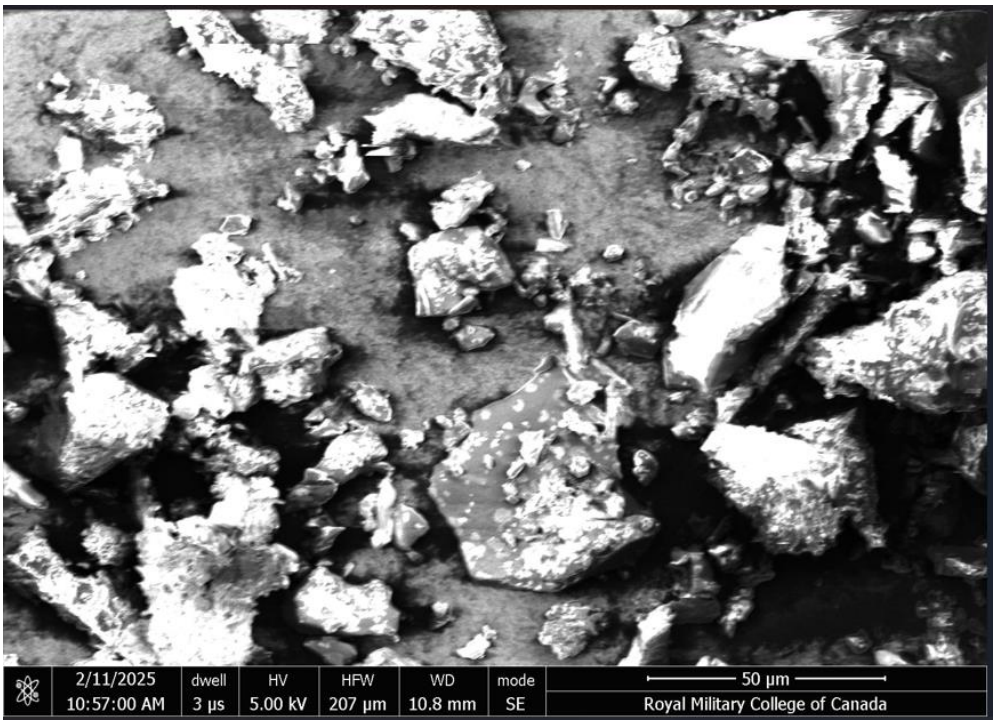

Figure E-6. Aged Comp B (Machined) SEM Image

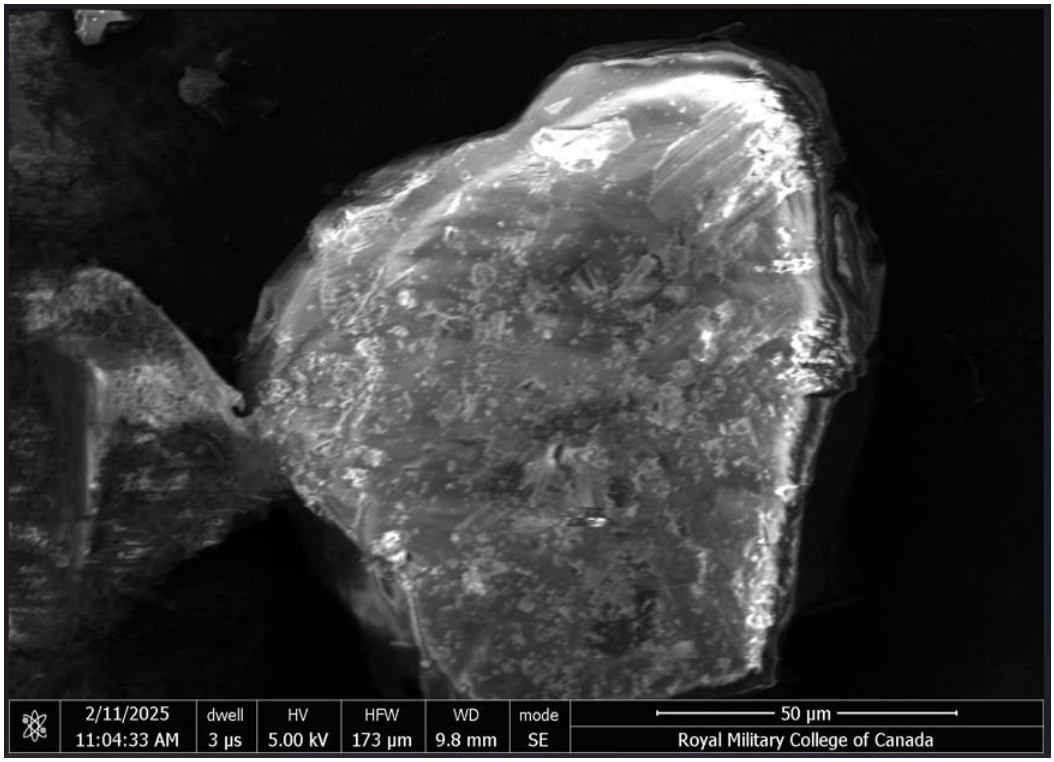

Figure E-7. Aged Comp B (Melted) SEM Image

Appendix F. TGA-DSC Thermograms

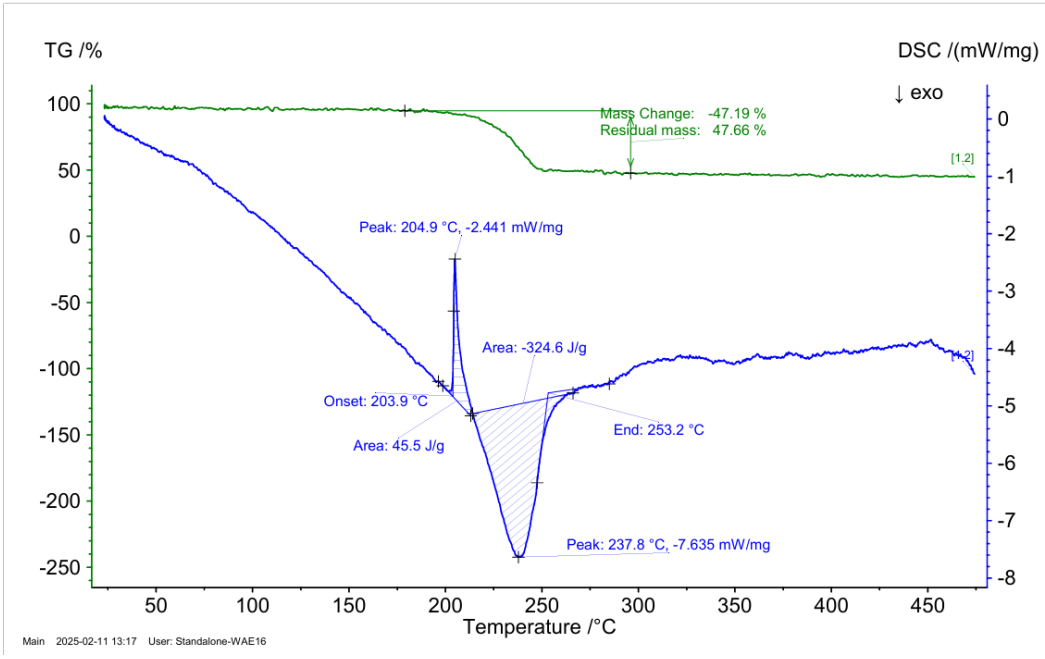

Figure F-1. Thermogram for Aged Comp A-3 (10 K/min)

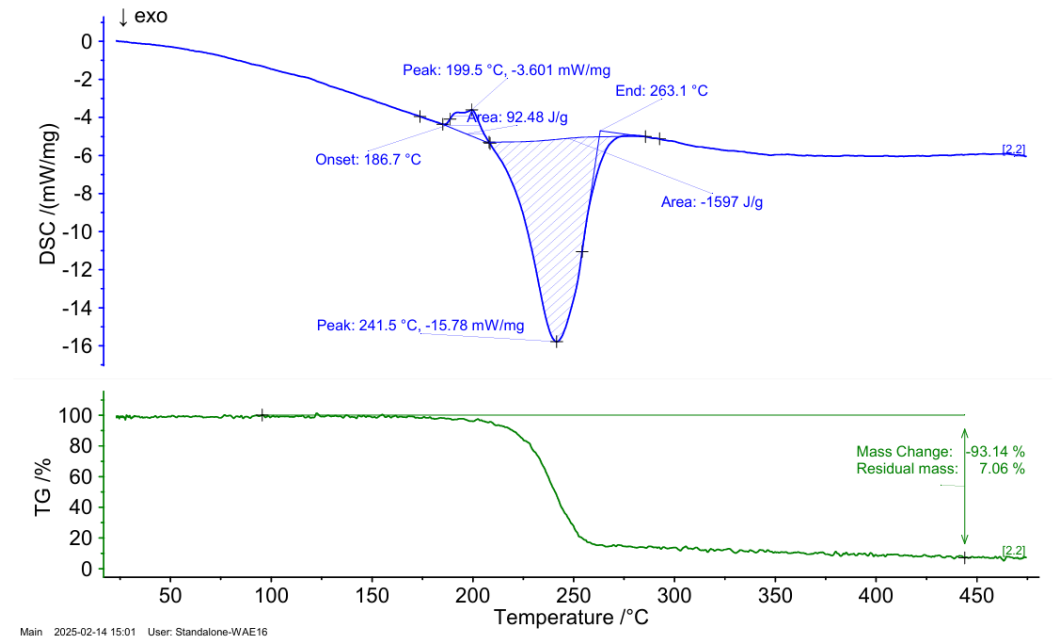

Figure F-2. Thermogram for Recent Comp A-3 (10 K/min)

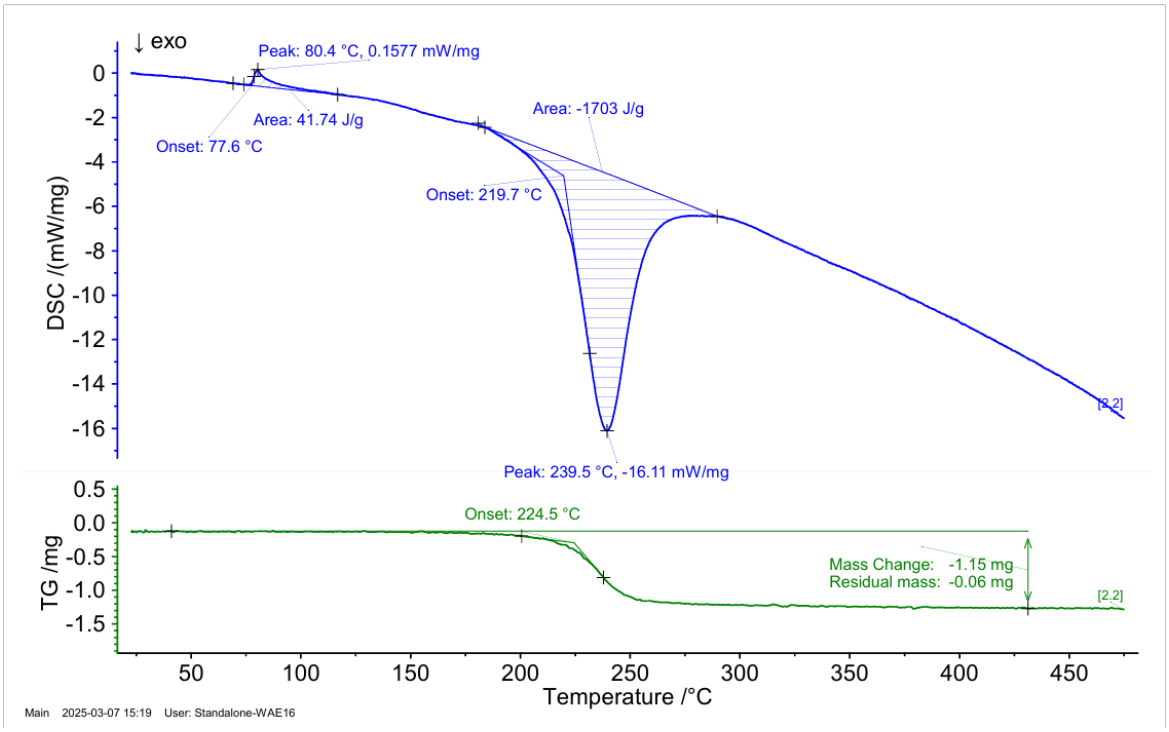

Figure F-3. Thermogram for Aged (Machined) Comp B (10 K/min)

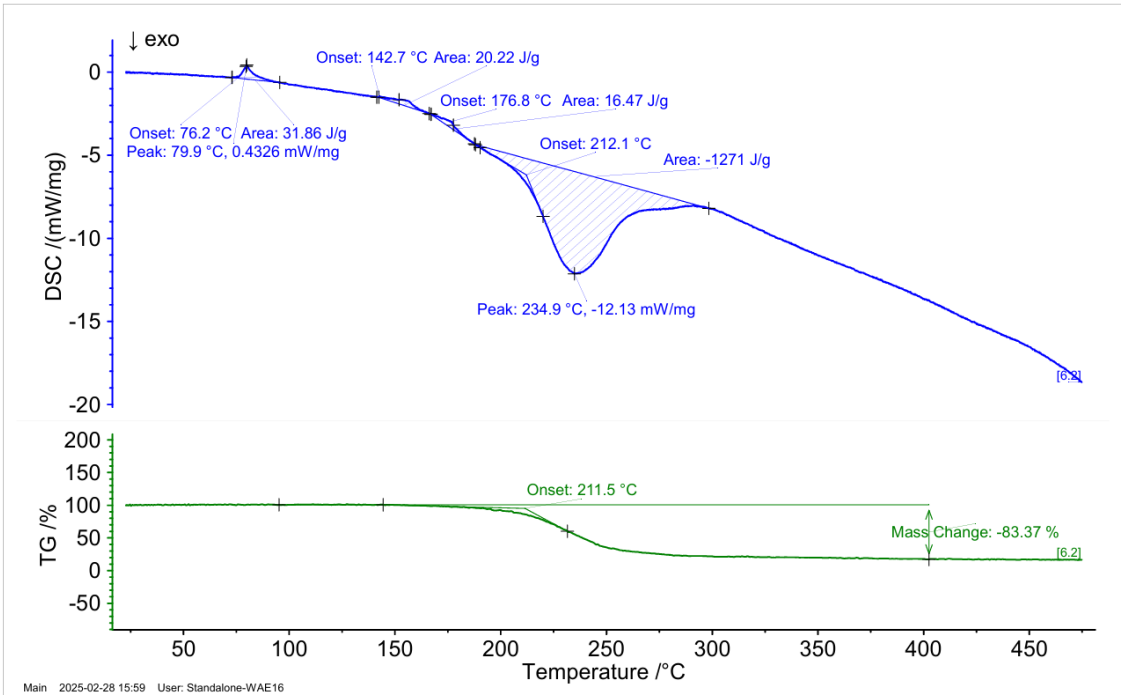

Figure F-4. Thermogram for Recent Comp B (10 K/min)

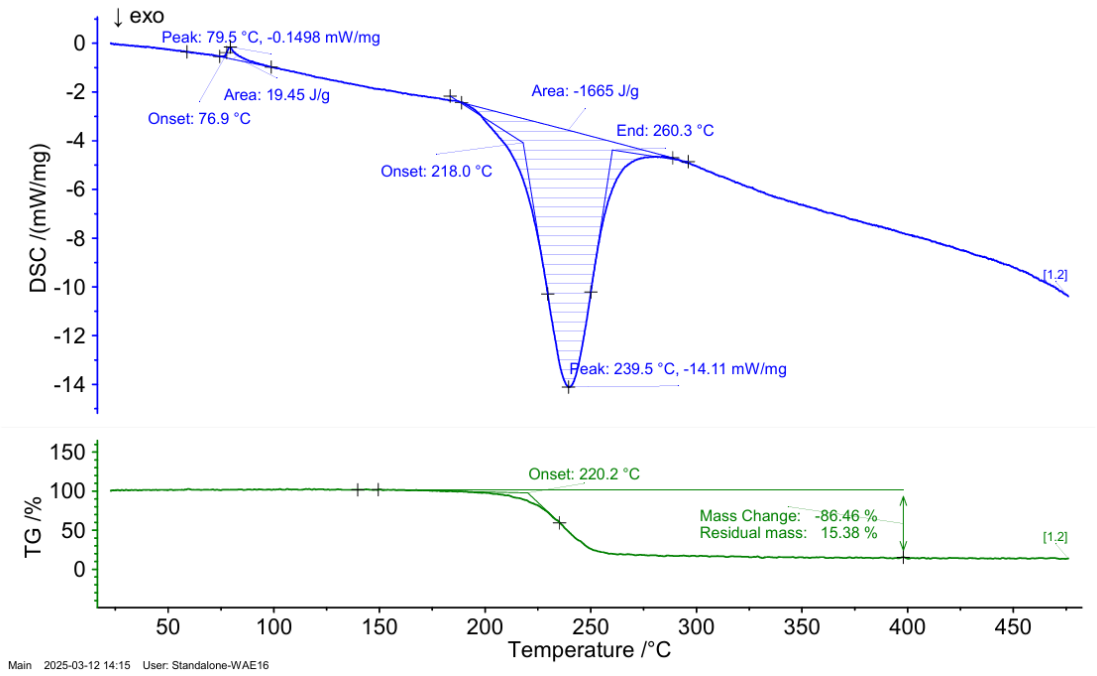

Figure F-5. Thermogram for Aged (Melted) Comp B (10 K/min)

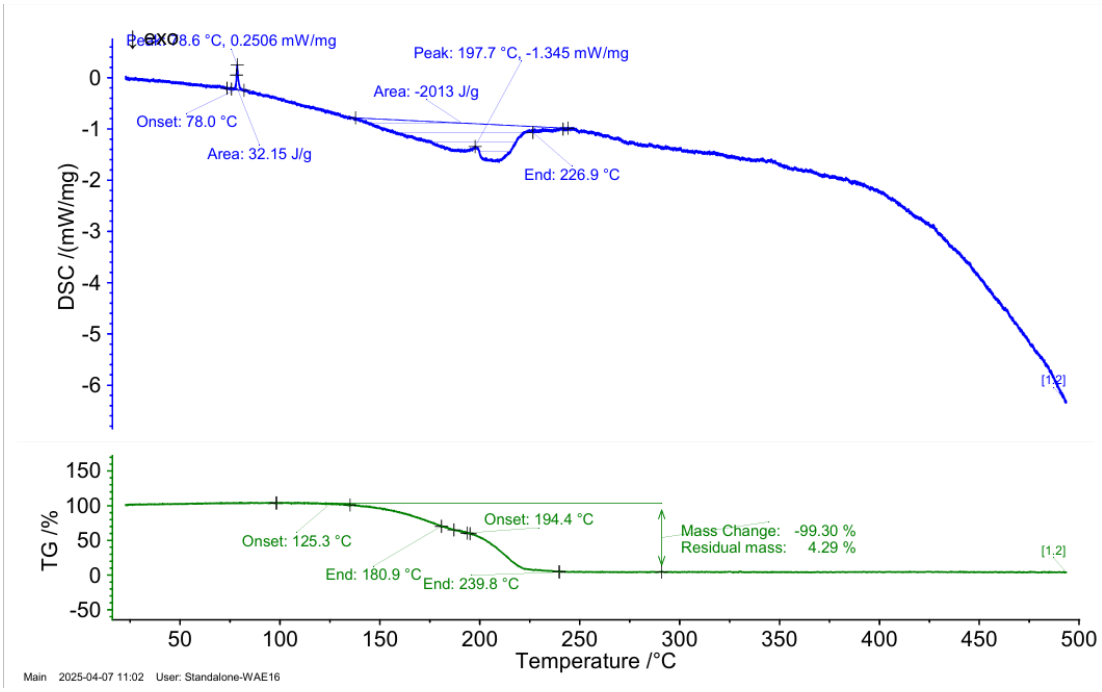

Figure F-6. Thermogram for Aged (Machined) Comp B (1 K/min)

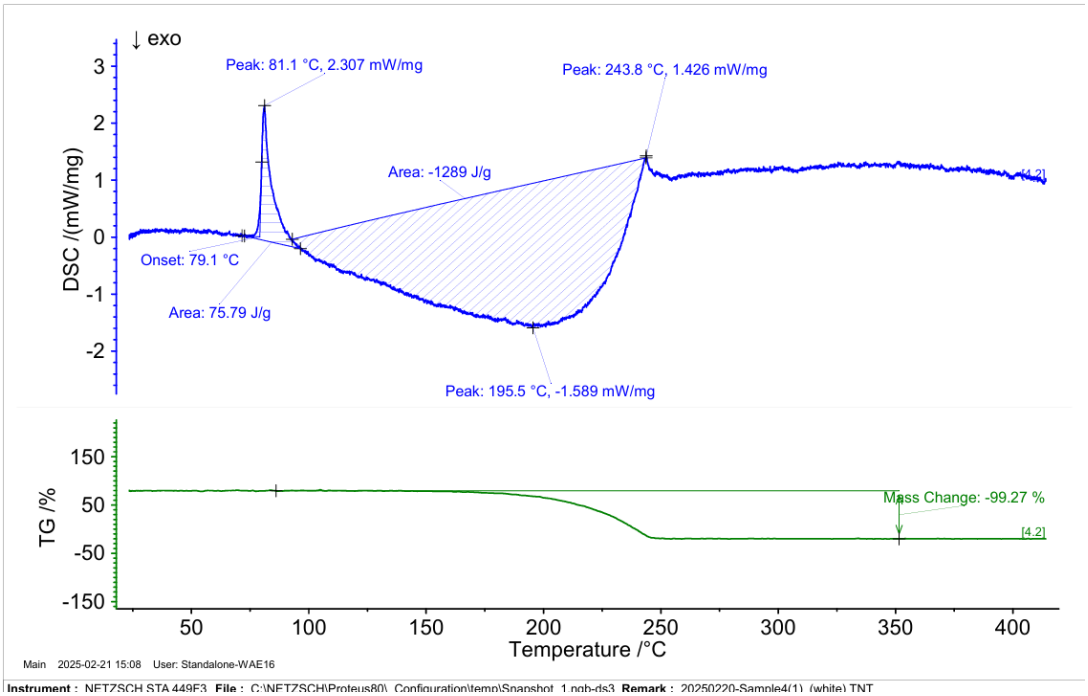

Figure F-7. Thermogram for Aged TNT (10 K/min)

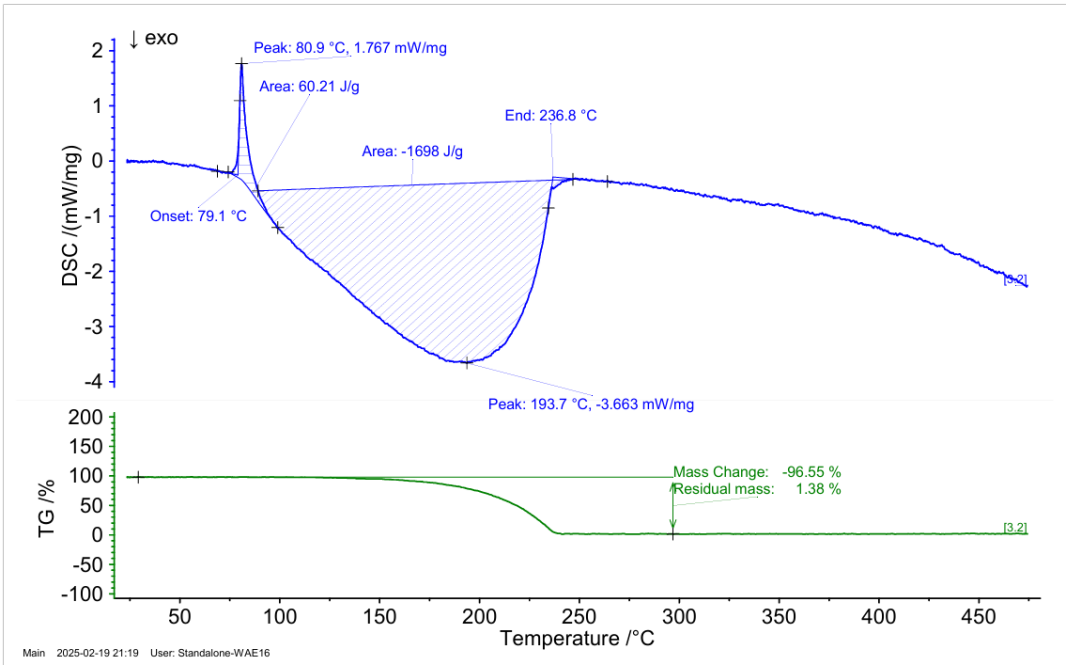

Figure F-8 Thermogram for Recent TNT (10 K/min)

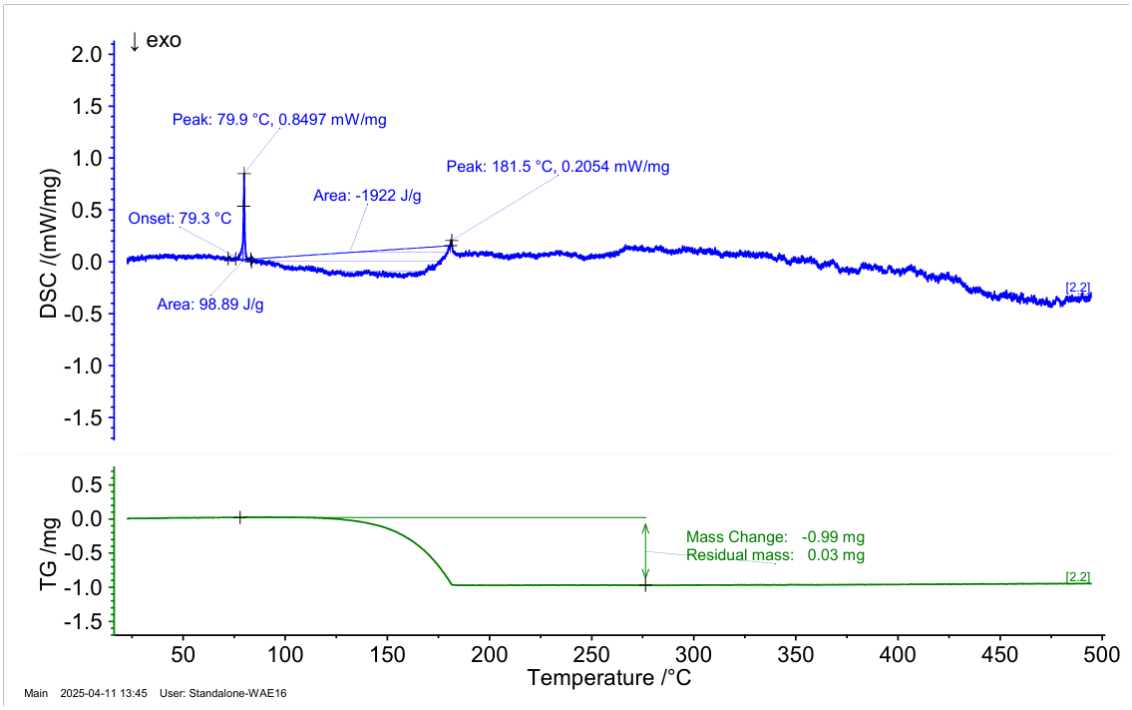

Figure F-9. Thermogram for Aged TNT (0.5 K/min)

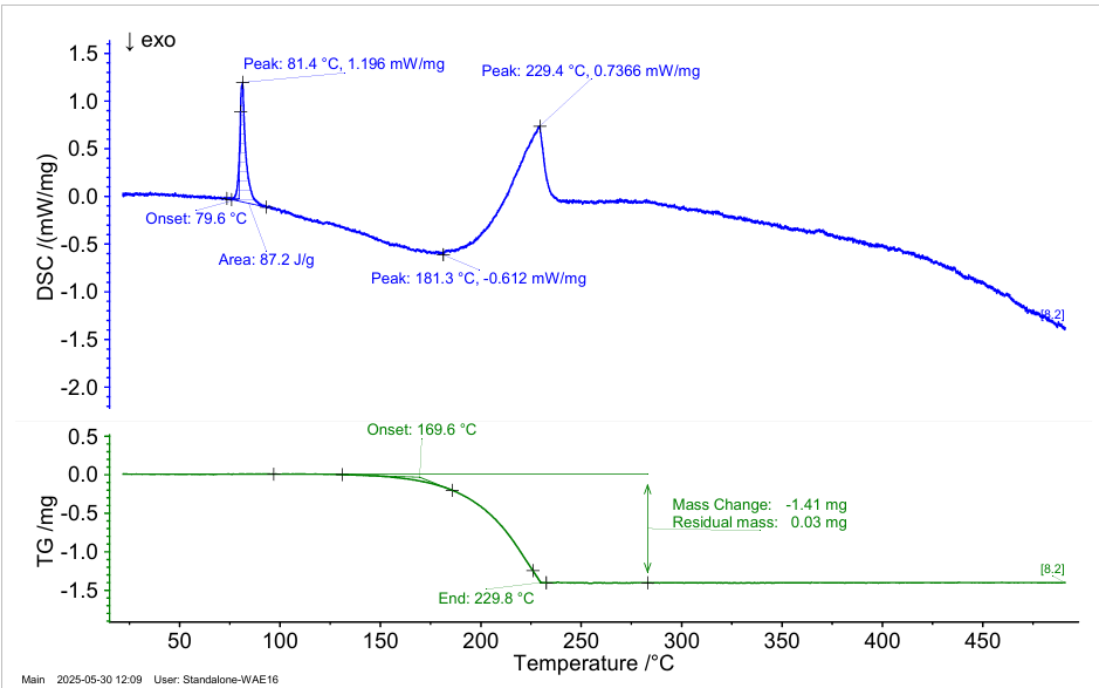

Figure F-10. Thermogram for Aged TNT (3 K/min)

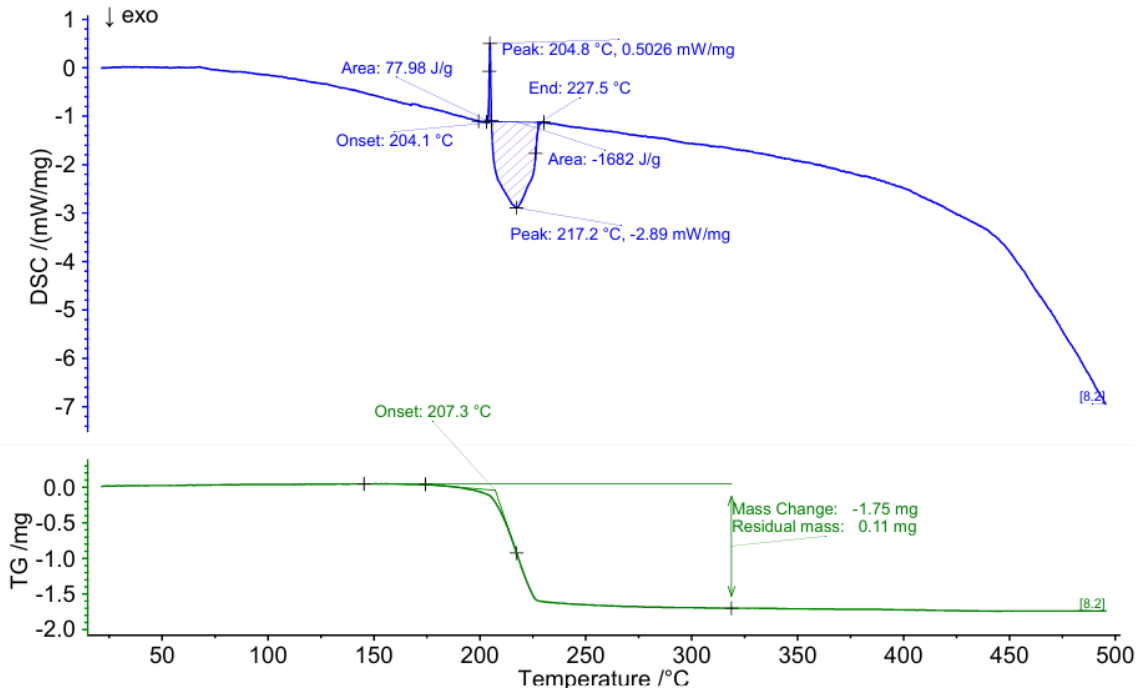

Figure F-12. Thermogram for Aged Comp A-3 (1 K/min)

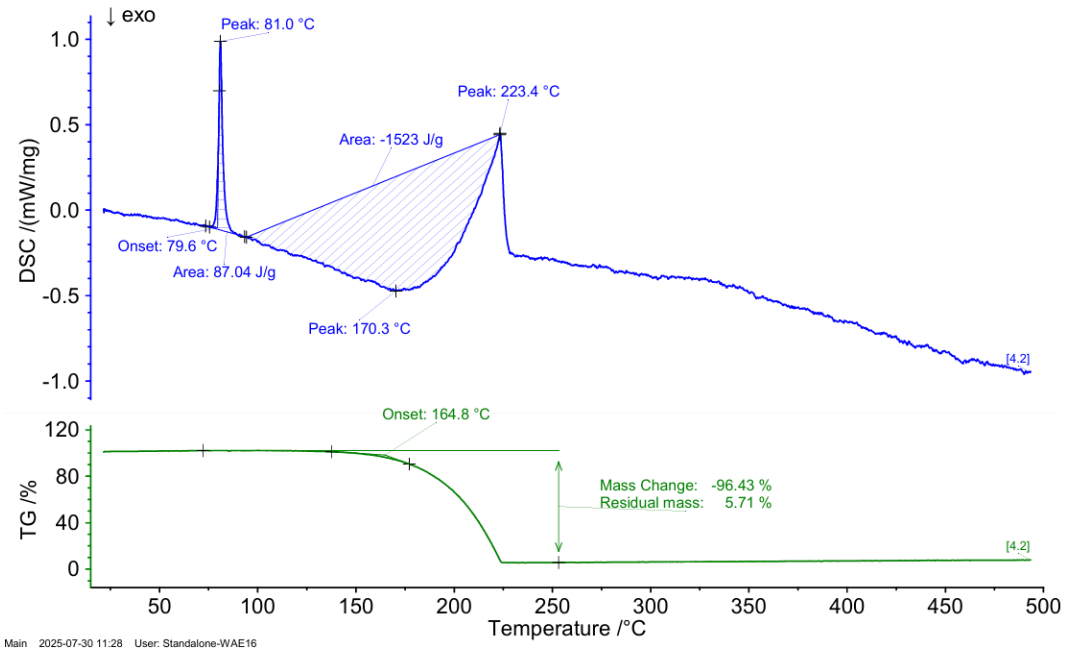

Figure F-13. Thermogram for Aged TNT (2 K/min)

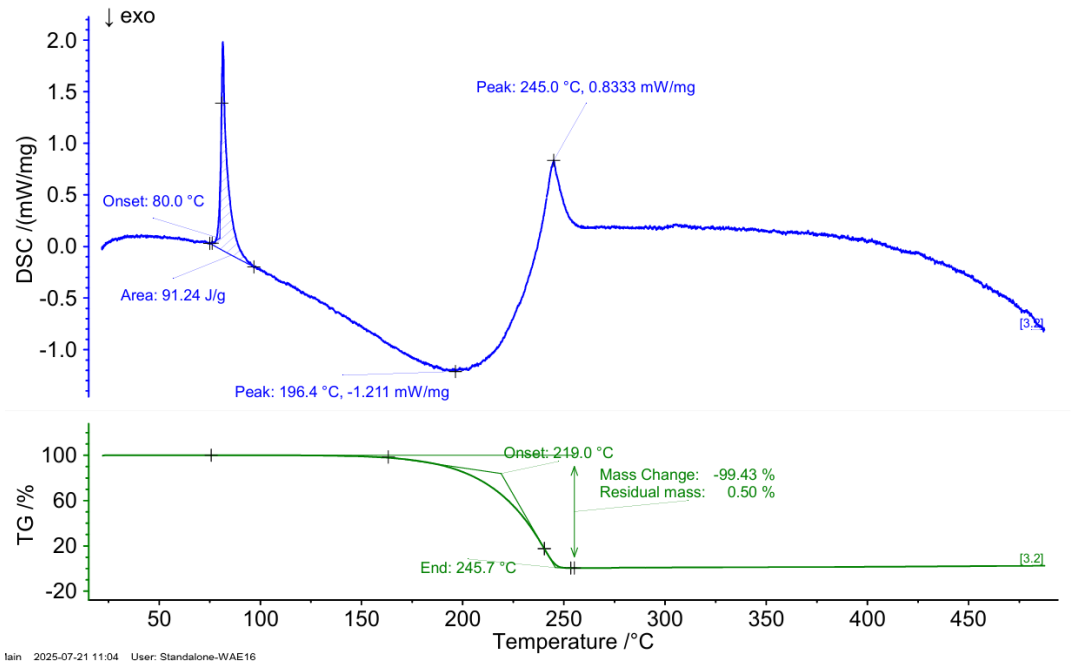

Figure F-14. Thermogram for Aged TNT (5 K/min)